

AD \_\_\_\_\_

Award Number: DAMD17-02-1-0706

TITLE: TARGET (Translational Approaches for the Reversal,  
Genetic Evaluation) of Lung Cancer

PRINCIPAL INVESTIGATOR: Waun Ki Hong, M.D.

CONTRACTING ORGANIZATION: The University of Texas M.D. Anderson  
Cancer Center  
Houston, Texas 77030

REPORT DATE: September 2003

TYPE OF REPORT: Annual

PREPARED FOR: U.S. Army Medical Research and Materiel Command  
Fort Detrick, Maryland 21702-5012

DISTRIBUTION STATEMENT: Approved for Public Release;  
Distribution Unlimited

The views, opinions and/or findings contained in this report are those of the author(s) and should not be construed as an official Department of the Army position, policy or decision unless so designated by other documentation.

Best Available Copy

20040415 014



**REPORT DOCUMENTATION PAGE**Form Approved  
OMB No. 074-0188

Public reporting burden for this collection of information is estimated to average 1 hour per response, including the time for reviewing instructions, searching existing data sources, gathering and maintaining the data needed, and completing and reviewing this collection of information. Send comments regarding this burden estimate or any other aspect of this collection of information, including suggestions for reducing this burden to Washington Headquarters Services, Directorate for Information Operations and Reports, 1215 Jefferson Davis Highway, Suite 1204, Arlington, VA 22202-4302, and to the Office of Management and Budget, Paperwork Reduction Project (0704-0188), Washington, DC 20503

<b>1. AGENCY USE ONLY</b> (Leave blank)		<b>2. REPORT DATE</b> September 2003	<b>3. REPORT TYPE AND DATES COVERED</b> Annual (1 Sep 2002 - 31 Aug 2003)	
<b>4. TITLE AND SUBTITLE</b> TARGET (Translational Approaches for the Reversal, Genetic Evaluation of) Lung Cancer			<b>5. FUNDING NUMBERS</b> DAMD17-02-1-0706	
<b>6. AUTHOR(S)</b> Waun Ki Hong, M.D.				
<b>7. PERFORMING ORGANIZATION NAME(S) AND ADDRESS(ES)</b> The University of Texas M.D. Anderson Cancer Center Houston, Texas 77030  <i>E-Mail:</i> whong@mdanderson.org			<b>8. PERFORMING ORGANIZATION REPORT NUMBER</b>	
<b>9. SPONSORING / MONITORING AGENCY NAME(S) AND ADDRESS(ES)</b> U.S. Army Medical Research and Materiel Command Fort Detrick, Maryland 21702-5012			<b>10. SPONSORING / MONITORING AGENCY REPORT NUMBER</b>	
<b>11. SUPPLEMENTARY NOTES</b> Original contains color plates: All DTIC reproductions will be in black and white.				
<b>12a. DISTRIBUTION / AVAILABILITY STATEMENT</b> Approved for Public Release; Distribution Unlimited				<b>12b. DISTRIBUTION CODE</b>
<b>13. ABSTRACT (Maximum 200 Words)</b> TARGET is focused on a series of projects designed to obtain data in the preclinical and clinical settings to help us further understand the epidemiology of lung cancer, the molecular biology, genetics and epigenetics of lung cancer in the context of tobacco-damaged aerodigestive tract tissue, and the anti-cancer activity of several promising new agents, and various treatment and drug delivery approaches in models of lung cancer and other aerodigestive tract tumors.				
<b>14. SUBJECT TERMS</b> Lung cancer, genetic markers, molecular epidemiology				<b>15. NUMBER OF PAGES</b> 98
				<b>16. PRICE CODE</b>
<b>17. SECURITY CLASSIFICATION OF REPORT</b> Unclassified	<b>18. SECURITY CLASSIFICATION OF THIS PAGE</b> Unclassified	<b>19. SECURITY CLASSIFICATION OF ABSTRACT</b> Unclassified	<b>20. LIMITATION OF ABSTRACT</b> Unlimited	



## TABLE OF CONTENTS

COVER.....	1
SF 298.....	2
INTRODUCTION .....	4
PROGRESS REPORT .....	5
<i>Project 1</i> .....	5
<i>Project 2</i> .....	6
<i>Project 3</i> .....	12
<i>Project 4</i> .....	14
<i>Project 5</i> .....	15
<i>Project 6</i> .....	17
<i>Project 7</i> .....	20
<i>Project 8</i> .....	27
<i>Project 9</i> .....	29
<i>Project 10</i> .....	31
<i>Core B</i> .....	33
KEY RESEARCH ACCOMPLISHMENTS .....	35
REPORTABLE OUTCOMES.....	35
CONCLUSIONS .....	36
APPENDIX .....	38



## INTRODUCTION

Lung cancer is the leading cause of cancer death for both men and women. More people die of lung cancer than colon, breast, and prostate cancers combined. In 2003, there will be about 171,900 new cases of lung cancer in the United States: 91,800 among men and 80,100 among women. About 157,200 people will die of this disease: 88,400 men and 68,800 women. About 87% of lung cancer deaths are caused by smoking. To reduce lung cancer incidence and mortality, we believe it is imperative to develop effective therapeutic approaches for patients with cancer, as well as effective cancer prevention strategies that target both current and former smokers who are at risk for development of cancer.

TARGET is focused on a series of projects designed to obtain data in the preclinical and clinical settings to help us further understand the epidemiology of lung cancer, the molecular biology, genetics and epigenetics of lung cancer in the context of tobacco-damaged aerodigestive tract tissue, and the anti-cancer activity of several promising new agents, and various treatment and drug delivery approaches in models of lung cancer and other aerodigestive tract tumors.

TARGET addresses the following specific goals:

- develop an integrated approach to study genetic susceptibility markers related to DNA repair capacity in lung cancer using both surrogate tissue and target tissue
- study the genetic instability induced by tobacco-related carcinogenesis and the effects of chemoprevention on its reversal
- identify and characterize novel biomarkers for early diagnosis of lung cancer to aid better understanding of the development and progress of lung cancer
- study the process of the hypermethylation of the promoter regions of important pro-apoptotic genes such as the death-associated protein (DAP) kinase and the p16 gene, and establish the relationship with disease-specific and overall survival in completely resected, early-stage non-small cell lung cancer in order to develop an independent molecular prognostic model utilizing these important parameters
- evaluate the effects of a histone deacetylase inhibitor on non-small cell lung cancer cell lines by studying interactions with nuclear retinoid genes, such as RAR- $\beta$ , and induction of apoptosis
- study the biological effects of the farnesyl transferase inhibitor SCH66336 on signal transduction and induction of apoptosis in aerodigestive tract cancer models
- better understand the global molecular changes in cellular responses and tumor suppressor gene FUS1 in order to elucidate its molecular mechanisms in lung cancer and thereby develop a gene replacement strategy using a FUS1-lipoplex in experimental mouse models of lung cancer
- characterize the potential efficacy of bcl-xl on human non-small cell lung cancer cell lines and develop a bcl-xl antisense adenoviral vector whose therapeutic effects will be tested in animal models of non-small cell lung cancer
- develop perfluorocarbon-mediated gene transfer to allow repeated gene transfer through reduction and mechanical disruption of the humoral response
- develop and validate different anti-angiogenic therapeutic approaches in lung cancer utilizing both orthotopic and metastatic lung cancer models in mice and identify optimal combinations in sequences of anti-angiogenic agents while studying surrogate markers for their response



## **PROGRESS REPORT**

### **Project 1                      Molecular Epidemiology of Lung Cancer**

**Principal Investigator: Margaret Spitz, M.D., M.P.H.**

#### **Specific Aim 1                      Create a specimen and data resource.**

We will enroll (over two years) a consecutive series of 100 lung cancer cases of any histology, age, gender and ethnicity, undergoing thoracotomy for definitive therapy. These patients will have detailed epidemiologic risk assessments including tobacco exposure, dietary intake and family history. Blood samples, bronchial washings and bronchial biopsies will be obtained on each patient.

**Update:** After receiving DoD approval of LAB03-0382 on May 12, 2003, the protocol was subsequently activated and the first patient was enrolled in June. Total patients registered to date are seven. All underwent lung resections for non-small cell lung cancer. We collected bronchial and buccal brushes, blood, interviews and questionnaires on all patients. On five of the seven patients, we retrieved normal bronchial epithelium, tumor tissue, and adjacent normal tissue. We were unable to collect tissue from two cases due to the surgeries being delayed into late evening hours. This is not expected to be a common occurrence.

#### **Specific Aim 2                      Determine the genetic susceptibility profile in surrogate tissue.**

We will perform a panel of genotypic (select polymorphisms in DNA repair genes) and functional (DNA repair capacity, mutagen sensitivity, and COMET) assays of genetic susceptibility on peripheral lymphocyte DNA from the 100 patients identified in Specific aim 1.

**Update:** All assays are established and ready to be run.

#### **Specific Aim 3                      Determine the genetic susceptibility profile in target tissue**

We will establish bronchial epithelial cell cultures from fresh tumor specimens at thoracotomy of the 100 lung cancer patients from Specific Aim 1 and perform, in parallel, phenotypic DNA repair capacity and mutagen challenge assays.

We will compare, using FISH analyses, the rate of concordance of DNA deletions at 3p21.3 and 10q22 loci in cells obtained from bronchial washings and peripheral lymphocyte cultures of 50 patients.

**Update:** DNA repair assay and FISH assay have been tested on epithelial cell cultures obtained from Dr. Lotan's lab.

We proposed to investigate the expression and regulation of the biomarkers in bronchial epithelial cells in cultures and to address whether the molecular alterations are persistent during development and differentiation of bronchial epithelium of the lung cancer patients. The source for epithelial cells is from bronchial biopsy tissues collected from the lung cancer patients who are undergoing surgery at M. D. Anderson Cancer Center, as described in Specific aim 1. So far, we have obtained 5 bronchial tissue specimens from surgically removed lung sections of 5 different patients, as described in Project 1. Bronchial epithelial cells from the 5 tissue specimens were successfully isolated and stored for further characterization. As soon as



characterization of the cells is completed, portions of the cells will be used for studies proposed in Project 3, Specific Aim 4 (Dr. Koo), and also distributed to Dr. Wu's and Dr. Wei's laboratories for their proposed studies on DNA repair capacity and mutagen sensitivity.

#### **Specific Aim 4      Assess concordance of findings in paired samples**

**Update:** As a pilot study, we compared telomere length in paired lymphocytes and bronchial brushings from the affected and unaffected sides of 20 patients with lung cancer (Table 1). Spearmans' correlation coefficients showed a significant close correlation between data from lymphocytes and bronchial brushings on normal side. This is important since PBLs are surrogate tissue and we do not know whether they reflect events in target tissue. We also find that there is no correlation between data from lymphocytes and bronchial brushings on tumor side. This is expected, since telomerase activity might be activated on tumor side.

**Table 1. Correlations between lymphocytes and brushings**

	<b>N</b>	<b>Correlation Coefficient</b>	<b>P value</b>
Lymphocytes/Brushings normal side	18	0.767	0.0002
Lymphocytes/Brushings tumor side	20	0.243	0.3030
Brushing normal /Brushings tumor side	18	0.644	0.0039

#### **Project 2      Genetic Instability by Smoking Status**

**Principal Investigator: Walter Hittelman, Ph.D.**

**Specific Aim 2.1      Determine the optimal conditions for detecting clonal changes using inter-simple sequence repeat PCR (Inter-SSR PCR). Standardize and validate inter-SSR PCR for application to bronchial biopsy specimens**

Our initial studies had suggested the inter-SSR PCR could be used to sensitively detect the presence of clonal outgrowths in small tissue specimens. The goal of this first Specific Aim was to improve the technology for use on tissue sections and to determine the sensitivity and reproducibility of this technique for detecting clonal and subclonal lung cell populations.

In order to make our analyses more amenable to quantification, we explored the use of fluorescence-labeled primers and then visualization and quantification of the PCR-derived bands on gels using the ABI 377 sequencer. A typical output of a run is shown in Figure 1 where reference markers are included to better carry out size determinations of the detected band peaks. The gels are scanned during the run and each lane's results can be plotted as a line plot.



One of the first tasks toward standardization was to identify the optimal PCR conditions for optimal visualization of product bands. These studies involved testing a variety of variables, including primer concentration,  $Mg^{2+}$  concentration, dNTP concentrations, and PCR reaction temperatures and cycle durations. The results shown in Figure 2 illustrate some results of this optimization process.

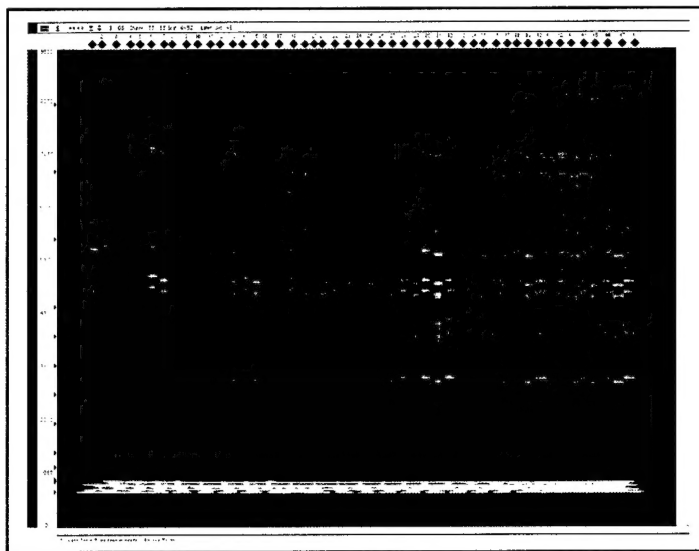
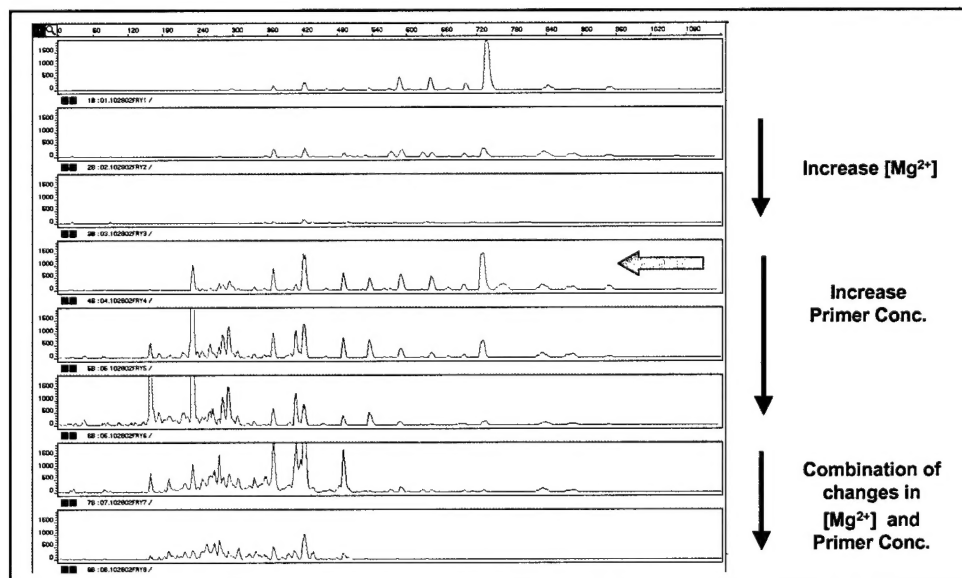


Figure 1. Illustration of typical output of a gel run of PCR products on the ABI 377 sequencer. The blue products are from the PCR reaction and the red products are the size references.

Figure 2.  
Optimization of the  
conditions of inter-  
SSR PCR for DNA  
fingerprinting.



To determine the reproducibility of the system in terms of parallel gel runs, we aliquoted the product of one PCR reaction into different lanes and checked for reproducibility of peak locations and amount (i.e., DNA fingerprints). As shown in Figure 2, the ABI 377 sequencer showed considerable reproducibility in parallel gel runs as seen by the superposition of patterns from different lanes.



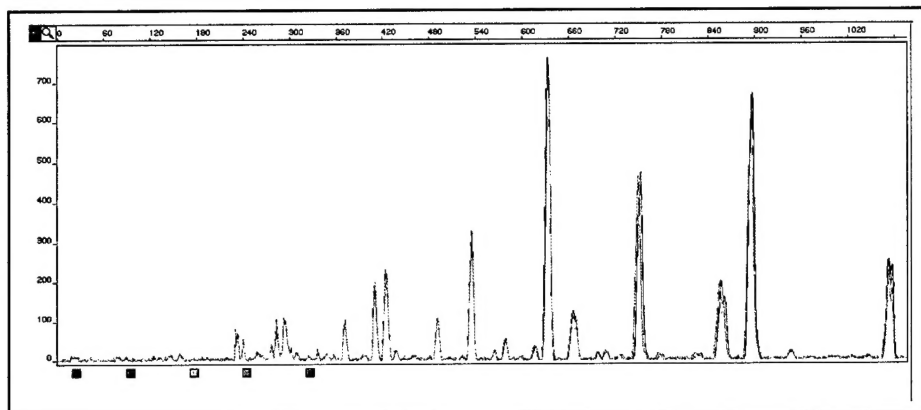


Figure 3. Superposition of results of aliquots of a PCR product run in different lanes

To determine the reproducibility of the PCR reaction under these conditions, we next took one DNA sample and aliquoted the sample into three portions, carried out parallel PCR reactions, and ran the PCR products in different gel wells on the ABI 377 sequencer. As shown in Figure 4, the results of different PCR reactions produced nearly identical DNA fingerprints.

Now that we had optimized the Inter-SSR PCR reaction for ABI 377 sequencer analysis, we wanted to determine whether this fingerprinting technique could detect cumulative clonal changes in lung cells as they progressed toward a malignant phenotype. For this purpose, we

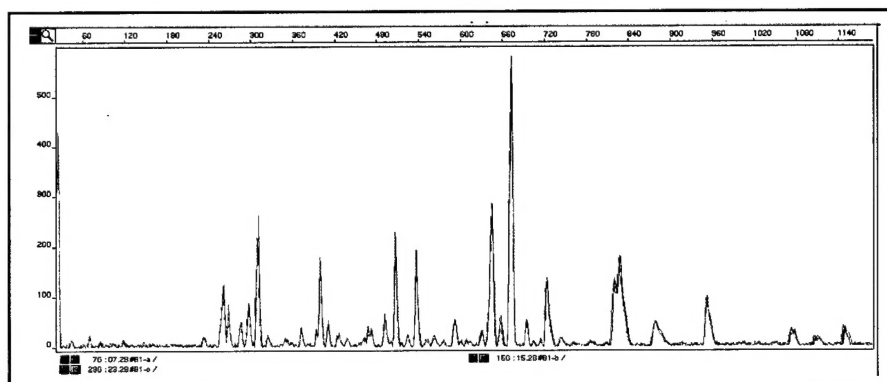


Figure 4. DNA fingerprints of repeat PCR products from the same DNA isolate

utilized a series of cell lines originally developed by Klein-Szanto whereby normal human bronchial epithelial cells were immortalized with SV40 (BEAS2B cells), allowed to grow in rat tracheal lining (1799 cells), and then treated with tobacco smoke condensate to generate non-tumorigenic (1198) and tumorigenic (11701) lines. As shown in Figure 5 and Table 1, inter-SSR PCR analysis of these cell lines demonstrated cumulative band changes as cells progressed toward the malignant phenotype.



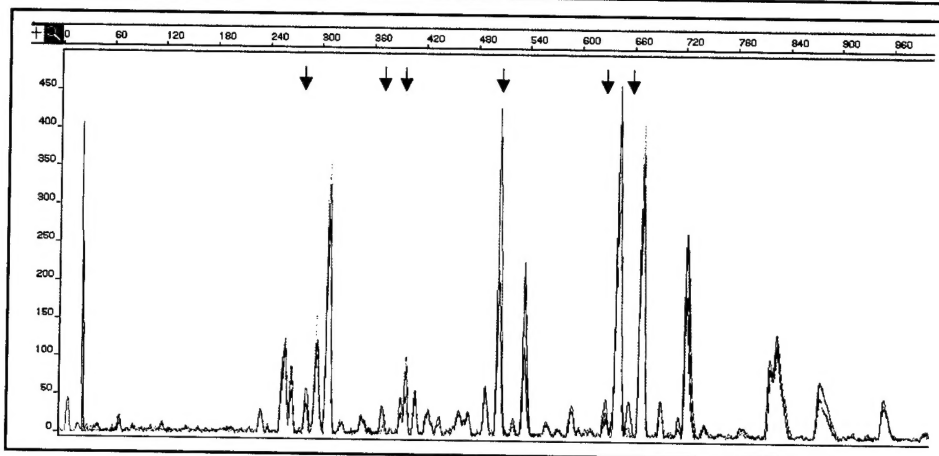


Figure 5: DNA fingerprints of BEAS2B (black), 1198 (green), 1799 (blue), and 1170I (red) cell populations. Arrows indicate band changes.

Cell Lines	Fam-(CA) <sub>n</sub> RG		Hex-(CA) <sub>n</sub> RY		Total
	Total # of bands	Result (# diff bands)	Total # of bands	Result (# diff bands)	
Beas 2B	51	0	21	0	0
1799	50	7 335L, 340L, 360L, 415L, 445g, 455g, 500g	20	2 540g, 660L	9
1198	51	6 335L, 340L, 360L, 415L, 455g, 500g	20	4 540g, 660L, 675L, 720g	10
1170I	50	7 335L, 340L, 360L, 445g, 455g, 470g, 500g	20	5 400L, 505g, 540g, 675L, 720g	12

Table 1. DNA fingerprint band changes during progression of lung cell lines from immortalized BEAS2B cells to 1170I tumorigenic cells.

To determine the sensitivity of Inter-SSR PCR for detecting subclonal variants, we subcloned the BEAS2B line into monoclonal outgrowths. We then chose two clones that differed in two bands (Figure 6) and then mixed their DNAs in different ratios prior to inter-SSR PCR analysis. As shown in Figure 7, subclonal variants occupying 25% of the population could be detected by this approach. We plan to carry out more quantitative assessments of standard deviations to better estimate the sensitivity of the technique to detect the presence of smaller subclonal variants.

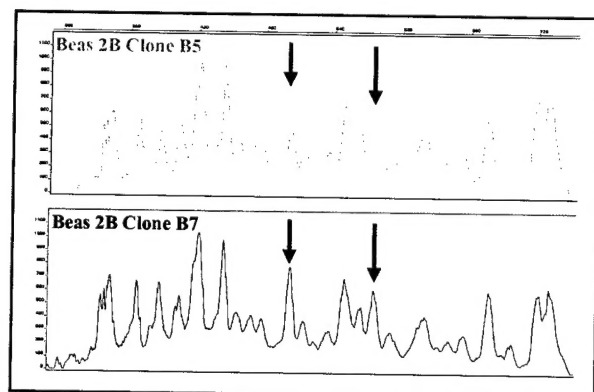


Figure 6. DNA fingerprints of two BEAS2B subclones with differing bands.

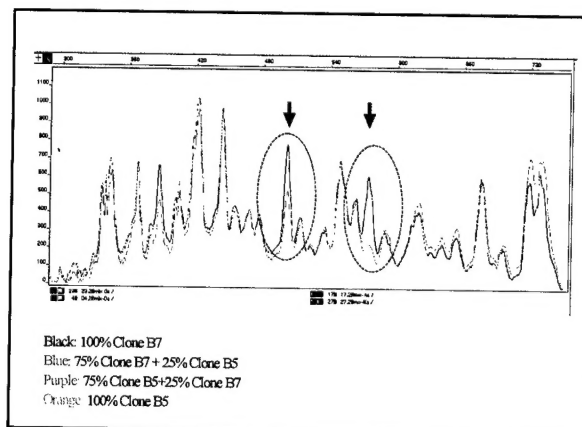


Figure 7: DNA fingerprints of mixtures of BEAS2B clones in different proportions.



Since our long term goal is to better understand how genetic instability leads to subclonal outgrowths in lung tissue, we were interested in comparing the degree of subclonal variation in immortal BEAS2B cells and tumorigenic 1170I cells. To this end, we isolated monoclonal fractions from each cell line and carried out inter-SSR PCR on each clonal outgrowth. As shown in Tables 2 and 3, both cell lines showed the presence of subclonal populations. However, as shown in Figure 8, the tumorigenic 1170I cell population had a higher level of clonal variation than did the immortal BEAS2B cell line. Interestingly, a significant fraction of the subclones from each cell line exhibited common individual bands that were not evident in the bulk population, suggesting some clonal selection in the setting of monoclonal outgrowth in multiwell cultures. A repeat study where monoclonal outgrowths were generated and analyzed by inter-SSR PCR showed a similar phenomenon, however the particular bands selected appeared different from the first study suggesting that the culture conditions can influence which subclones in the population are selected.

Table 2: Subclonal changes in BEAS2B cells

Beas 2B		Fam-(CA) <sub>n</sub> RG	Hex-(CA) <sub>n</sub> RY	Total # Change
Serial	Clone #	Result (# diff bands)	Result (# diff bands)	
1	B1	520L, 840L	0	2
2	B2	0	960g	1
3	B3	0	0	2
4	B5	590g, 700g	400g, 960g	3
5	B6	700g	400g, 960g	7
6	B7	520L, 590g, 700g, 840L	300L, 400g, 960g	3
7	B11	700g	400g, 960g	6
8	B13	590g, 700g, 840L, 900L	400g, 960g	5
9	B14	700g, 840L, 900L	400g, 960g	3
10	B15	700g	400g, 960g	3
11	B16	700g	400g, 960g	4
12	B17	700g	400g, 670g, 960g	8
13	B18	0	400g, 650L, 960g	3
14	B19	560g, 590g, 680L, 700g, 840L	400g	2
15	B20	680L, 700g	400g, 670g	4
16	B21	700g	400g	2
17	B22	590g, 700g	400g	3
18	B23	700g	400g	2
19	B24	590g, 700g	400g	2
20	B25	700g	400g	3
21	B29	560L, 700g	400g	5
22	B30	700g	400g, 480g, 700g, 960g	5
23	B32	650L, 700g	400g, 670g, 960g	2
24	B33	0	400g, 960g	3
25	B34	700g	400g, 670g	4
26	B36	700g	400g, 670g, 960g	3
27	B37C	700g	400g, 670g	6
28	B39	700g	305L, 310L, 400g, 650L, 670g	4
29	B41	700g	305L, 310L, 400g	

Table 3. Subclonal changes in 1170I cells

1170I		Fam-(CA) <sub>n</sub> RG	Hex-(CA) <sub>n</sub> RY	Total Changes
Serial	Clone #	Result (# diff bands)	Result (# diff bands)	
1	1	560L, 730g, 910g, 980g	670g, 610g, 830g	7
2	2	335g, 365g, 405g, 415g, 435g, 490g	670g	7
3	3	0	670g	1
4	4	560g, 720g, 730g, 910g, 980g	0	5
5	5	720g, 730g, 910g	400g, 670g, 810g, 830g	7
6	6	720g, 730g, 910g	0	3
7	7	560g, 730g, 910g, 980g	0	4
8	8	345g, 365g, 500g, 720g, 730g	640g, 670g	7
9	9	120g, 335g, 370g, 380g, 420L, 620L	0	6
10	11	365g, 415g, 435g, 490g	670g	5
11	12	335g, 345g, 730g	670g	4
12	13	730g	670g	2
13	14	720g, 730g, 910g	670g	4
14	15	345g	400g, 505L, 670g, 810g, 820g	8
15	16	335g, 365g, 410g, 435g, 490g	400g, 505L, 670g, 810g, 820g	10
16	17	335g, 340g, 345g, 380g, 390g, 840L, 910L	0	7
17	18	0	670g	1
18	19	720g, 730g	400g, 505L, 670g, 810g, 820g	7
19	20	720g, 730g, 910g	400g, 670g, 810g, 820g	7
20	21	730g, 910g, 980g	670g, 810g, 820g	6
21	22	345g, 730g	505L, 670g	4
22	23	730g, 980g	670g	3
23	24	0	670g	1
24	25	0	670g	1
25	26	0	665g, 670g	2
26	27	345g	505L, 670g	3
27	28	345g	665g, 505L, 670g	4
28	29	0	670g	1
29	30	810L	400g, 810g, 820g	4
30	31	345g, 460g, 500L, 910L	400g, 505L, 670g, 810g, 820g	9
31	32	345g	500g	2
32	33	345g	0	1
33	34	345g	505L	2
34	35	500L	505L, 670g	3
35	36	0	500g	1
36	37	0	0	0
37	38	0	670g	1
38	39	0	670g	1
39	40	0	505L	1
40	41	345g	505L, 670g	3
41	42a	345g	0	1
42	43a	0	0	0
43	44	365g	0	1

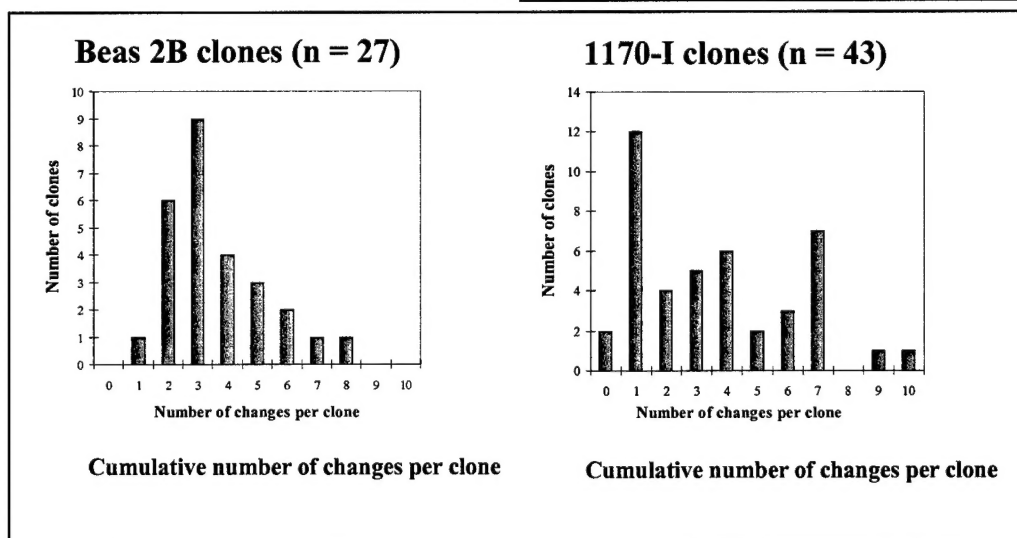


Figure 8. Clonal variation frequencies in BEAS2B and 1170I cell populations as assessed by inter-SSR PCR. Note increased numbers of 1170I subclones with high numbers of band changes from the bulk population.



We have now initiated studies to determine our ability to carry out inter-SSR PCR analysis on cells dissected from paraffin embedded specimens. The first studies will be carried out on cell culture pellets that have been formalin-fixed and embedded in paraffin. Once the technology is worked out in this setting, we will move to analysis of microdissected bronchial biopsy specimens.

**Specific Aim 2.2      Determine whether smoking status influences changes in clonal frequency and determine whether chemopreventive intervention has differential impact on clonal outgrowths in current and former smokers**

The initiation of these studies awaits the completion of Specific Aim 2.1 where we will standardize and validate inter-SSR PCR for use on bronchial biopsy specimens.

Abstract: Lu T and Hittelman WN. Assessment of subclonal evolution in human bronchial epithelial cell lines progressing toward malignancy by fluorescence inter-simple sequence repeat PCR. Proc AACR 44:894, 2<sup>nd</sup> ed., 2003.



### **Project 3      Epithelial Biomarkers of Lung Cancer: Evaluation of Airway Secretions to Study Lung Carcinogenesis**

**Principal Investigator: Ja Seok Koo, Ph.D.**

**Specific Aim 1      Identify proteins whose secretion or release is different in squamous metaplastic tracheobronchial epithelial cells as compared to normal mucous epithelial cells**

Phenotypes of the cultures of primary normal human tracheobronchial epithelial (NHTBE) cell are dependent on retinoic acid (RA) when the cultures are maintained in air-liquid interface (ALI) culture method. Cultures maintained in RA-sufficient media generate a fully-differentiated mucociliary bronchial epithelium mimicking *in vivo* tracheobronchial epithelium, in contrast the cultures become squamous metaplasia in RA-deficient media. To identify proteins whose secretion or release is different in squamous metaplastic tracheobronchial epithelial cells as compared to normal mucous epithelial cells, apical surface liquid (ASL) from the NHTBE cell cultures grown in RA-sufficient (mucous) or RA-deficient (squamous) media were collected by apical washing with PBS. Protein profiles of the ASL from the squamous metaplastic NHTBE were analyzed by two dimensional polyacrylamide gel electrophoresis (2-D PAGE). Initial identification of protein spots on the 2-D PAGE was performed by matrix assisted laser desorption/ionization-time of flight-mass spectrometry (MALDI-TOF) and nanoelectrospray-tandem mass spectrometry (nES-MS/MS) analysis in collaboration with Proteomics Core Facility in our institution. The data are shown in Table 1.

**Specific Aim 2      Identify and characterize abnormal proteins secreted by lung squamous cell carcinomas**

This study is scheduled in Year 2.

**Specific Aim 3      Evaluate the efficacy of these differently-secreted proteins to serve as novel biomarkers using readily-accessible clinical specimens**

This study is scheduled in Year 3.

**Specific Aim 4      Establish primary bronchial epithelial cells in culture and evaluate the expression of candidate biomarkers in bronchial epithelium of lung cancer patients.**

We proposed to investigate the expression and regulation of the biomarkers in bronchial epithelial cells in cultures and to address whether the molecular alterations are persisted during development and differentiation of bronchial epithelium of the lung cancer patients. The source for epithelial cells is from bronchial biopsy tissues collected from 100 newly diagnosed, and previously untreated lung cancer patients who are undergoing surgery at M. D. Anderson Cancer Center, as described in Project 1 (PI: Margaret Spitz) of the TARGET program. So far, we have obtained 5 bronchial tissue specimens from surgically removed lung sections of 5 different patients, as described in Project 1. Bronchial epithelial cells from the 5 tissue specimens were successfully isolated and stored for further characterization. As soon as characterization of the cells is completed, portions of the cells will be used for studies proposed in the Specific Aim 4 and also distributed to Dr. Spitz's laboratory for their proposed studies.



Fig. 1. 2-D PAGE analysis of the ASL from squamous metaplastic NHTBE cell cultures.

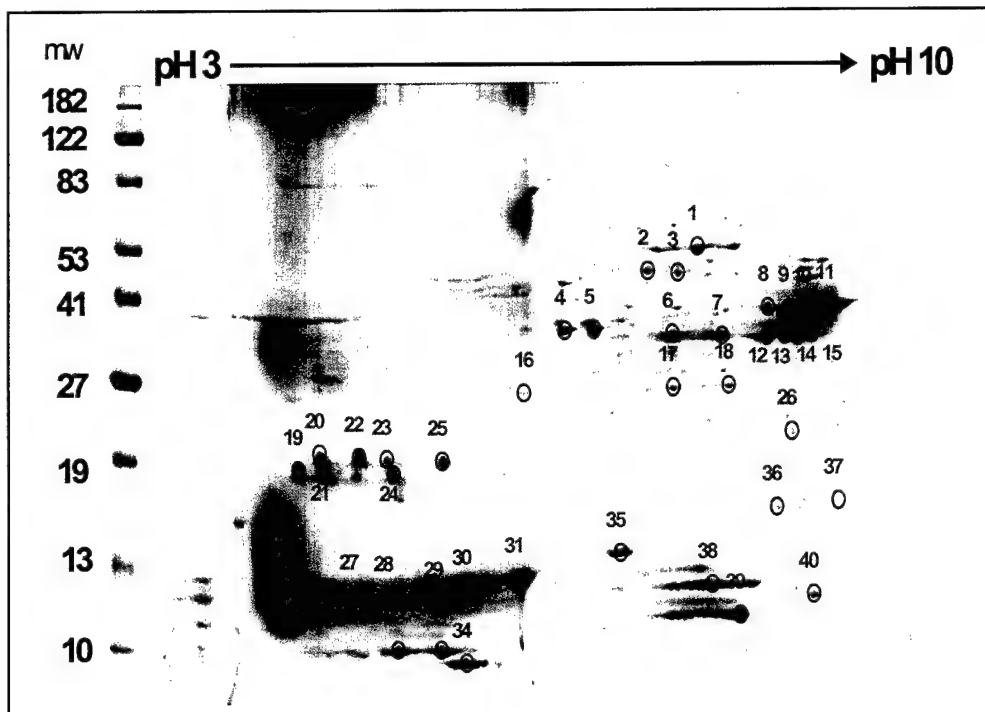


Table 1. Identification of protein in the apical surface liquid from squamous NHTBE cells using 2-D PAGE and MALDI-MS spectrophotometry.

Spot #	Protein ID	Accession Number	MW (Da)	pI
1	$\alpha$ -enolase	P06733	47169	7.0
2 - 5	Squamous cell carcinoma antigen 1	P29508	44565	6.3
6 - 7, 12 - 15	Annexin 1	P04083	38715	6.6
8 - 11	Glyceraldehyde 3-phosphate dehydrogenase	P04406	36054	8.6
16	Unknown			
17 - 18	Triosephosphate isomerase (TIM)	P00938	2667	6.4
19	MAGUK P55 subfamily member 2 (MPP2 protein)	Q14168	64614	6.3
20	Unknown			
21 - 22, 27, 29	Cystatin A (Stefin A)	P01040	11007	5.4
23	Glycodelin precursor (GD)	P09466	20624	5.4
24	Unknown			
Spot #	Protein ID	Accession Number	MW (Da)	pI
25, 28	Camitine O-palmitoyl transferase 1	P50416	88429	8.8
26	ADP-ribosylation factor-like protein 6	Q9H0F7	21098	8.7
30 - 31	Calgranulin B	P06702	13242	5.7
32	Defensin 6 precursor	Q01524	10975	5.2
33	Calcyclin	P06703	10180	5.3
34	Ubiquitin	P02248	8565	6.6
35	Unknown			
36	G-substrate	Q96001	17852	8.5
37	Unknown			
38	Bifunctional methylenetetrahydrofolate dehydrogenase/cyclohydrolase	P13995	37321	8.9
39	Diacylglycerol kinase, beta	Q9Y6T7	90596	8.1
40	D-beta-hydroxybutyrate dehydrogenase, mitochondrial precursor (BDH)	Q02338	38303	8.9



## **Project 4     Prognostic Role of Promoter Hypermethylation of Death-Associated Protein (DAP) Kinase and p16 Genes in Early-Stage Non-Small Cell Lung Cancer**

**Principal Investigator: Charles Lu, M.D.**

- Specific Aim 1        To examine the relationship between hypermethylation of the death-associated protein (DAP) kinase gene promoter and disease-free, disease-specific, and overall survival in completely resected, early-stage NSCLC**
- Specific Aim 2        To examine the relationship between hypermethylation of the p16 gene promoter and disease-free, disease-specific, and overall survival in completely resected, early-stage NSCLC**
- Specific Aim 3        To examine the relationship between hypermethylation of the p16 gene promoter and history of tobacco smoke exposure in early-stage NSCLC**
- Specific Aim 4        To determine the independent prognostic significance of these two molecular biomarkers after adjusting for relevant clinicopathologic variables (T-stage, N-stage, age, gender, histology, type of surgery, performance status, weight loss, smoking status)**

The specific goal of this research proposal is to determine the prognostic importance of promoter hypermethylation of selected candidate genes in patients with early-stage, resected NSCLC who have been followed as part of a clinical research database. This study will create a high-quality database that includes clinical information in addition to surgical pathology specimens.

Subjects in this study are identified from a clinical research database of patients who have undergone surgical resection by faculty members of the Department of Thoracic and Cardiovascular Surgery, The University of Texas M. D. Anderson Cancer Center. This database was established in 1997, and includes all patients who undergo thoracic surgical resection at M. D. Anderson Cancer Center. Detailed demographic, clinical, and pathologic data are recorded using standardized data collection forms. Follow-up clinical information is also collected at each clinic visit. Patients with completely resected NSCLC with pathologic stages I or II who do not receive post-operative adjuvant therapy (either chemotherapy or chest radiotherapy) are eligible for this protocol. The projected sample size is 300 subjects.

A query of the Department of Thoracic Surgery clinical research database yielded an initial list of 436 patients who underwent surgery between January 1, 1997 and December 31, 2000. To date the medical records of 363 patients have been screened, and 218 (60.1%) eligible subjects have been identified. Our collaborators in the Department of Pathology are reviewing these screened patients to determine if sufficient surgical tissue samples (paraffin blocks) exist to perform the required hypermethylation assays. If tissue is available, we will formally include the subject in our research study and complete the clinical data abstraction for the subject. This data set will include gender, age, tumor histology, pathologic stage, preoperative clinical variables (performance status, weight loss, smoking status), date of disease recurrence, date of death/last follow-up. Promoter hypermethylation assays will then be performed for our genes of interest, DAP kinase and p16.

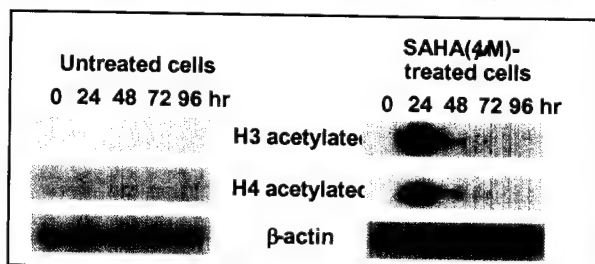


## Project 5 An Epigenetic Approach to Lung Cancer Therapy

Principal Investigator: Reuben Lotan, Ph.D.

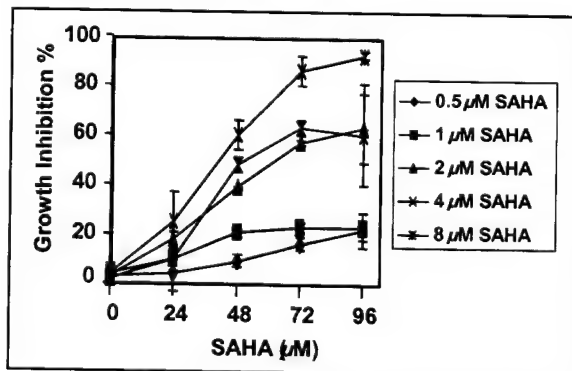
- Specific Aim 1** Determine the ability of SAHA and 5-aza-CdR used as single agents and in combination to inhibit growth and induce apoptosis in normal bronchial and small airway epithelial cells, immortalized, premalignant, transformed and tumorigenic lung cells, and several established non-small cell lung cancer cell lines *in vitro*
- Specific Aim 2** Explore the mechanisms of interactions between SAHA and 5-aza-CdR
- Specific Aim 3** Determine the ability of SAHA, 5-aza-CdR and their combinations to inhibit the growth of human NSCLC cells implanted subcutaneously in athymic nude mice
- Specific Aim 4** Investigate the mechanisms of *in vivo* activity, especially those related to inhibition of cell growth and induction of apoptosis

During the last year, we have made progress in specific aim 1. First, we found that the histone deacetylase inhibitor SAHA increased transiently the acetylation of both histones H3 and H4 in the NSCLC cell line CALU-1 (Fig. 1). Similar results were obtained in other NSCLC cells (not shown). The increase was detected by 24 and subsided by 72 hr.



**Fig. 1.** Calu-1 cells were treated with 4  $\mu$ M SAHA for the indicated times and then the cells were lysed and histones were isolated by acid extraction. Acetylation was detected by Western blotting using specific anti-acetylated H3 and H4 antibodies. The membranes were reprobbed with anti-actin antibodies to control for differences in loading in different lanes.

We then explored the effects of SAHA on the growth of 5 NSCLC cell lines. We found that SAHA inhibited the growth of these cell lines with IC<sub>50</sub> at 72 hr of between 1 and 4  $\mu$ M (see an example in Fig. 2). ATRA (1  $\mu$ M) alone had only a minimal effect on the growth of these cell lines and when it was added to SAHA there was no increase in growth inhibition relative to that obtained with SAHA alone.



**Fig. 2.** H157 cells were seeded in 96 well plates and treated with the indicated concentrations of SAHA for the indicated times. The cells were harvested at 24 hr intervals and their numbers were estimated by the sulforhodamine B assay. The results are the mean  $\pm$  SD of triplicate determinations.



The H157 were resistant to 5-aza-CdR alone and even in combination with SAHA and all-trans retinoic acid (ATRA). The combinations did not give growth inhibition beyond what was observed with SAHA alone. It appears that unlike what we had observed in head and neck cancer cell lines; and others have observed in colon cancer and breast cancer, in NSCLC there is no synergistic or even additive effect of various growth inhibitors and SAHA.

**Future plans:** We will examine whether combinations of SAHA and 5-aza-Cdr or retinoic acid or both can modulate cell invasion and migration. We will also pursue in vivo studies.



## **Project 6                      The Role of the Farnesyl Transferase Inhibitor SCH66336 in Treatment of Carcinoma of the Aerodigestive Tract**

**Principal Investigator: Fadlo Khuri, M.D.**

Farnesyl transferase inhibitors (FTIs) are a new class of anticancer drugs whose mechanism of action is still incompletely understood. We were the first group to show evidence for clinical synergy between paclitaxel and lonafarnib in the clinic (1, 2).

**Specific Aim 1              Evaluate the effects of SCH66336 on Ras downstream signaling events by evaluating its effect on downstream molecules such as Raf, Erk-1/2, Akt-2, and jun-terminal kinase (jnk-1), assaying apoptosis and also examining SCH66336's effect on angiogenesis in both lung and head and neck squamous cell carcinoma cell lines**

We investigated lonafarnib (SCH66336), an FTI, in head and neck squamous cell carcinoma (HNSCC) and non-small cell lung cancer (NSCLC) cell lines. Lonafarnib treatment inhibited cell growth by inducing G2/M phase arrest. In the head and neck cancer cell line, UMSCC38, p-Raf levels were decreased after lonafarnib treatment; however, Erk1/2 activity was not modulated. In contrast, Akt protein expression was decreased and over-expressed a constitutively active Akt, partially rescued the G2/M arrest, and increased cdc2 activity. Furthermore, we found no evidence of transcriptional regulation of Akt; rather, we detected a decrease in exogenous Akt protein level, replenished by MG132, a proteasome inhibitor. In conclusion, we have evidence for a novel mechanism of action of lonafarnib in which Akt protein is degraded through a ubiquitin-based mechanism, reducing Akt expression, decreasing cdc2 activity and leading to G2/M phase cell-growth arrest (3).

Although FTIs were originally designed to target Ras activation, many studies indicate that they may inhibit cell growth and induce apoptosis independent of Ras mutation status. Thus, their action mechanisms remain largely unknown. PI3 kinase-Akt pathway has been proposed to be a target for FTI's action, but its role in mediating FTI's biological effects is still controversial. We examined the effect of lonafarnib on the growth of a panel (11) of human non-small cell lung cancer (NSCLC) cell lines and the role of the Akt pathway in mediating its growth inhibitory effects (4). Lonafarnib was effective to inhibit the growth of NSCLC cell lines, particularly after a 5-day treatment, regardless of Ras mutation status. The IC50s for a 3-day and a 5-day treatment ranged from 2.1 to 9.8  $\mu$ M and from 0.14 to 3.12  $\mu$ M, respectively. Under normal culture condition (5% serum), lonafarnib induced apoptosis only in a few cell lines but G1 or G2/M arrest in most cell lines. However, cells underwent rapid apoptosis when exposed to lonafarnib in low serum (0.1%) culture medium. The majority of NSCLC cell lines expressed an undetectable level of active or phospho-Akt (p-Akt). Lonafarnib at up to 10  $\mu$ M did not decrease either the Akt level or the p-Akt level in any of the tested cell lines, even after 48 h treatment. Unexpectedly, lonafarnib increased p-Akt level in one cell line, which, however, was as sensitive as the other cell lines to lonafarnib treatment and underwent G2/M arrest. The PI3 kinase inhibitor LY294002 at 10  $\mu$ M decreased the p-Akt level but failed to induce apoptosis. It suppressed elevated p-Akt by 1 or 5  $\mu$ M lonafarnib but failed to enhance the effect of lonafarnib on induction apoptosis. Although 10  $\mu$ M LY294002 in combination with 10  $\mu$ M lonafarnib did synergistically induce apoptosis, the p-Akt level remained increased. Therefore, we conclude that Akt is not likely to be a target for lonafarnib's effect on growth arrest and apoptosis induction in human NSCLC cells. This is further supported by our finding that addition of 0.15% bovine serum albumin (BSA), which approximately equals the protein amount in 5% serum,



prevented cells from apoptosis, which occurred in 0.1% serum medium. This result clearly indicates that low serum conditions enhance the effect of lonafarnib on induction of apoptosis by simply increasing its intracellular concentration due to less binding of lonafarnib to protein rather than inactivating PI3 kinase-Akt survival pathway.

**Specific Aim 2      Evaluate the effects of SCH66336 on protein expression in both lung and head and neck cancer cell lines by identifying proteins whose expression is altered by treatment with SCH66336 and determining the role of these proteins as biomarkers and effectors of response to treatment with farnesyl transferase inhibitors**

We also investigated the effect of lonafarnib on modulation of proteins in head and neck cancer. We found that several proteins are upregulated and others downregulated by FTI. To reveal novel mechanisms of FTI induced tumor growth inhibition or induction of apoptosis, we performed two-dimensional electrophoresis (2-DE) and mass spectrometry to identify differentially expressed proteins after lonafarnib treatment (5). We visualized over 500 proteins were visualized using colloidal coumassie blue staining. Thirty five differentially expressed proteins were found compared to the protein expression profile of the untreated control. The identity of twenty-two of the 35 proteins were obtained through mass peptide fingerprinting. All of the proteins identified were unlikely to be direct substrates of farnesyl transferase because they lack a CAAX motif, and include (1) heat shock proteins, (2) receptors, (3) binding proteins, (4) enzymes and (5) proteins with unknown properties. Further studies to identify their function and significance are ongoing.

**Specific Aim 3      Evaluate the efficacy of SCH66336 as an inhibitor of growth and as an inducer of apoptosis in an orthotopic model of head and neck squamous cell carcinoma, where we can obtain serial tissue to evaluate changes in cell signaling, induction of apoptosis and inhibition of angiogenesis**

To be carried out years 2 and 3 of the TARGET Grant.

**Specific Aim 4      Expand on our preliminary data to focus on the underlying mechanisms by which farnesyl transferase inhibitors induce apoptosis in combination with retinoids such as 4-HPR, or taxanes such as docetaxel or paclitaxel, in non-small cell lung cancer and squamous head and neck cancer cell lines**

To be carried out years 2 and 3 of the TARGET Grant.

In summary, lonafarnib is active in inducing growth arrest and apoptosis in human NSCLC and HNSCC cells, through mechanisms independent of Ras mutation and Akt activation in NSCLC. This suggests a completely novel, Akt-independent mechanism of action for these compounds in lung cancer, unlike our previous data generated with head and neck cell lines.

#### **Publications:**

1. Khuri FR, Glisson BS, Kim ES, Meyers ML, Herbst RS, Thall PF, Munden RF, Statkevich YP, Bangert S, Thompson E, Cascino M, Shin DM, Papadimitrakopoulou V, Kurie JM, Kies MS, Lee JS, Fossella FV, Hong WK. Phase I study of farnesyl transferase inhibitor



- (FTI) SCH66336 with paclitaxel in solid tumors. *Journal of Clinical Oncology*, submitted 2003.
2. Kim ES, Kies MS, Fossella FV, Glisson BS, Zaknoen S, Baum CM, Summey C, Lu C, Papadimitrakopoulou V, Hong WK, Khuri FR. Phase II study of the farnesyltransferase inhibitor (FTI) lonafarnib with paclitaxel in patients with taxane-refractory/resistant non-small cell lung cancer. *Journal of Clinical Oncology*, submitted 2003.
  3. Hassan KA, Lee H-Y, Kim E, Bishop WR, Kirschmeier P, Mao L, Khuri FR. A novel mechanism of farnesyltransferase inhibitor (SCH66336) arresting head and neck squamous cell carcinoma cells. *Proceeding of the American Association for Cancer Research*, 44, abstract #800, pp. 156, 2003.
  4. Sun S-Y, Zhou Z, Wang R, Khuri FR. Akt is not a target for the growth inhibition and apoptosis induction by the farnesyltransferase inhibitor SCH66336 in human lung cancer cells. Manuscript in preparation.
  5. Wu W, Hassan KH, Hong WK, Mao L, and Khuri FR. Proteomic identification of proteins associated with farnesyltransferase inhibitor treatment. *Proceeding of the American Association for Cancer Research*, 43, abstract #4667, pp. 943, 2002.



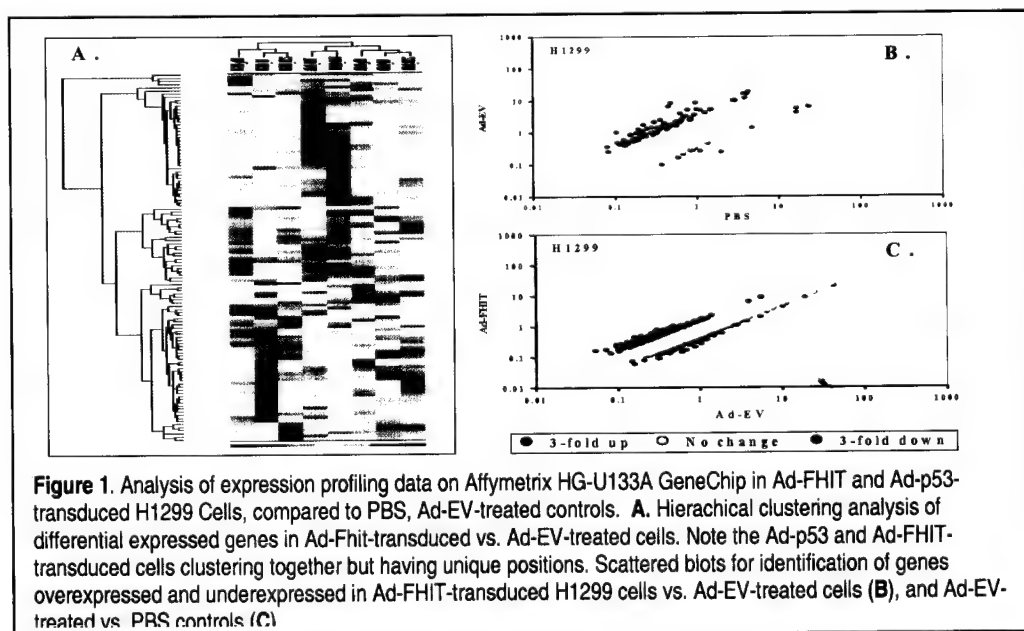
## Project 7      Mechanisms and Therapeutic Applications of the Tumor Suppressor Gene *FUS1* in Lung Cancer

Co-Principal Investigators: Lin Ji, Ph.D.  
Rajagopal Ramesh, Ph.D.

**Specific Aim 7.1      To determine the global molecular changes and cellular responses to *FUS1*-mediated tumor-suppressor activities in human NSCLC cells by high throughput gene and protein expression profiling.**

The advanced technologies of functional genomics—DNA microarrays and ProteinChip arrays—and a novel, inducible expression system are used to determine the gene and protein expression patterns mediated by overexpression of *FUS1* in Ad-*FUS1*-transduced NSCLC cells or by expression of *FUS1* at a physiological level. The specific targets of *FUS1* will be identified by comparison of the gene and protein expression profiles, and proteins of interest will be isolated. Since *FUS1* is a newly identified novel 3p21.3 tumor suppressor gene, and biological function and molecular mechanism of *FUS1*-mediated tumor suppressor activities are unknown, we first used the well studied p53 and a novel FHIT tumor suppressor gene (located at 3p14.2 region)-mediated tumor, suppressing activities in human NSCLC A549 and H1299 cells, as a model system for the development and validation of the technology.

In this pilot study, we used a complementary gene and protein expression profiling with DNA microarray and ProteinChip technologies, as proposed in Specific Aim 1.1, to quantitatively monitor cellular changes in gene and protein expression and discover the molecular targets of the novel FHIT TSG in non-small cell lung carcinoma (NSCLC) cells. We performed gene expression profiling analysis, using the Affymetrix HG-U133A GeneChips, in Ad-FHIT-transduced NSCLC H1299 and A549 cells, compared with those of PBS-treated mock and empty vector (Ad-EV) or Ad-LacZ-treated negative controls. A comparative analysis of the gene and protein expression profiling revealed several unique cellular targets and signaling pathways involved in FHIT tumor suppressing activity, including the significantly down-regulated expression of proteins in the Ras/Rho GTPase super-family, the cytoskeleton- and tubulin-forming components, and the growth factors and the up-regulated protein mediators in cell death and apoptosis pathways (Fig. 1 and Fig. 2). Our data demonstrated that the complementary gene and protein expression technology is a powerful tool for generation of hypothesis and for identification of specific cellular targets and signaling pathways mediated by a specific gene product in a complex biological network.





We are now using the technologies and protocols developed in this pilot study to study FUS1-mediated gene and protein modulations in lung cancer cells. We have established FUS1-stable transfectants of NSCLC cell lines, which allow us to monitor gene and protein expression changes mediated by FUS1 expression under physiological conditions (Fig. 3).

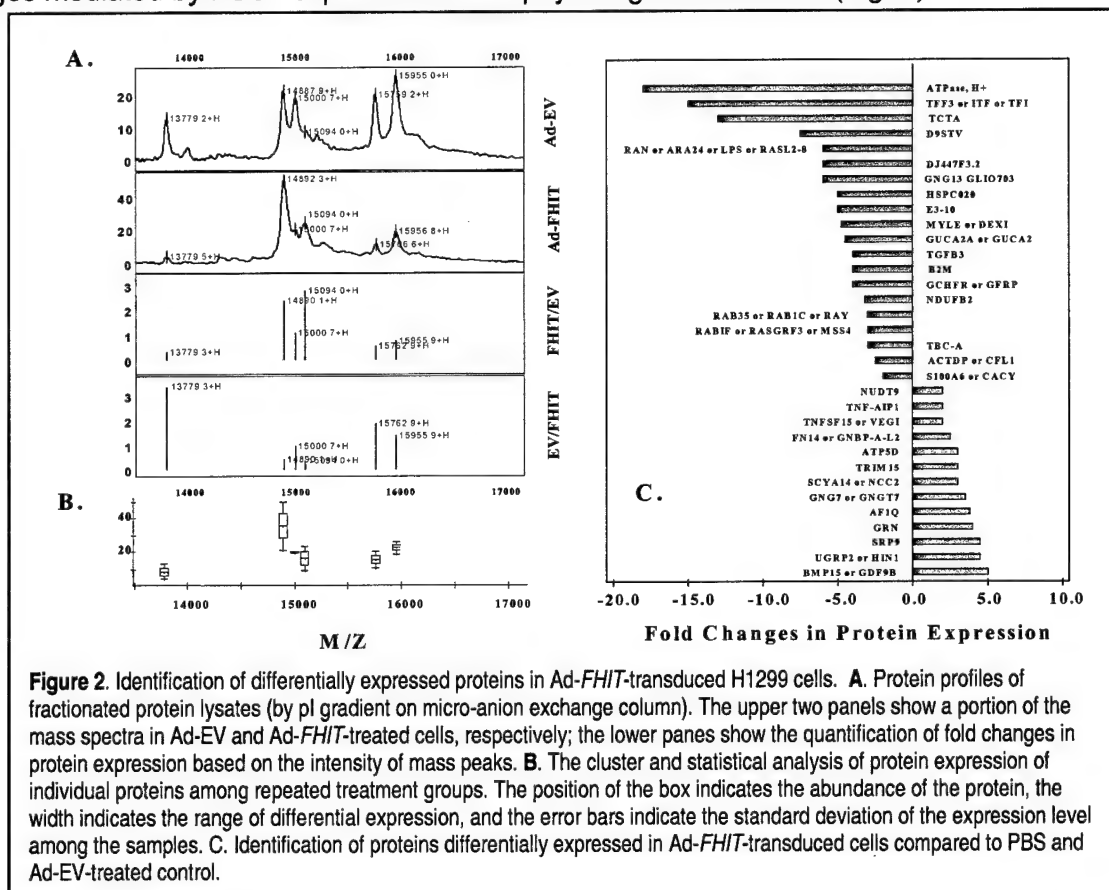
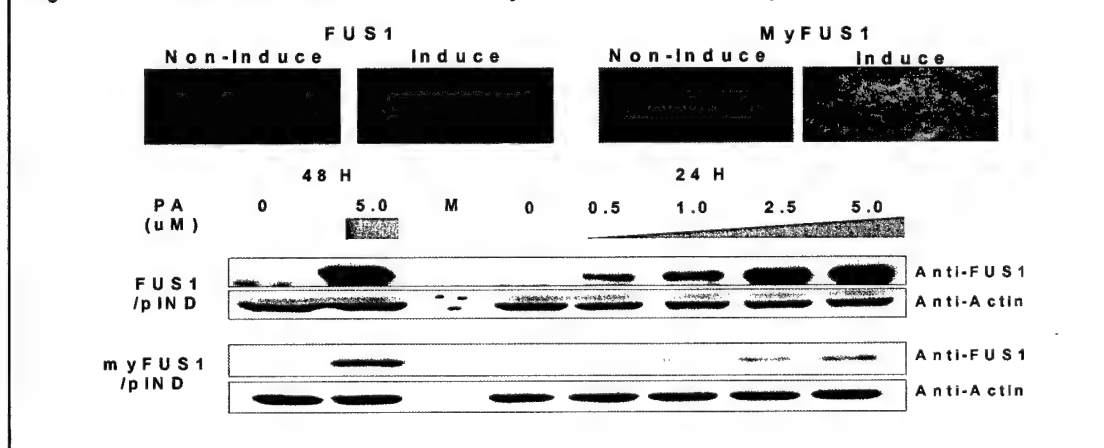


Figure 3. Establishment of FUS1/myFUS1/C-delFUS1 protein inducible clone:





**Specific Aim 7.2      To elucidate the molecular mechanism of FUS1 in lung cancer pathogenesis by determining the expression and subcellular localization of the FUS1 protein in human normal lung tissue and tumor samples at various stages of development.**

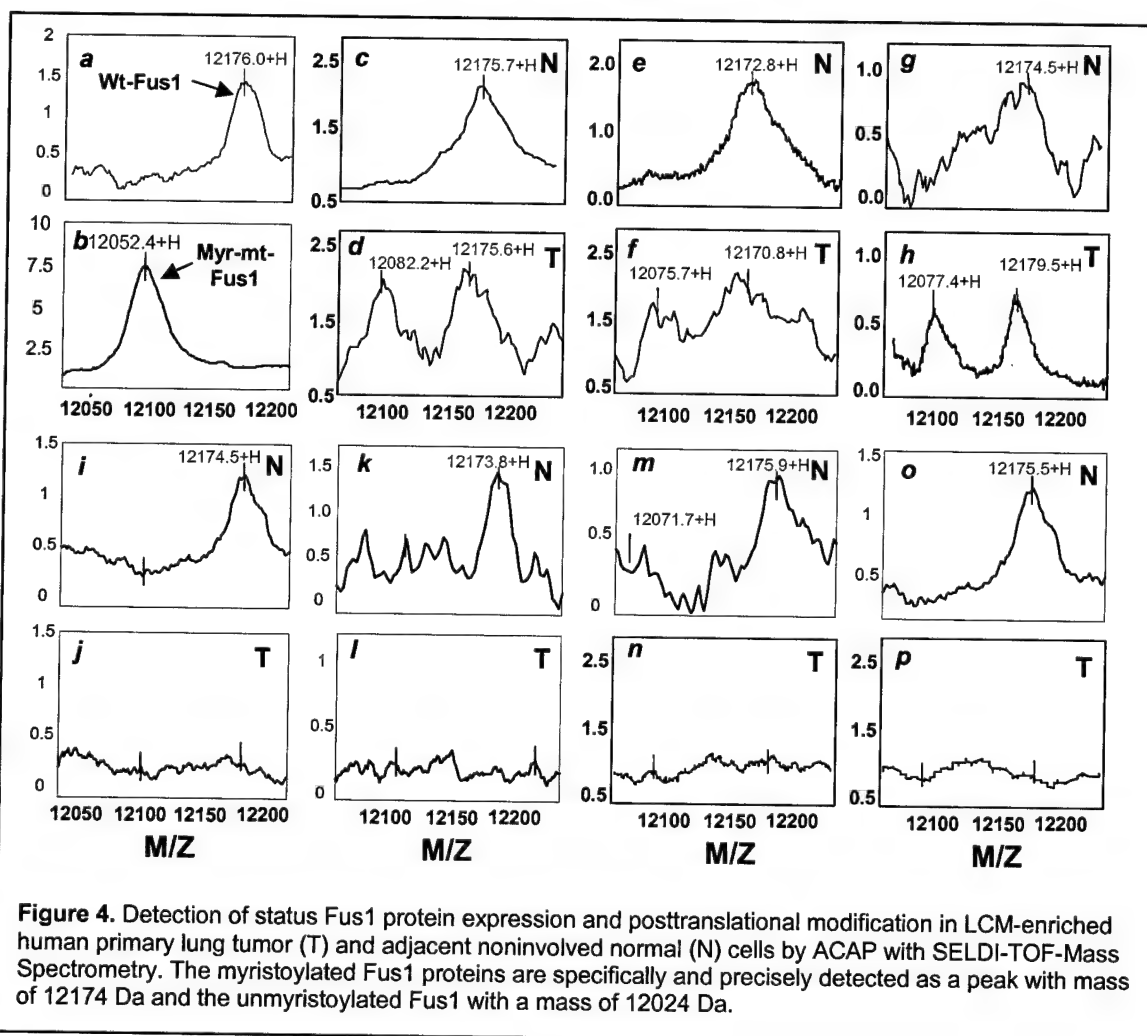
We proposed to use both conventional tissue sections and available tissue arrays to examine the *FUS1* expression and cellular localization by immunohistochemical analysis with anti-FUS1 antibodies. In our preliminary studies, we examined 40 primary lung cancers and found that mutation of the *FUS1* gene was infrequent and there were only a few nonsense mutations and a C-terminal deletion mutation that arose from aberrant mRNA splicing. In addition, we found no evidence for *FUS1* promoter region methylation (data not shown). *FUS1* expression has been detected in various normal human tissues; including brain, heart, pancreas, prostate, kidney, and lung, based on quantifying Expressed Sequence Tags (ESTs) in Unigene clusters, as summarized in GeneCards. Although endogenous *Fus1* protein expression could be detected in normal human bronchial epithelial cells and fibroblast cells (WI-38) by immunoblot analysis, and *FUS1* mRNA transcription could be seen on Northern blots of RNAs prepared from lung cancer cell lines, we could not detect endogenous *Fus1* protein in these lung cancer cell lines on immunoblots using the affinity-purified, anti-*Fus1* peptide antibodies developed. Furthermore, we performed immunohistochemical staining on a set of paired normal lung and lung cancer tissue sections. We found that normal lung epithelial cells express *Fus1*, but many lung cancer cells (15 out of 20, >70%) did not. We also found that even in those tumor samples with *FUS1*-positive staining, the staining was not uniformly detectable in all tumor cells. Based on both the lung cancer-growth suppressing properties of the *Fus1* protein in vitro and in animal models and the observed loss of protein expression in primary tumors and tumor-derived cell lines, we hypothesized that *FUS1* would have to act as a TSG in a haploin sufficient manner (since most primary lung cancers experienced allelic loss in this 3p21.3 region), and that both loss of expression and deficient posttranslational modification of *Fus1* protein might lead to loss of its tumor suppression function and lung cancer development.

Since mutation of *FUS1* is infrequent and no evidence has been found for methylation or mutation of the *FUS1* promoter region in lung cancers, other factors such as haploinsufficiency, low expression, abnormal products arising from aberrant mRNA splicing, and posttranslational modification of *Fus1* may play important roles in lung tumorigenesis. We used ACPA analysis with SELDI-TOF-MS to evaluate the protein expression and myristoylation status in primary lung tumor and uninvolved normal lung tissue samples. Molecular analysis of tumors and their precursor lesions requires the isolation of specific cell subpopulations (normal, preneoplastic, and tumors) from a composite background of multiple cell types in tumor-tissue biopsies. This was accomplished with laser-captured microdissection (LCM) technology. To evaluate *Fus1* protein expression and posttranslational modifications in human lung tumors and noninvolved tissues, we used LCM combined with appropriate tissue-preparation methods to separate and enrich tumor or noninvolved normal cells, and the resulting separated cell populations (about 500 - 1000 cells) were used for the *Fus1*-specific ACPA analysis by SELDI-TOF-MS. We found that only myristoylated protein species could be detected in normal cells (13 out of 15,  $P = 0.0003$  by a Nonparametric 2x2 contingency table, McNemar Chi-square test), but both the unmyristoylated and myristoylated *Fus1* protein were detected in tumor cells (5 out of 15 samples,  $P = 0.0442$ ) as indicated by the precise mass of *Fus1* protein on the mass spectra. The mixed status of *Fus1* protein in the tumor cells may be a reflection of the tumor-cell molecular heterogeneity. In some tumor samples (7 out of 15 samples,  $P = 0.0030$ ), neither form of *Fus1* proteins could be captured, consistent with the immunohistochemical analysis in these tumor and normal tissue samples. The remaining three samples tested were un-resolvable due to the ambiguous spectra (spectra not shown). The difference in the observed



Fus1 protein myristoylation status between the normal and the tumor cell populations is significant as indicated by a Nonparametric McNemar Marginal Homogeneity test for the equality of categorical responses from two paired and dependent populations ( $P < 0.001$ ) (Fig. 4).

To study the molecular mechanisms of FUS1 tumor suppressing activities, we used a SELDI-Mass spectrometry analysis on an anti-Fus1-antibody-capture ProteinChip array and identified wild-type Fus1 as an N-myristoylated protein. Loss of expression or a defect of myristoylation of the Fus1 protein was observed in human primary lung cancer and cancer cell lines. A myristoylation-deficient mutant of the Fus1 protein abrogated its ability to inhibit tumor cell-induced clonogenicity in vitro, to induce apoptosis in lung tumor cells, to suppress the growth of tumor xenografts and lung metastases in vivo, and rendered it susceptible to rapid proteasome-dependent degradation. Our results show that myristoylation is required for Fus1-mediated tumor-suppressing activity, and suggest a novel mechanism for the inactivation of TSGs in lung cancer and a role for deficient posttranslational modification in TSG-mediated carcinogenesis.



**Figure 4.** Detection of status Fus1 protein expression and posttranslational modification in LCM-enriched human primary lung tumor (T) and adjacent noninvolved normal (N) cells by ACAP with SELDI-TOF-Mass Spectrometry. The myristoylated Fus1 proteins are specifically and precisely detected as a peak with mass of 12174 Da and the unmyristoylated Fus1 with a mass of 12024 Da.



**Specific Aim 7.3 To quantitatively evaluate interactions of the *FUS1* gene with other 3p21.3 TSGs for their tumor-suppressing activities *in vitro* and *in vivo*.**

We propose to study the additive, synergistic, or antagonistic effects of the interactions of the *FUS1* gene with other 3p21.3 tumor suppressor genes. These interactions will be quantitatively determined using our recently developed two-dimensional (2D) and multidimensional isobologram-modeling and statistical analysis methods in Ad-3p21.3-transduced NSCLC cells *in vitro* and in Ad-3p21.3-treated lung cancer tumors in animal models. These studies are to be undertaken in years 2 and 3.

**Specific Aim 7.4 To determine the dose-limiting toxicity and biodistribution of the *FUS1*-lipoplex in a murine model and in a non-human primate model and to evaluate the therapeutic effect of the *FUS1*-lipoplex in local, solid tumors and experimental metastatic lung tumors.**

Dose-escalation studies are to be performed to determine the maximum tolerated dose (MTD), of *FUS1*-lipoplex. Biodistribution studies will be performed to determine in which tissues the transgene (*FUS1*) is expressed. Human tumor-xenograft mouse models of metastatic lung cancer will be used to assess the anticancer efficacy of *FUS1*-lipoplex treatment. For the disseminated disease model, the therapeutic effect of *FUS1*-lipoplex treatment will be measured by counting the number of pulmonary metastases and determining animal survival rates.

Construction of plasmid DNA expression vector. We have recently developed a plasmid DNA expression vector system for expressing high levels of transgene in human cells. This vector system consists of a mammalian gene-expression cassette driven by a CMV minimum promoter with an E1 enhancer at the 3' end and a BGH-poly A signal sequence at the 5' end to ensure the efficient expression of the transgene *in vivo*. The kanamycin-resistance gene was chosen as the selectable marker to avoid development of antibiotic-resistance in patients. A minimum pMB1 origin of replication (ori) sequence is used to drive high-copy replication and production of the plasmid in the bacterial host strain DH5a. The plasmid backbone is minimal to ensure a higher yield of plasmid DNA production and a higher concentration of recombinant plasmid DNA per plasmid DNA preparation. In the present proposal we intend to use this plasmid DNA vector (pLJ143/KGB) to evaluate the toxicity and therapeutic efficacy of 3p21.3 genes cloned at the multiple cloning site (mcs). Production and purification of the plasmid DNA was carried out using standard published techniques. Using this plasmid vector we assessed the expression of one of the 3p21.3 genes, *FUS1*, *in vitro* in human lung tumor cells (H1299). The expression of the *FUS1* protein in lung tumor cells was confirmed by western blot assay after transfection with DOTAP:cholesterol (DOTAP:Chol) liposome. Transfection of cells with lipoplex resulted in a strong *FUS1* specific band (14.3 kD), whereas mock transfection with PBS resulted in undetectable *FUS1* protein expression. *FUS1* protein expression was observed at 24 and 48 hours after transfection. These results demonstrated that the plasmid DNA vector is efficient in expressing the transgene.

Suppression of Tumor Growth by Intratumoral Delivery of *FUS1*-lipoplex. To test whether delivery of TSGs (*FUS1*, and p53) complexed to DOTAP:Chol-liposome (*FUS1*-lipoplex) resulted in tumor suppression *in vivo*, preliminary therapeutic studies were conducted. For this purpose human lung cancer xenografts were established in nude mice by inoculating H1299 tumor cells subcutaneously into the dorsal flanks of nude mice. In comparison with treatments with PBS or DOTAP:Chol-CAT complex, treatment with DOTAP:Chol-*FUS1* complex significantly suppressed growth of H1299 tumors ( $P < 0.01$ ) (Figure 6A). Most PBS, or



DOTAP:Chol-CAT complex treated tumor-bearing mice were euthanized by day 25 because their tumors were necrotic or had exceeded 1.5 cm in diameter. The growth of the tumors treated with DOTAP:Chol-FUS1 complex was well suppressed until day 25 on the average, after which they began to regrow gradually. Immunohistochemical analysis of tumors by TUNEL staining 2 days after the last injection of DOTAP:Chol-FUS1 revealed tumor cell apoptosis (Figure. 6B). No significant induction of apoptosis was observed in control tumors. Furthermore, no observable side effects were found in the mice treated with DOTAP:Chol-FUS1 complex (data not shown), suggesting that such treatment was well tolerated.

Since the main aim of the present proposal is to develop and deliver therapeutic genes via the systemic route, we tested the therapeutic effect of FUS1 gene on experimental lung metastasis and animal survival. Preliminary studies were conducted in a nude mouse model bearing experimental A549 lung metastasis. Treatment with DOTAP:Chol-FUS1 resulted in a significant inhibition ( $P = 0.01$ ) of tumor metastasis as indicated by the reduction in number of tumor nodules in the lungs (Figure 7A). Animals treated with PBS, DOTAP:Chol.liposome alone, plasmid DNA alone, and DOTAP:Chol-CAT complex served as controls in these experiments. Correlating with these observations was the prolonged survival of lung tumor bearing animals (mean = 80 days;  $P = 0.01$ ) treated with DOTAP:Chol-FUS1 complex (Figure 7B) compared to animals treated with PBS (mean = 47.8 days), treated with DOTAP:Chol. liposome (mean = 47.2 days), treated plasmid DNA (mean = 51.6 days), and treated with DOTAP:Chol-CAT complex (mean = 47.8 days). These preliminary results indicate the tumor suppressive function of FUS1 gene and support the findings of Ji et al. 58. Similarly, intravenous treatment subcutaneous H1299 tumor bearing nude mice with PEI-p53 complex demonstrated significant tumor suppression compared to control animals that were treated with PBS, and treated with PEI-b gal complex. These results demonstrate the feasibility of using these vectors for systemic therapy. However, further analyses using other xenograft models as well as toxicity studies are warranted prior to testing these vectors and genes in the clinic.

Toxicity Study of Injected b-gal-Lipoplex. On the basis of results from recent studies by Templeton et al., who have described efficient systemic delivery using a DOTAP:cholesterol lipid formulation, we conducted preliminary studies and have demonstrated the feasibility of in vivo gene delivery via systemic routes. Liposomes (20 mM DOTAP:cholesterol) were synthesized as described and mixed with b-gal plasmid DNA to give a final concentration of 150 mg of liposomes per 300 ml of b-gal-lipoplex. A single 50 mg dose of lipoplex was intravenously injected into immunocompetent female C3H mice via the tail vein, and mice were monitored for toxicity, as determined by mortality and morbidity rates. Animals were also evaluated for liver enzyme profiles 24 and 48 hours after injection. Preliminary results showed no signs of toxicity as no animals died. Liver enzyme profiles (OT/PT and AP) showed no significant differences in enzyme levels between treated and untreated animals.

Related Publications (published and submitted) (2002-2003):

Futoshi, U., Sasaki, J., Nishizaki, M., Carboni, G., Xu, K., Gao, B., Kondo, M., Atkinson E.N., Lerman, M.I., Minna, J.D., Roth, J.A, Ji, L. Myristoylation of Fus1 protein is required for tumor suppression in lung cancer. Science, 2003 (submitted).

Ji, L., Xu, K., Sasaki, J., Nishizaki, M., Carboni, G., Girard, L., Garner, H., Minna, J.D., and Roth J.A. Gene and Protein Expression Profiling Reveal Unique Cellular Targets and Signaling Pathway of Tumor Suppressor Gene FHIT in Lung Cancer. The 94th American Association for Cancer Research (AACR) Annual Meeting, Washington, DC, July 11-14, 2003 (presentation).



Futoshi, U., Sasaki, J., Nishizaki, M., Carboni, G., Xu, K., Minna, J.D., Roth, J.A., and Ji, L. Myristoylation of Fus1 protein plays an important role in Fus1-mediated tumor suppressing activities in human lung cancer cells. The 94th American Association for Cancer Research (AACR) Annual Meeting, Washington, DC, July 11-14, 2003.

Patent:

Ji, L., Roth, J.A., L., Minna, J.D., and Lerman, M.I. Chromosome 3p21.3 genes as tumor suppressors. U.S. Patent pending NO. 60/217, 112; International Patent Application No. PCT/US01/2178; European Patent Application Based on PCT/US01/21781.



## **Project 8      Therapeutic Targeting bcl-xl Expression In Non-Small Cell Lung Cancer**

**Principal Investigator: W. Roy Smythe, M.D.**

The bcl-xl gene is a member of the bcl-2 family of genes that controls mitochondrial membrane potential and interacts with other members of this family to control apoptosis, or programmed cell death. When over-expressed, the bcl-xl protein leads to inhibition of apoptosis as well as decreases sensitivity to conventional treatments (i.e. chemotherapy and irradiation). Decreasing expression of this gene product by various means may conversely induce apoptosis in cancer cells and render them sensitive to more conventional available therapies. The following specific aims were proposed for this grant. Following each specific aim is a description of the work completed and/or ongoing in this area.

### **Specific Aim 1      Characterize the in vitro effects of bcl-xl ASO exposure on human NSCLC cells and evaluate such exposure as a prime for other pro-apoptotic therapies**

We have evaluated a panel of bcl-xl antisense oligonucleotides (ASO) on the human non-small cell carcinoma cell lines A549 and H1299. We have identified one particular construct (ISIS 15999) that can decrease cell viability in a lipid delivery system by 60%-90%. We have also demonstrated the ability of this in vitro treatment to increase the apoptotic (subg1 by FACS analysis) fraction of cells by more than 30%. This has also effectively sensitized these cell lines to cisplatin, with significant increases in both cell death and apoptosis over either monotherapy approach.

Due to a concern regarding the in vivo applicability of this approach, we have been evaluating an RNA silencing approach for down regulation of bcl-xl expression as well. Following sequence rules, we have designed and evaluated 5 separate siRNA double stranded constructs and have tested them on non-small cell lines in vitro. Two of these constructs were able to effectively decrease bcl-xl expression at both protein (Western blot) and mRNA (real-time PCR) levels. The most promising construct was utilized to develop a hairpin loop plasmid delivery system. Both the siRNA double stranded and plasmid constructs are able to induce apoptotic cell death in vitro. Notably, the bcl-xl siRNA plasmid construct delivered with a lipid delivery system can sensitize NSCLC cells to cisplatin and decrease the amount of cisplatin required to kill 50% of these cells (IC50) by a full log.

### **Specific Aim 2      Develop an adenoviral vector capable of transferring an antisense bcl-xl gene construct**

A full length, rather than short segment, bcl-xl antisense adenoviral gene therapy vector (xl22) was developed (second generation replication deficient human type 5 construct). This has been characterized by sequencing as the intended sequence.

### **Specific Aim 3      Characterize the in vitro effects of bcl-xl antisense adenoviral vector exposure on human NSCLC cells and evaluate such exposure as a prime for other pro-apoptotic therapies**

The xl22 vector was evaluated in vitro in NSCLC cells. This vector has been demonstrated to down regulate bcl-xl protein expression (Western Blot) and induce apoptotic cell death.



**Specific Aim 4      Characterize the therapeutic effects of bcl-xl antisense targeting with both ASO and adenoviral vectors in animal models of non-small cell lung carcinoma and evaluate such exposure as a prime for other pro-apoptotic therapies in vivo**

We have demonstrated thus far the ability of ASO to decrease intraperitoneal tumor burden in a xenograft model of mesothelioma (identical bcl-2 family expression pattern) by 30%-40%. Likewise, we have demonstrated that the xl22 construct can decrease tumor burden by more than 60%. We have recently demonstrated the ability to transfer the backbone siRNA plasmid system with a reporter gene (E. Coli beta galactosidase) utilizing a dotap:cholesterol delivery method into in vivo intraperitoneal xenograft tumor. These experiments are currently being repeated in a xenograft model of human NSCLC.



## Project 9 Improved Pulmonary Gene Delivery with Partial Liquid Ventilation for Treatment of Pulmonary Malignancies

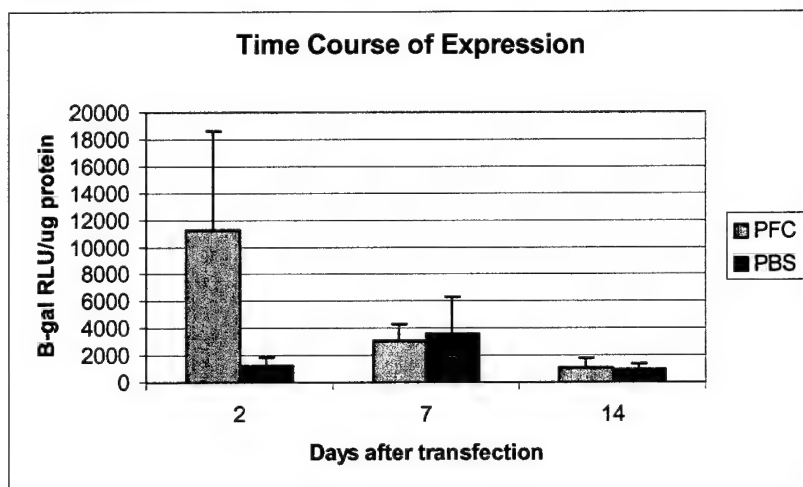
Principal Investigator: Ara Vaporciyan, M.D.

**Specific Aim 1** To determine PFC's ability to diminish the immune response, both innate and the later cellular and humoral responses, to intratracheal administration of adenoviral vector

### Task A Evaluation of the innate immune and later cell-mediated response at the cellular level

We have begun to collect data on the immune response after adenoviral transfection with  $\beta$ -galactosidase gene (B-gal) when delivered intratracheally with phosphate buffered saline (PBS) or perfluorocarbon (PFC). Initial experiments involved confirmation of PFC's ability to enhance adenoviral transfection given endotracheally. Due to the extent of time between these experiments and our preliminary data, we utilized a new recently produced batch of B-gal adenovirus. All subsequent experiments will be performed with this batch of adenovirus. The dose of adenovirus was  $5 \times 10^8$  viral particles in 100  $\mu$ l PBS. Control animals received only this dose endotracheally while experimental animals received a similar dose followed by 3 ml (10 ml/kg) PFC. At 2 days after transfection, animals in the experimental group had whole lung expression at least 10 fold greater than control animals (relative light units per mg protein  $\pm$  standard error of the mean;  $13539 \pm 8348$  vs.  $1293 \pm 706$ ,  $p=0.06$ ). This demonstrates the ability of PFC to enhance expression of B-gal. This enhanced expression is most likely due to increased transfection either through improved delivery of the virus to the alveolar cells or through interference of pulmonary mechanisms of viral clearance.

Assessment of expression at later time points was evaluated to identify the rate of clearance of



transfected cells. This clearance is a function of the hosts' immune response to the transfected cells. The ability of perfluorocarbons to interfere with the inflammatory response has been suggested by some investigators.

Although our studies were conducted with a single dose of PFC it is possible that this isolated dose could interfere with the normal clearance mechanisms. Using a similar dose of adenovirus and PFC, animals were harvested at 14

days after transfection. A rapid clearance of B-gal expression was observed in the PFC treated animals with nearly similar expression values for experimental and control animals at 14 days ( $1107 \pm 709$  vs.  $931 \pm 452$ ). A number of hypotheses could account for the rapid clearance of PFC-mediated expression. One hypothesis is that the enhanced expression associated with PFC may lead to a more pronounced inflammatory response and improved clearance. Blood specimens were collected from all animals at the time of sacrifice and these will be analyzed for



the levels of cytokines associated with antiviral immune response. In addition, levels of anti-adenoviral antibodies will be measured. This work is scheduled for year two of this project. A second hypothesis is that the increased expression is due to increased protein production per cell (i.e. increased transfection of each cell rather than greater numbers of cells transfected). This would allow a similar rate of cellular clearance in control and experimental animals to result in a rapid reduction of expression in the experimental group.

**Task B            Evaluation of the innate immune and later cell-mediated response at the molecular level**

Serum samples are being collected from all experiments underway so far. Animals sacrificed at 2, 7 and 14 days have serum specimens collected and snap frozen in liquid nitrogen then placed at  $-70^{\circ}\text{C}$  till ready for cytokine evaluation. All cytokine assays will be performed simultaneously once all specimens have been collected. This is scheduled for year two of our project.

Early assessment of the cellular immune response has begun. Blood specimens have been collected from 2 day animals and white blood cell counts with differential determination has been performed. This is a nonspecific assessment of the cellular response to adenoviral transfection with and without the use of PFC. These experiments were initially performed with a higher dose of adenovirus,  $10^{10}$  viral particles. Animals that received only vehicle, adenovirus, or adenovirus with PFC down the airway had a WBC count ( $\times 1000/\square\text{l}$ ) of  $4.7 \pm 0.4$ ,  $6.1 \pm 0.7$ , and  $5.1 \pm 0.5$ . This was a 71.4% reduction in the total WBC ( $p=0.2$ ) relative to the baseline WBC observed in the animals that received vehicle alone.

**Specific Aim 2            To determine PFC's ability to enhance repeated gene transfer through reduction and mechanical disruption of the humoral response**

We have just begun performing these long-term repeat dosing experiments and no data are available as yet. These projects are scheduled for the latter part of the first year and to be completed during the second year.

**Specific Aim 3            To determine PFC's ability to allow continued penetration of the pulmonary parenchyma in the setting of an animal model of severe emphysema**

These experiments are scheduled for the second and third year of this project.

**Specific Aim 4            To determine the ability of PFC mediated gene transfer to effectively transduce a model of multifocal lung cancer**

These experiments are scheduled for the second and third year of this project.



**Project 10     Development of an Orthotopic Model to Study the Biology and Therapy of  
Primary Human Lung Cancer in Nude Mice**

**Co-Principal Investigators: Michael S. O'Reilly, M.D.  
Roy S. Herbst, M.D.**

- Specific Aim 1     Develop and validate orthotopic and metastatic murine lung cancer models for testing the efficacy of anti-angiogenic agents alone and in combination with cytotoxic agents**
- Specific Aim 2     Compare the effects of anti-angiogenic therapy alone and in combination with chemotherapeutic agents in different sites of primary and metastatic disease**
- Specific Aim 3     Identify optimal combinations and sequencing of anti-angiogenic agents with chemotherapy for treatment of lung cancer**
- Specific Aim 4     Develop surrogate markers of response to therapy using immunohistochemical and gene expression analysis of tumor tissues**

We have worked to develop biologically relevant animal models of human lung cancer, which are reproducible, inexpensive and easy to perform. Human lung adenocarcinoma (PC14PE6), bronchioloalveolar carcinoma (NCI-H358), squamous cell carcinoma (NCI-H226), poorly differentiated non-small cell lung cancer (NCI-H1299 and A549), or small cell lung cancer (NCI-H69) cells in Matrigel were injected percutaneously into the left lung of nude mice. The growth pattern of the different lung cancer tumors was studied. For PC14PE6 and NCI-H358, the growth pattern in the subcutis and the response to Paclitaxel were also studied.

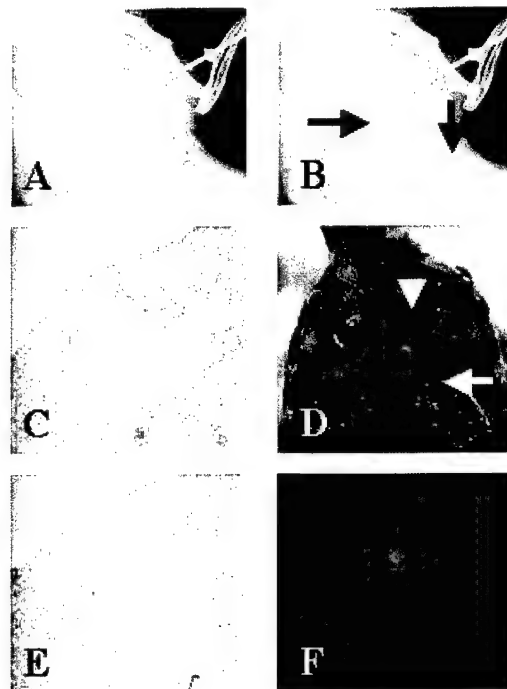
As is observed for human primary lung cancer, tumors formed from a single focus of disease and progressed to a widespread and fatal thoracic process characterized by diffuse dissemination of lung cancer in both lungs and metastasis to intra- and extra-thoracic lymph nodes. When the lung cancer cell lines were implanted subcutaneously, systemic therapy with Paclitaxel induced tumor regression. However, only a limited therapeutic response to Paclitaxel was observed when the same cells were implanted orthotopically into the lung. Immunohistochemical analysis of tumor tissue revealed increased expression of the pro-angiogenic factors IL-8, bFGF, and VEGF/VPF.

Our orthotopic models of human lung cancer confirm the "seed and soil" concept and likely provide more clinically relevant systems for the study of both non-small cell lung cancer (NSCLC) and small cell lung cancer (SCLC) biology and for characterizing novel therapeutic strategies.

Fig. 1 A To demonstrate fluid spreading after injection into the thorax, a 27.5-gauge needle was inserted into the left lung of a nude mouse (Faxitron® x-ray image). B, The image was taken immediately following an injection of 75 µl iohexol (omnipaque™), an iodinated contrast agent. The fluid blunted the tip of the needle in the lung parenchyma and accumulated in the pleura according to gravity forces (arrows). C, The solitary nodules surrounded by a normal lung developed several days after injection of tumor cells with Matrigel, which anchored them and prevented cell suspension spread. PC14PE6 (adenocarcinoma) tumor, 9 days after tumor implantation. D, Diffuse thoracic disease involving the injected site, the contra-lateral lung and lymph nodes. Note the heart (arrowhead) and the small portion of the lung (arrow). E, IHC



staining revealed that lung cancer in this system expressed bFGF from an early stage of disease. *F*, To study the sequence of metastasis we transfected two cell lines with green fluorescent protein (GFP). The lesion is a microscopic left lung tumor on day 4 after injection of PC14PE6 cells with Matrigel. At this time, we found metastasis in the regional lymph nodes and the right lung.





## **Core B: Biostatistics and Data Management**

**Director: J. Jack Lee, Ph.D.**

**Co-Director: B. Nebiyu Bekele, Ph.D.**

### **Core Goals:**

- To provide the statistical design, sample size and power calculations for each project.
- To facilitate prospective data collection and quality control of data for the clinical trials, animal experiments, and basic science studies associated with the TARGET program.
- To provide all statistical data analysis including descriptive statistical analysis, hypothesis testing, estimation, modeling of prospectively generated data.
- To generate statistical reports for all projects.
- To collaborate and assist all project investigators in the publication of scientific results.

From the inception of the TARGET program, the Biostatistics and Data Management Core has worked actively with all the Projects in their research efforts, especially in the area of biostatistical advice and consulting in the initial design of studies, analysis of experimental result and development of a decision analytic model to assess the effect of prophylactic cranial irradiation for patients with small cell lung cancer.

In collaboration with Dr. Ruth Katz, we have analyzed deletions of the 3p and 10q genes from 15 lung cancer patients and a group of 15 controls. We have performed penalized logistic regression to predict group membership. Because of the small sample size, we used a leave-one-out validation technique to assess the quality of the prediction associated with the 3p and 10q gene deletion. We also performed survival analyses using the Cox proportional hazards model. This research is in progress.

In collaboration with Lin Ji, we have analyzed the relationship between the expression of FUS1 protein in tumor tissue compared to normal tissue. We used the marginal homogeneity test to test for differences between the paired samples (Normal Vs. Tumor). The marginal homogeneity test, a generalization of McNemar's test, assesses the equality of categorical responses from two populations, where the data consist of paired, dependent categorical responses, one from each population. This research is in progress.

In collaboration with Dr. Scott Cantor (a decision scientist) and Dr. Jin-Soo Lee (Director of National Cancer Center of Korea) we have developed a decision analytic model to examine the effects of PCI on quality adjusted life years (QALYs). Utility assessments of the effects of PCI (and associated neurotoxicity) were elicited from Dr. Jin-Soo Lee (an expert in this field). Survival times for both the PCI group and the no PCI group were modeled using a log normal distribution which mimicked survival times reported in the literature. Quality adjusted survival time and expected QALYs are estimated for current survival rates and assuming the cure rate will increase in the future due to improved therapy and management of this disease. This research is in progress.



### Publications

Bekele BN\*, Lee JJ\*, Cantor SB, Zhou X, Lee LS (2003) " Decision Analysis of Prophylactic Cranial Irradiation for Patients with Small Cell Lung Cancer", M. D. Anderson Department of Biostatistics Technical Report #002-03. (\*Equal Effort).



## KEY RESEARCH ACCOMPLISHMENTS

- Activated LAB03-0382 (Project 1) and enrolled 5 patients to date.
- DNA repair assay and FISH assay to be tested on epithelial cell cultures.
- Optimized conditions for inter-simple sequence PCR in cultured bronchial epithelial cells.
- Characterized clonal evolution in cell lines with progression from immortalization to the tumor phenotype.
- Identified distinct clonal variants within cell lines with progression to the tumor phenotype.
- Proteins in the apical surface liquid from squamous metaplastic bronchial cells in culture were separated by 2 dimensional polyacrylamide gel electrophoresis.
- Initial identification of 40 protein spots was performed by MALDI-MS method. Thirty-five out of 40 proteins were identified and further verification is underway.
- 363 medical records screened, 218 subjects identified as eligible for study database. Tissue sample assessment ongoing.
- SAHA inhibited the growth of 5 NSCLC cell lines. In NSCLC, there is no synergistic or even additive effect of various growth inhibitors and SAHA.
- Studied molecular mechanisms of a novel tumor suppressor gene (TSG) FUS1; identified the wild-type Fus1 as an N-myristoylated protein; presented first-hand evidence for the loss of expression or a defect of myristoylation of the Fus1 protein in human primary lung cancer and cancer cell lines; showed that myristoylation is required for Fus1-mediated tumor-suppressing activity in vitro and in vivo.
- Evaluated the toxicity and therapeutic effects of systemic administration of DOTAP:Cholesterol:FUS1 DNA (Fus1-lipoplex) on development of human lung metastases and animal survival, and found that the treatment with FUS1-lipoplex resulted in significant inhibition of tumor metastases and no signs of toxicity at those therapeutic dose levels, no animal death and significant increase of liver enzyme (OT/PT and AP) profiles observed.
- Novel ras-dependent and independent effects of farnesyl transferase inhibitors uncovered.
- Proteomic analysis of FTI-treated cell lines detects several important classes of proteins that are upregulated or downregulated by this class of compounds.
- Intratracheal administration of adenoviral vector in the presence of perfluorocarbon achieves 8 to 10 fold improved expression than vector administered without perfluorocarbon.
- Perfluorocarbon-mediated expression returns to baseline levels at a similar rate as expression seen with vector alone.
- Developed biologically relevant animal models of human lung cancer.

## REPORTABLE OUTCOMES

### **Abstract:**

Lu T, Hittelman WN. Assessment of subclonal evolution in human bronchial epithelial cell lines progressing toward malignancy by fluorescence inter-simple sequence repeat PRC. *Proc AACR* 44:894, 2003.

Hassan KA, Lee HY, Kim E, Bishop WR, Kirschmeier P, Mao L, Khuri FR. A novel mechanism of farnesyltransferase inhibitor (SCH66336) arresting head and neck squamous cell carcinoma cells. *Proc AACR* 44:183, 2003.

### **Patent Pending:**



Ji L, Roth JA, Minna JD, Lerman MI. Chromosome 3p21.3 genes as tumor suppressors. U.S. Patent pending No. 60/217, 112; International Patent Application No. PCT/US01/2178; European Patent Application Based on PCT/US01/21781

**Publications:**

Khuri FR, Glisson BS, Kim ES, Meyers ML, Herbst RS, Thall PF, Munden RF, Statkevich YP, Bangert S, Thompson E, Cascino M, Shin DM, Papadimitrakopoulou V, Kurie JM, Kies MS, Lee JS, Fossella FV, Hong WK. Phase I study of farnesyl transferase inhibitor (FTI) SCH66336 with paclitaxel in solid tumors. *Journal of Clinical Oncology*, submitted 2003.

Kim ES, Kies MS, Fossella FV, Glisson BS, Zaknoen S, Baum CM, Summey C, Lu C, Papadimitrakopoulou V, Hong WK, Khuri FR. Phase II study of the farnesyltransferase inhibitor (FTI) lonafarnib with paclitaxel in patients with taxane-refractory/resistant non-small cell lung cancer. *Journal of Clinical Oncology*, submitted 2003.

Sun SY, Zhou Z, Wang R, Khuri FR. Akt is not a target for the growth inhibition and apoptosis induction by the farnesyltransferase inhibitor SCH66336 in human lung cancer cells. Manuscript in preparation.

Futosh U, Sasaki J, Nishizaki M, Carbone G, Xu K, Gao B, Kondo M, Atkinson EN, Lerman MI, Minna JD, Roth RA, Ji L. Myristoylation of Fus1 protein is required for tumor suppression in lung cancer. *Science*, submitted 2003.

Bekele BN\*, Lee JJ\*, Cantor SB, Zhou X, Lee LS. Decision Analysis of Prophylactic Cranial Irradiation for Patients with Small Cell Lung Cancer. M. D. Anderson Cancer Center Department of Biostatistics Technical Report #002-03, 2003. (\*Equal Effort)

**Presentations:**

Ji L, Xu K, Sasaki J, Nishizaki M, Carboni G, Girard L, Garner H, Minna JD, Roth JA. Gene and Protein Expression Profiling Reveal Unique Cellular Targets and Signaling Pathway of Tumor Suppressor Gene FHIT in Lung Cancer. The 94<sup>th</sup> American Association for Cancer Research (AACR) Annual Meeting, Washington, DC, July 11-14, 2003.

Futosh U, Sasaki J, Nishizaki M, Carboni G, Xu K, Minna JD, Roth JA, Ji L. Myristoylation of Fus1 protein plays an important role in Fus1-mediated tumor suppressing activities in human lung cancer cells. The 94<sup>th</sup> American Association for Cancer Research (AACR) Annual Meeting, Washington, DC, July 11-14, 2003.

**CONCLUSIONS**

**Projects 1,3-5, 8-10:** No conclusions can be drawn at the present time.

**Project 2:** These results demonstrate the power of inter-simple sequence PCR analysis to detect clonal evolution and increases in clonal heterogeneity as cell populations progress through the multistep tumorigenesis process. More advanced cell populations appear to demonstrate increased genetic instability and clonal outgrowth.

**Project 6:** Lonafarnib is active in inducing growth arrest and apoptosis in human NSCLC and HNSCC cells, through mechanisms independent of Ras mutation and Akt activation in NSCLC.



This suggests a completely novel, Akt-independent mechanism of action for these compounds in lung cancer, unlike our previous data generated with head and neck cell lines.

**Project 7:** Our results elucidated an essential role for the protein myristoylation or the deficient posttranslational modification in FUS1-mediated carcinogenesis, and suggest a novel mechanism for the inactivation of FUS1 in lung cancer. Our results also suggest that it may be possible to prevent and delay tumorigenesis and suppress lung tumor growth and progression through gene transfer of the wt-Fus1 by systemic administration of FUS1-lipoplex.



## **APPENDIX**



[Back](#)

Abstract Number: 4511

**Assessment of subclonal evolution in human bronchial epithelial cell lines progressing toward malignancy by fluorescence inter-simple sequence repeat PCR****Tao Lu, Walter N. Hittelman. UT MD Anderson Cancer Center, Houston, TX.**

Tumors of the aerodigestive tract reflect a field cancerization process whereby carcinogen-exposed tissue progresses through a multistep process of clonal evolution driven by genetic instability and chronic wound healing. Prior chromosome in situ hybridization studies on bronchial biopsies of current and former smokers demonstrated the presence of chromosome changes throughout the exposed epithelial field. Spatial chromosome and molecular analyses of the bronchial epithelium suggested that with chronic tobacco exposure, the lung become a mosaic of clones and subclones, the extent of which is related to the degree and duration of tobacco exposure. These clones/subclones remain for years following smoking cessation. Because a high frequency of subclonal outgrowths are found in normal and premalignant epithelium adjacent to lung tumors, it is postulated that an assessment of the degree of genetic instability and clonal outgrowth in the bronchial epithelium of smokers may provide a risk marker for lung cancer development. We sought a quantitative technique with sufficient dynamic range that could be used to probe bronchial epithelium for the frequency of clonal/subclonal outgrowths. Fluorescence inter-simple sequence repeat PCR (ISSR-PCR) is a DNA fingerprinting technique whereby unique sequences between simple sequence repeat segments are amplified leading to a series of bands on a DNA sequencing gel. Genetic changes such as deletions, insertions, and rearrangements in the unique sequences lead to changes in the number and locations of bands. The numbers of bands changed from normal reflect the accumulated numbers of clonal alterations. To test the feasibility of this approach for quantifying clonal changes during malignant development, we applied ISSR-PCR (using two sets of fluorescence-labeled oligo primers with two anchor nucleotides at the 3' end of a (CA)<sub>8</sub>-repeat) to four sequentially evolved lung cell lines derived from large T-antigen immortalized normal human bronchial epithelial cells (Beas-2B), grown in vivo (1799), treated with cigarette smoke condensate (1198), and evolved to cancer (1170I). We observed 7 altered bands from Beas-2B to 1799, 3 additional bands to 1198, and 3 additional bands to 1170I. For comparison of dynamic range, we carried out a preliminary microsatellite LOH analyses using 5 primer pair sets (2 for chromosome (Chr) 3p14, 2 for Chr 9p21, and 1 for Chr 13q14) and found a total of 2 changes between Beas-2B and 1170I cells. These results suggest that ISSR-PCR has promise for quantifying the extent of subclonal outgrowth in cell populations and may prove useful in the assessment of lung cancer risk when applied to the analysis of bronchial epithelium. Supported in part by DAMD17-02-1-0706, CA-68437, CA70907, and EDNRN NCI CA-86390.

Presenter: Walter N. Hittelman

Affiliation: UT MD Anderson Cancer Center, Houston, TX . Email: [whittelm@mail.mdanderson.org](mailto:whittelm@mail.mdanderson.org)

Copyright © 2003 American Association for Cancer Research. All rights reserved.

Citation for abstracts scheduled for publication: Proceedings of the AACR, Volume 44, 2nd ed., July 2003.

Citation for abstracts not scheduled for publication: Proceedings of the AACR, Volume 44, 1st ed., March 2003.



[Back](#)

Abstract Number: 800

## **A novel mechanism of farnesyltransferase inhibitor (SCH66336) arresting head and neck squamous cell carcinoma cells**

**Khaled A. Hassan, Ho-Young Lee, Edward Kim, W. Robert Bishop, Paul Kirschmeier, Li Mao, Fadlo R. Khuri. M. D Anderson Cancer Center, Houston, TX; Schering Plough Research Institute, Kenilworth, NJ; Winship Cancer Institute, Emory University School of Medicine, Atlanta, GA.**

Farnesyltransferase (FTase) is a critical enzyme that post-translationally modifies proteins containing a CAAX motif such as Ras. FTase inhibitors (FTI) can regulate the growth of a variety of tumor cells in culture and in animal models. In a phase I clinical trial conducted by our group, a significant response to induction treatment with short (8-14 days) courses of SCH66336 has been documented in head and neck squamous cell carcinoma (HNSCC). To investigate the mechanism that mediates the cell growth inhibitory effect of SCH66336 on HNSCC, flow cytometry was performed on an HNSCC cell line UMSCC38. We found that SCH66336 causes cell cycle arrest with an accumulation of cells in the G2 phase. Furthermore, ph-Raf and ph-Akt expression was decreased indicating that SCH66336 inhibits Ras activity. However, it has been shown that Ras mutational status does not correlate with FTI sensitivity, implicating other mechanisms in the observed cell cycle arrest. In fact, total Akt protein level was downregulated by SCH66336. Metabolic labeling studies showed that endogenous and exogenous Akt protein is degraded after SCH66336 treatment, indicating a novel mechanism of action of SCH66336. To associate Akt degradation and cell growth inhibition, infection with active Akt adenovirus showed partial rescue from G2 phase arrest at pharmacologically achievable doses of SCH66336. Experiments supporting this correlation are ongoing. As a conclusion, SCH66336 may exert its effect through inhibiting Ras activity in head and neck cancer cell lines, as well as decreasing the stability of Akt through different mechanisms. Supported in Part by the BESCT program to WKH/FRK/LM (DAMD17-01-1-01689-1) and Schering Plough Research Institute Grant to FRK (CS99-265).

Presenter: Khaled A. Hassan

Affiliation: M. D Anderson Cancer Center, Houston, TX . Email: [khaledhassan@mail.com](mailto:khaledhassan@mail.com)

Copyright © 2003 American Association for Cancer Research. All rights reserved.

Citation for abstracts scheduled for publication: Proceedings of the AACR, Volume 44, 2nd ed., July 2003.

Citation for abstracts not scheduled for publication: Proceedings of the AACR, Volume 44, 1st ed., March 2003.



# **Myristoylation of the Fus1 Protein is Required for Tumor Suppression in Human Lung Cancer Cells**

**Futoshi Uno,<sup>1\*</sup> Jiichiro Sasaki,<sup>1\*</sup> Masahiko Nishizaki,<sup>1\*</sup> Giovanni Carboni,<sup>1</sup> Kai Xu,<sup>1</sup>  
Masashi Kondo,<sup>2</sup> Edward N. Atkinson,<sup>3</sup> John D. Minna,<sup>2</sup> Jack A. Roth,<sup>1</sup> Lin Ji,<sup>1†</sup>**

<sup>1</sup>Section of Thoracic Molecular Oncology, Department of Thoracic and Cardiovascular Surgery and <sup>3</sup>Department of Biomathematics, The University of Texas M.D. Anderson Cancer Center, Houston, TX 77030; <sup>2</sup>Department of Internal Medicine and Pharmacology, Hamon Center for Therapeutic Oncology Research, The University of Texas Southwestern Medical Center, Dallas, TX 75390;

**Key Words:** *FUS1* tumor suppressor gene, myristoylation, human chromosome 3p21.3, lung cancer.

**Category: Reports**

**\*These authors contributed equally to this work**

**†Correspondence should be addressed to:** Lin Ji, Ph.D., Assistant Professor, Department of Thoracic and Cardiovascular Surgery, Box 445, The University of Texas M. D. Anderson Cancer Center, 1515 Holcombe Blvd., Houston, TX 77030.

Phone: (713) 745-4530. Fax: (713) 794-4901. E-mail: [lji@mdanderson.org](mailto:lji@mdanderson.org)



### Abstract

*FUS1* is a novel tumor suppressor gene (TSG) identified in the human chromosome 3p21.3 region that is deleted in many cancers. Using SELDI-Mass spectrometry analysis on an anti-Fus1-antibody-capture ProteinChip array, we identified wild-type Fus1 as an *N*-myristoylated protein. Loss of expression or a defect of myristoylation of the Fus1 protein was observed in human primary lung cancer and cancer cell lines. A myristoylation-deficient mutant of the Fus1 protein abrogated its ability to inhibit tumor cell-induced clonogenicity *in vitro*, to induce apoptosis in lung tumor cells, to suppress the growth of tumor xenografts and lung metastases *in vivo*, and rendered it susceptible to rapid proteasome-dependent degradation. Our results show that myristoylation is required for Fus1-mediated tumor-suppressing activity, and suggest a novel mechanism for the inactivation of TSGs in lung cancer and a role for deficient posttranslational modification in TSG-mediated carcinogenesis.



Tumor suppressor genes (TSGs) play a major role in the pathogenesis of human lung cancer and other cancers. Lung cancer cells harbor mutations and deletions in multiple known oncogenes and TSGs; however, genetic alterations and allelic losses on the short arm of chromosome 3 are among the most frequent and earliest cancer abnormalities detected in the pathogenesis of lung cancers and have been shown to occur in 96% of non-small cell lung cancers (NSCLC) and in 78% of preneoplastic lung lesions (1). The frequent and early loss of heterozygosity and the overlapping homozygous deletions observed in the 3p21.3 region in lung and breast cancers suggest a critical role of one or more 3p21.3 genes as “gatekeepers” in the molecular pathogenesis of these cancers (2,3).

The novel *FUS1* TSG is one of the candidate TSGs that have been identified in a 120-kb homozygous-deletion region in human chromosome 3p21.3 (2,4,5). The cloned cDNA of *FUS1* (GeneBank ID: AF055479) is 333 bp and encodes a protein of 110 amino acid residues (Fig. 1A). However, the *FUS1* gene does not show homology with any known genes and proteins in databases. We have previously demonstrated that exogenous expression of the wild-type (wt)-*FUS1* by plasmid- or adenoviral vector-mediated gene transfer significantly inhibits tumor cell growth, induces apoptosis, and alters cell cycle kinetics in 3p21.3-deficient NSCLC cells *in vitro* and efficiently suppresses tumor growth and inhibits tumor progression and metastases in various human lung cancer xenograft mouse models (4-6).

However, the mechanisms involved in the inactivation of the *FUS1* gene in primary human cancers remain unknown. In a previous study, we examined 40 primary lung cancers and found that mutation of the *FUS1* gene was infrequent and there were only a few nonsense mutations and a C-terminal deletion mutation that arose from aberrant mRNA splicing (Fig. 1A) (5). In addition, we found no evidence for *FUS1* promoter region methylation (data not shown).



*FUS1* expression has been detected in various normal human tissues; including brain, heart, pancreas, prostate, kidney, and lung, based on quantifying Expressed Sequence Tags (ESTs) in Unigene clusters, as summarized in GeneCards (7). Although endogenous Fus1 protein expression could be detected in normal human bronchial epithelial cells and fibroblast cells (WI-38) by immunoblot analysis and *FUS1* mRNA transcription could be seen on Northern blots of RNAs prepared from lung cancer cell lines, we could not detect endogenous Fus1 protein in these lung cancer cell lines on immunoblots using the affinity-purified, anti-Fus1 peptide antibodies developed (Fig. 1B). Furthermore, we performed immunohistochemical staining on a set of paired normal lung and lung cancer tissue sections (Fig. 1C). We found that normal lung epithelial cells express Fus1 (Fig.1C, b-d), but many lung cancer cells (15 out of 20, >70%) (Fig.1C, f-h) did not. We also found that even in those tumor samples with Fus1-positive staining, the staining was not uniformly detectable in all tumor cells (Fig.1C, e). Based on both the lung cancer-growth suppressing properties of the Fus1 protein *in vitro* and in animal models and the observed loss of protein expression in primary tumors and tumor-derived cell lines, we hypothesized that *FUS1* would have to act as a TSG in a haploinsufficient manner (since most primary lung cancers experienced allelic loss in this 3p21.3 region) (8), and that both loss of expression and deficient posttranslational modification of Fus1 protein might lead to loss of its tumor suppression function and lung cancer development.

To test this hypothesis, we first performed a computer-based homologous structure modeling and functional domain prediction of Fus1 protein to assess its biochemical and biophysical properties and to obtain possible leads to its biological function (Fig. 1A). The secondary protein structure prediction featured the wt-Fus1 protein as a highly hydrophobic protein with extensive helix-coils domain structures lacking transmembrane elements (Fig. 1A).



The functional domains of Fus1 protein were predicted using a motif-based profile scanning program (9) and showed a potential myristoylation site at the *N*-terminus, a protein kinase A (PKA) interaction site, an A kinase anchoring protein (AKAP) interaction (protein/protein) site, and a PDZ class II domain (Fig. 1A). From these analytical comparisons of Fus1 protein structure and function, we predict that Fus1 is a myristoylated member of the novel cAMP-dependent protein kinase A and A-kinase anchoring protein families, which are associated with a wide range of cellular processes, including transcription, signal transduction, metabolism, ion channel regulation, cell cycle progression, and apoptosis (10,11).

To verify myristoylation of the Fus1 protein, we constructed a plasmid vector expressing either the wt-*FUS1* or a myristoylation-site deficient mutant (myr-mt-*FUS1*), in which the predicted myristoylation site of glycine (G<sub>2</sub>) was replaced with an alanine (A<sub>2</sub>) (Fig. 1A) by site-directed mutagenesis. A double mutant (dmt-*FUS1*) in the C-terminal region, in which two highly hydrophobic isoleucine (I) residues (I<sub>87</sub> and I<sub>91</sub>) were replaced with two neutral and rigid-conformation- promoting proline residues (P<sub>87</sub> and P<sub>91</sub>) (Fig. 1A), was also constructed as another control to confirm the biological significance and specificity of myristoylation-deficient mutation of Fus1 protein. The wt-Fus1 and mutant-Fus1-expressing plasmid vectors were used to transfect Fus1-deficient human non-small cell lung cancer (NSCLC) NCI-H1299 cells. The expression and posttranslational modification status of these wild type and mutant Fus1 proteins were analyzed by surface-enhanced laser desorption and ionization and time of flight-mass spectrometry (SELDI-TOF-MS) on an anti-Fus1-antibody-capture ProteinChip array (ACPA) (12) (Ciphergen Biosystems, Fremont, CA) (Fig. 2A). The expressed Fus1 proteins in transfected H1299 cells were specifically captured on the protein chip and detected in the SELDI-TOF-MS spectra (Fig. 2A), but no protein peaks at corresponding mass positions were detected in the



spectra with an anti-101F6 (a protein with encoding gene co-located in 3p21.3 region with *FUS1*) antibody-coated chip as a non-specific control (Fig. 2B). The wt-Fus1 protein was identified as a myristoylated protein based on the detected mass of the captured wt-Fus1 protein (Fig. 2A), which showed a protein peak with a mass/charge (M/Z) of  $12174 \pm 6.25$  d, compared to the predicted MW of 12072.98 d for the un-myristoylated wt-Fus1 or 12174.2 d for the myristoyl-Fus1 protein. The myristoylation mutant (12024.6 d) and the C-terminal deletion mutant (8783.5 d) of Fus1 protein were also captured and detected on the protein array by SELDI-MS, respectively, by comparing them with their calculated masses (Fig. 2A). No captured Fus1 proteins were detected in either the untransfected or p*LacZ*-transduced cells (Fig. 2A). Based on the 232 d mass-shift between the detected myristoylated Fus1 (12174 d) and the predicted un-myristoylated Fus1 protein (11942 d, without the first methionine residue as the methonine residue is removed during myristoylation), we predict that the Fus1 protein is acylated at the G<sub>2</sub> with a 14-carbon myristate (C<sub>14</sub>H<sub>28</sub>O<sub>2</sub>, 228.4 d). The myristoylation of Fus1 protein is also further confirmed by immunoblot analysis and immunoprecipitation analysis of the <sup>14</sup>C-myristate-labeled and acylated Fus1 protein in the p*FUS1*-transfected cells (Fig. 2D) (12).

Since mutation of *FUS1* is infrequent and no evidence has been found for methylation or mutation of the *FUS1* promoter region in lung cancers, other factors such as haploinsufficiency, low expression, abnormal products arising from aberrant mRNA splicing, and posttranslational modification of Fus1 may play important roles in lung tumorigenesis (2,3). We used ACPA analysis with SELDI-TOF-MS to evaluate the protein expression and myristoylation status in primary lung tumor and uninvolved normal lung tissue samples. Molecular analysis of tumors and their precursor lesions requires the isolation of specific cell subpopulations (normal, preneoplastic, and tumors) from a composite background of multiple cell types in tumor-tissue



biopsies. This was accomplished with laser-captured microdissection (LCM) technology (13). To evaluate Fus1 protein expression and posttranslational modifications in human lung tumors and noninvolved tissues, we used LCM combined with appropriate tissue-preparation methods to separate and enrich tumor or noninvolved normal cells, and the resulting separated cell populations (about 500 - 1000 cells) were used for the Fus1-specific ACPA analysis by SELDI-TOF-MS. LCM, cell lysate preparation, ACPA analysis (12), and SELDI-TOF-MS analysis were performed according to the manufacturer's instructions and procedures described by von Eggeling *et al.* (14). We found that only myristoylated protein species could be detected in normal cells (13 out of 15,  $P = 0.0003$  by a Nonparametric 2x2 contingency table, McNemar Chi-square test), but both the unmyristoylated and myristoylated Fus1 protein were detected in tumor cells (5 out of 15 samples,  $P = 0.0442$ ) as indicated by the precise mass of Fus1 protein on the mass spectra (Fig. 2C). The mixed status of Fus1 protein in the tumor cells may be a reflection of the tumor-cell molecular heterogeneity. In some tumor samples (7 out of 15 samples,  $P = 0.0030$ ), neither form of Fus1 proteins could be captured (Fig. 2C), consistent with the immunohistochemical analysis in these tumor and normal tissue samples. The remaining three samples tested were un-resolvable due to the ambiguous spectra (spectra not shown). The difference in the observed Fus1 protein myristoylation status between the normal and the tumor cell populations is significant as indicated by a Nonparametric McNemar Marginal Homogeneity test for the equality of categorical responses from two paired and dependent populations ( $P < 0.001$ ).

To explore the possible mechanism(s) for the involvement of the unmyristoylated (or demyristoylated) Fus1 protein and the loss of its expression in inactivation of Fus1 protein in primary lung cancer, we evaluated the stability of the exogenously expressed wt-Fus1 and myr-



mt-Fus1 proteins in H1299 cells. We found that the duration of transient expression of myr-mt-Fus1 protein was much shorter than that of wt-Fus1. Myr-mt-Fus1 protein expression peaked at 36 h posttransfection and was almost undetectable after 60 h, while the wt-Fus1 protein was expressed at high levels beyond 60 h posttransfection (Fig. 2E). The half-life of the myr-mt-Fus1 protein was shorter than that of wt-Fus1, being approximately 6 h for the former and 12 h for the latter, as shown by pulse-chase of protein synthesis after treatment with the protein synthesis inhibitor cyclohexamide (CHA) (Fig. 2F). These results suggest unmyristoylated Fus1 protein may be degraded more rapidly than the myristoylated form. Therefore, we investigated the effect of proteasome inhibitor (15), MG132, on degradation of Fus1 proteins. We found that the unmyristoylated Fus1 protein levels increased in myr-mt-*FUS1*-transfected H1299 cells treated with MG132 at the various concentrations of MG132 (Fig. 2G). The MG132-induced recovery of the myr-mt-Fus1 protein could be detected at a very low level (1  $\mu$ M) (Fig. 2G) and was independent of protein synthesis, as demonstrated by significant protein accumulation upon treatment with 10  $\mu$ M of MG132 either in the presence or the absence of the protein synthesis inhibitor CHA (Fig. 2H), with no effect shown on wt-Fus1 protein under the same experimental conditions (Fig. 2H). These results suggest that myristoylation may stabilize Fus1 protein, and demyristoylation may result in rapid degradation of Fus1 protein through a proteasome-dependent pathway.

The identification of *N*-myristoylation of the wt-Fus1 protein provides an important clue to its biological function. One of the biochemical and biological functions of protein myristoylation is the facilitation of efficient interactions with cell membranes necessary for correct subcellular localization (16-18). Therefore, we analyzed the subcellular localization of myristoylation positive wt-Fus1 and the myristoylation-deficient mt-Fus1 proteins in plasmid-



transfected H1299 cells by immunofluorescence image analysis using fluorescein isothiocyanate-conjugated anti-Fus1 antibodies (Fig. 3A). The myr-mt-Fus1 lost its characteristic intracellular membrane localization (Fig. 3A), suggesting the important role of myristoylation in the cellular localization of Fus1 protein.

To evaluate the biological role of myristoylation in Fus1 protein-mediated tumor-suppression, we compared the clonogenicity of the wt-Fus1 and myr-mt-Fus1-expressing H1299 cells *in vitro* (Fig. 3D and E). The exogenous expression of both the *FUS1* genes and proteins in these H1299 transfectants was confirmed by RT-PCR (Fig. 3B) and by Western-blot (Fig. 3C) analysis, respectively. A significant inhibition of clonogenicity was observed in myristoylated wt-Fus1-expressing H1299 cells, but no significant growth inhibition was observed in myr-mt-Fus1-expressing cells, compared with the Fus1 non-expressing controls (Fig. 3D and E). The C-terminal double mutation of Fus1 (dmt-Fus1), which was theoretically expected to severely alter the hydrophobic and conformational properties in this region of Fus1 protein, was still able to significantly inhibit clonogenicity comparable to that of wt-Fus1 (Fig. 3B and C). A third artificial mutant provided a specificity control and further supports the essential role of the myristoylation site in Fus1-mediated-tumor suppressing activity.

To determine the role of myristoylation of Fus1 protein *in vivo*, we evaluated the effects of wt-Fus1 and myr-mt-Fus1 protein expression on tumor growth in H1299 subcutaneous tumor xenografts in nu/nu mice by intratumoral injection of DOTAP-cholesterol complexed with either wt-*FUS1* or myr-mt-*FUS1*-expressing plasmid DNAs (*FUS1*-lipoplexes) (19), along with PBS as a mock control and *LacZ* plasmid vector as a negative control (Fig. 4A ). The human NSCLC xenograft model, DNA-lipoplex preparation, and treatment procedures were previously described (4,6,19). The growth of tumors was recorded from the first injection until 31 days



after the last injection. Tumor volumes were normalized by calculating the percentage increase in tumor-volume after treatment relative to volume at the beginning of treatment in each group. All of the tumors treated with wt-*FUS1* showed significantly suppressed growth ( $P < 0.001$ ), compared with mouse groups treated with PBS or p*LacZ* controls (Fig. 4A). However, the tumor suppressing activity of the myristoylation-deficient mutant (myr-mt-*FUS1*) of Fus1 protein was significantly reduced compared with the wt-Fus1 ( $P < 0.001$ ), although it retained a small inhibitory effect compared with the PBS and p*LacZ* controls, (Fig. 4A).

We further evaluated the effect of the myristoylation of Fus1 protein on development of lung metastases using the human NSCLC A549 xenograft metastasis mouse model by systemic (intravenous) administration of the wt-*FUS1* or myr-mt-*FUS1*-lipoplexes, compared to PBS, p*LacZ*, and lung cancer-originated C-terminal deletion mutant of wt-*FUS1*, dmt-*FUS1* plasmid vector controls (4,6). The development of A549 pulmonary metastases was significantly inhibited ( $P < 0.001$ ) and the numbers of metastatic tumor colonies found on the surfaces of lungs from mice inoculated with A549 cells were reduced more than 85% in animals treated with wt-*FUS1*, compared with those in control treatment groups (Fig. 4B). However, no significant reduction ( $P < 0.003$ ) of metastases formation was observed in animals treated with myr-mt-*FUS1*. The formation of metastases was significantly reduced ( $P < 0.001$ ), in animals treated with dmt-*FUS1* compared with those controls treated with either PBS or *LacZ*, but the inhibitory effect was weaker than that observed in the wt-*FUS1*-treated group (Fig. 4B). The size of any remaining metastatic tumor nodules, as shown in hematoxylin and eosin-stained sections of mouse lung tissues (Fig. 4C), was reduced in animals treated with wt-*FUS1* but not in those treated with myr-mt-*FUS1*, compared with either PBS or *LacZ*-treated controls. We analyzed the induction of apoptosis in these Fus1-expressing tumor cells by *in situ* apoptosis analysis with



FITC-dUTP-labeled TUNEL staining (Roche Biochemicals) (Fig. 4D). Induction of apoptosis was only detected in the wt-Fus1-expressing tumors (Fig. 4D,b) but not in myr-mt-Fus1-expressing (Fig. 4D, c) or PBS-treated (Fig. 4E, a) tumors, providing direct evidence for the need for both Fus1 expression and myristoylation in Fus1-mediated tumor suppression and apoptosis *in vivo*.

Together, these results strongly support the biological importance of myristoyl modification of Fus1 and warrant an extensive study of the role of the expression and posttranslational modification of Fus1 protein in the pathogenesis of lung and other human cancers. The *N*-myristoyl modification of proteins is achieved by a co-translational linkage of myristic acid via an amide bond to the *N*-terminal glycine residues of a variety of cellular and viral proteins in eukaryotic cells (20). Covalent modification of proteins by fatty acids such as myristate and palmitate is now a widely recognized form of protein modification and about 100 proteins are known to be myristoylated (16,18). *N*-myristoyl-proteins play essential roles in diverse biological functions, such as regulating cellular structure, directing protein intracellular localization, mediating protein-protein and protein-substrate interactions, and regulating calcium and ion channel activities (16-18,20). The requirement for myristoylation of the viral p60src protein to mediate its transforming and oncogenic properties demonstrated the biological importance of this hydrophobic myristoyl moiety (21). Recent genetic, biochemical, and cell biological studies have provided insight into the molecular mechanisms of the regulation of protein myristoylation and explored strategies for modulating this process *in vivo* for therapeutic applications (16-18,20). Our present evidence that primary lung cancers are deficient for myristoylation of Fus1 protein and the requirement of myristoylation for Fus1-mediated tumor



suppressing activity *in vitro* and *in vivo* also implies the cancer preventive and therapeutic potential of positively regulating or re-activating myristoylation for Fus1.

Although the mechanism of demyristoylation is not known, the demyristoylation of the myristoylated alanine-rich C-kinase substrate (MARCKS) as shown by mass determinations of the myristoylated or demyristoylated MARCKS proteins with electrospray mass spectrometry, has been found in brain (22), and the reduced expression of MARCKS has been reported in various cell lines after oncogenic or chemical transformation and in melanoma cells compared to normal choroidal melanocytes (23). The existence of a nonmyristoylated pool of a G protein alpha subunit (Gpa1p) in yeast has also been reported and the myristoylated Gpa1p is required for specific targeting of the protein to the plasma membrane; however, it is not clear how the nonmyristoylated proteins are generated and maintained (18,24). Since point mutations of *FUS1* are infrequent, no mutation has been identified in its myristoylation site, and no evidence of epigenetic DNA methylation has been found in the *FUS1* promoter region in lung cancers, the observed reduced or lost expression and the deficient myristoylation of the Fus1 proteins in primary lung tumor cells and tumor-derived cell lines probably results from a deregulated myristoylation process or the accelerated proteasome-dependent degradation of demyristoylated Fus1 proteins. Since most lung cancers experience allelic loss in this 3p21.3 region, haploinsufficiency may play a critical role in inactivation of Fus1 protein in lung cancer (3). The importance of TSG haploinsufficiency in tumor cell biology has recently drawn increasing attention and it may have profound effects on gene transcription, protein expression, posttranslational modification, stability, and does-dependent activity of TSGs, due to the resulting decreased genomic stability, unbalanced chromosomal spatial symmetry, increased



susceptibility to stochastic delays of gene initiation, altered transcriptional and translational stoichiometry, and interrupted gene expression (25).

Our findings point to an essential role for protein myristoylation in human cancer pathogenesis and warrant further studies of alternative mechanisms involved in the inactivation of novel TSGs such as 3p21.3 *FUS1* gene by posttranslational modification, loss of expression, and haploinsufficiency. Our results also suggest that it may be possible to prevent and delay tumorigenesis by neutralizing the effects of 3p haploinsufficiency before progression of premalignant lesions to invasive cancer and suppress tumor growth by inducing apoptosis and altering cell cycle processes after tumor onset through wt-*FUS1* gene transfer.

#### Reference List and Notes

1. M. I. Lerman *et al.*, *Nucleic Acids Res.* 18, 205 (1990).
2. M. I. Lerman and J. D. Minna, *Cancer Res.* 60, 6116-6133 (2000).
3. Zabarovsky ER, Lerman MI, Minna JD., *Oncogene* 21, 6915-6935 (2002).
4. L. Ji *et al.*, *Cancer Res.* 62, 2715-2720 (2002).
5. M. Kondo *et al.*, *Oncogene* 20, 6258-6262 (2001).
6. R. Ramesh *et al.*, *Mol. Thera. J. Ameri. Soci. Gene Thera.* 3, 337-350 (2001).
7. <http://bioinfo.weizmann.ac.il/cards-bin/carddisp?FUS1>, by the Crown Human Genomics Center and Yeda Research and Development Co. Ltd. (Rehovot, Israel)
8. I. I. Wistuba *et al.*, *Cancer Res.* 60, 1949-1960 (2000).



9. M. B. Yaffe *et al.*, *Nat. Biotech.* 19, 348-353 (2001).
10. A. Feliciello, M. E. Gottesman, E. V. Avvedimento, *J. Mol. Biol.* 308, 99-114 (2001).
11. F. W. Herberg, A. Maleszka, T. Eide, L. Vossebein, K. Tasken, *J. Mol. Biol.* 298, 329-339 (2000).
12. ACPA Analysis. The endogenous or exogenous wt-Fus1 or mutant Fus1 proteins were captured with affinity-purified rabbit Fus1 polyclonal antibodies developed in our laboratory from cultured cells or LCM-separated and enriched human primary lung tumor and non-involved normal cells. Protein lysate was prepared in RIPA buffer containing 1% Nonidet P-40, 0.5% sodium deoxycholate, 0.1% SDS, and complete proteinase inhibitors (Roche Biochemicals, Germany) in 1x PBS. 5  $\mu$ l (about 10  $\mu$ g) of protein lysate was spotted on a Fus1 antibody-coated preactivated surface (PS20) ProteinChip<sup>TM</sup> array, analyzed by SELLDI-MS in the presence of CHCA matrix solution, and both internal and external standards were used for mass/Charge ( $m/z$ ) calibration (Ciphergen Biosystems, Fremont CA). [B. Davies *et al.*, *Biotechniques*. 27, 1258 (1999); E. von Eggeling *et al.*, *Biotechniques*. 29, 1066 (2000); H. Cai *et al.*, *Nat. Neurosci.* 4, 233 (2001)]
13. A. Maitra *et al.*, *Nat. Med.* 5, 459-463 (1999).
14. F. von Eggeling *et al.*, *Biotechniques* 29, 1066-1070 (2000).
15. W. Baumeister, J. Walz, F. Zuhl, E. Seemuller, *Cell* 92, 367-380 (1998).
16. J. B. Ames, T. Tanaka, L. Stryer, M. Ikura, *Curr. Opin. Struct. Biol.* 6, 432-438 (1996).



17. J. B. Ames *et al.*, *Nature* 389, 198-202 (1997).
18. M. D. Resh, *Biochim. Biophys. Acta* 1451, 1-16 (1999).
19. N. S. Templeton *et al.*, *Nat. Biotech.* 15, 647-52 (1997).
20. R. S. Bhatnagar *et al.*, *Nat. Struct. Biol.* 5, 1091-1097 (1998).
21. M. P. Kamps, J. E. Buss, B. M. Sefton, *Proc. Natl. Acad. Sci. U.S.A.* 82, 4625-4628 (1985).
22. S. Manenti, O. Sorokine, A. Van Dorsselaer, H. Taniguchi, *Biochem. Soci. Transact.* 23, 561-564 (1995).
23. S. Manenti, F. Malecaze, H. Chap, J. M. Darbon, *Cancer Res.* 58, 1429-1434 (1998).
24. J. Song, J. Hirschman, K. Gunn, H. G. Dohlman, *J. Biol. Chem.* 271, 20273-20283 (1996).
25. Y. Zhu *et al.*, *Science*, 296, 920 (2002); A. Celeste *et al.*, *Science*, 296, 922 (2002); M. E. McLaughlin, T. Jacks, *Cancer Cell*, 1, 408 (2002); R. A. Veitia, *BioEssays*, 24, 175 (2002); J.G. Seidman, C. Seidman, *J. Clin. Inves.*, 109, 451 (2002); J. Dworkin, R. Losick, *Cell*, 107, 339 (2001); D.L. Cook *et al.*, *Proc. Natl. Acad. Sci. USA*, 95, 15641 (1998)
26. We thank Dr. Sandra Hofmann at U.T. Southwestern Medical Center, Dallas for her critical review of the manuscript, Drs. Nebiyu Bekele and Michael Gilcrease at M.D. Anderson Cancer Center for performing McNemar statistical analysis and for pathological



evaluation of immunohistochemically stained human tissue sections, respectively, and Dr. Charlotte Clarke from Ciphergen Biosystems, Inc., for her technical assistance with SELDI-TOF-MS technology. This work was partially supported by: grants from the National Cancer Institute, the National Institutes of Health (SPORE CA70970; CA71618); a W. M. Keck Gene Therapy Career Development grant [L.J]; grants from the Department of Defense BESCT (DAMD17-01-1-0689) and TARGET (DAMD17-02-1-0706) Lung Cancer Programs; gifts to the M.D. Anderson Cancer Center Division of Surgery Core Laboratory Facility from Tenneco and Exxon; the M. D. Anderson Cancer Center Support Core Grant (CA16672); a grant from the Tobacco Settlement Funds as appropriated by the Texas State Legislature, and a sponsored research agreement with Introgen Therapeutics, Inc. (SR93-004-1).



## Figure Legends

**Figure 1.** Predicted secondary structure and functional domains of Fus1 protein and its expression in normal lung and primary lung tumors and tumor-derived cell lines. **A.** Predicted secondary structure and functional domains of wt-Fus1 and C-del-Fus1. The predicted functional elements and domains, including a potential myristoylation site, protein kinase A (PKA) targeting site, AKAP interface, and a PDZ class II domain are indicated. Mutants, myr-mt-Fus1, in which the codon GGC for Gly<sub>2</sub> was changed into GCC for Ala<sub>2</sub>, and Dmt-Fus1, in which codon ATT for Ile<sub>87</sub> and ATC for Ile<sub>91</sub> were changed into CCT for Pro<sub>87</sub> and CCC for Pro<sub>91</sub>, respectively, were constructed by site-directed mutagenesis. The C-del-Fus1 is a tumor-related C-terminal deletion mutant, derived by abnormal mRNA splicing. **B.** Immunoblot analysis of endogenous Fus1 protein expression in normal lung fibroblast WI-38 cells grown in phosphate-buffered saline (PBS), under conditions of contact inhibition (over-confluence growth) or after exposure of the cells to ultraviolet irradiation (100 j for 5 min) and in NSCLC cells. The same blots were also probed for  $\beta$ -actin to ensure equal loading. **C.** Immunofluorescence image analysis in wt-*FUS1*-transfected H1299 cells with FITC-conjugated rabbit anti-Fus1 antibodies (**a**) and immunohistochemical analysis of Fus1 protein expression in the normal lung (**b** and **c**) and bronchial epithelial (**d**), and primary lung tumors (**e-h**) cells in formalin-fixed/paraffin-embedded tissue samples. The wt-Fus1 was shown to have a typical mitochondria /ER membrane localization in cytoplasm (**a**); expression of Fus1 was detected in cytoplasm in normal lung (**a** and **b**) and bronchial epithelia (**c**); Fus1 expression was also detected in some tumor cells in one primary NSCLC (**e**) but undetectable in other primary NSCLCS (**f, g, h**), using rabbit anti-Fus1 polyclonal antibodies at 1:2000 dilution. Magnifications are: 400x (**e**); 1000x (**c, d, f, g, h**).



**Figure 2.** Verification and detection of myristoylation of Fus1 protein by a SELDI-TOF-MS spectrometry analysis on an anti-Fus1-ACPA. **A.** Detection of Fus1 proteins captured on the anti-Fus1 antibody-coated preactivated surface (PS20) chip in wt-*FUS1* or myr-mt-*FUS1*-containing plasmid-transfected H1299 cells. The myristoylated Fus1 proteins are specifically and precisely detected as a peak with a mass of 12174 d and the unmyristoylated Fus1 (myr-mt-Fus1) with a mass of 12024 d, compared with the calculated mass of 12174 d for the myristoylated wt-Fus1 and 12025 d for the myr-mt-Fus1, respectively. No Fus1 proteins were detected in either phosphate-buffered saline (PBS) mock or *LacZ* control cells. **B.** ACPA assay with PS20 chips coated with nonspecific antibodies (anti-101F6). No Fus1 proteins were detected on these mass spectra when the same protein lysates in **A** were applied. **C.** Detection of status of Fus1 protein expression and posttranslational modification in LCM-enriched human primary lung tumor (T) and adjacent noninvolved normal (N) cells, shown as representative pairs (*c-d* to *o-p*) from 15 tissue samples tested, by ACAP assay as described in **B**. The protein lysate prepared from wt-*FUS1* (*a*) or myr-mt-*FUS1* (*b*) transfected H1299 cells were used as positive controls. A single peak of myristoylated wt-Fus1 protein with a mass of  $12174 \pm 5.2$  d was detected in normal cells, whereas two peaks, one with a mass of 12174 d for the myristoylated wt-Fus1 and another with a mass of  $12075 \pm 8.5$  d for the unmyristoylated wt-Fus1 proteins, were detected in tumor cells. In some tumors no Fus1 peptides were detected. **D.** Western blot (WB) and immuno-precipitation western blot (IP-WB) analyses for verification of myristoylation of Fus1 proteins in H1299 transfectants. H1299 cells were transfected with either wt-*FUS1* or myr-mt-*FUS1* plasmid vectors for 48 h and then incubated with  $^{14}\text{C}$ -labeled myristic acid (American Radiolabeled Chemicals, St. Louis, MO) in a final concentration of 5  $\mu\text{Ci/ml}$  for 90



min. Cells were lysed in RIPA buffer containing 1% Nonidet P-40, 0.5% sodium deoxycholate, 0.1% SDS, and complete proteinase inhibitors (Roche, Germany) in 1 X PBS and then 80 µg of crude protein lysate was loaded onto each lane for WB. 1-2 mgs of protein lysate with 1-2 µg anti-Fus1 antibodies were used for IP. **E** and **F**. Effect of myristoylation on Fus1 protein synthesis and stability by Western-blot analysis during a 60-h time course posttransfection (**E**) and with a 3-h interval pulse-chase after treatment with 50 µM of protein synthesis inhibitor cyclohexamide (cHA) (**F**) in *wt-FUS1* (left panels) or *myr-mt-FUS1* (right panels) transfected H1299 cells. **G** and **H**. Effect of proteasome inhibitor MG132 on demyristoylation-induced degradation of Fus1 proteins. H1299 cells were transfected with *wt-FUS1* or *myr-mt-FUS1* plasmid DNAs for 24 h and then treated with DMSO (0) and varied concentrations (1-50 µM) of MG132 (**G**), or treated with 10 µM of MG132 in the presence (+) or the absence (-) of 50 µM of cHA (**H**). Expression of Fus1 proteins was analyzed by Western blot with anti-Fus1 antibodies. These experiments were carried at least twice with duplicates for each.

**Figure 3.** Effects of myristoylation on Fus1 protein subcellular localization and Fus1-mediated tumor-suppressing activity *in vitro*. **A**. Immunofluorescence image analysis of Fus1 protein expression and subcellular localization. H1299 cells were transfected with either *wt-Fus1*-expressing (*a* and *b*) or *myr-mt-Fus1* (*c* and *d*)-expressing plasmid vectors. Fus1 proteins were probed with FITC-conjugated anti-Fus1 antibody (green) and the nucleus was stained with Hoechst dye (blue; Sigma Chemical Co., St. Louise, MO). **B** and **C**, Expression of Fus1 genes and proteins in H1299 transfectants were verified by RT-PCR (**B**) and by Western-blot (**C**) analysis. **D** and **E**. Effect of myristoylation of Fus1 protein on tumor cell-derived clonogenicity *in vitro*. H1299 cells ( $1 \times 10^6$ ) were transfected with plasmid DNAs using FUGEN 6 *in vitro*



transfection reagent (Roche Molecular Biochemicals, Indianapolis, IN). Four micro-grams of wild-type (wt-*FUS1*), myristoylation-deficient mutant (myr-mt-*FUS1*), or hydrophilic double mutant (dmt-*FUS1*) of Fus1-expressing plasmids were co-transfected with 1 µg of the neomycin-resistant gene-containing pcDNA3.1 vector (Invitrogen, Carlsbad, CA); the pcDNA3.1 (1 µg) vector alone and the pcDNA3.1 plus wt-p53 plasmid were used as negative and positive controls, respectively. Twenty-four hours after transfection, cells were harvested, stained with trypan blue, and counted. Five thousand cells were re-plated on a 100-mm tissue culture dish in triplicate and grown in 5% fetal bovine serum supplemented-RPMI 1640 medium containing 40 µg/ml of G418 for 2-3 weeks. The numbers of G418-resistant colonies were counted after staining with Crystal Violet (D) and the quantitative analysis is shown in E. The experiments were repeated at least three times. The error bars represent the standard deviations, and the differences between the pcDNA3.1 vector alone and each testing construct is statistically analyzed by two-tailed student *t*-test.  $P \leq 0.05$  is considered significant.

**Figure 4.** Effect of myristoylation of Fus1 protein on Fus1-mediated tumor-suppressing activity *in vivo*. **A.** Effect on H1299 human tumor xenograft growth in nude mice. The human NSCLC H1299 cells were inoculated subcutaneously in nude mice. When the tumor reached 5 to 10 mm in diameter 2 weeks after tumor inoculation, it was injected with DOTAP-cholesterol-complexed wt-*FUS1* or myr-mt-*FUS1* plasmid vectors (*FUS1*-Lipoplex) at a dose of 25 µg plasmid DNA:10 nmol liposome /tumor each in 100 µl of D5W (5% Dextrose in water) for three times within a week. PBS and *Lac-Z* were used as mock and negative controls, respectively. Results were reported as the mean  $\pm$  SD in 5-10 mice for each treatment group. Tumor volumes were normalized by the percentage increase of tumor sizes after treatment relative to those at the



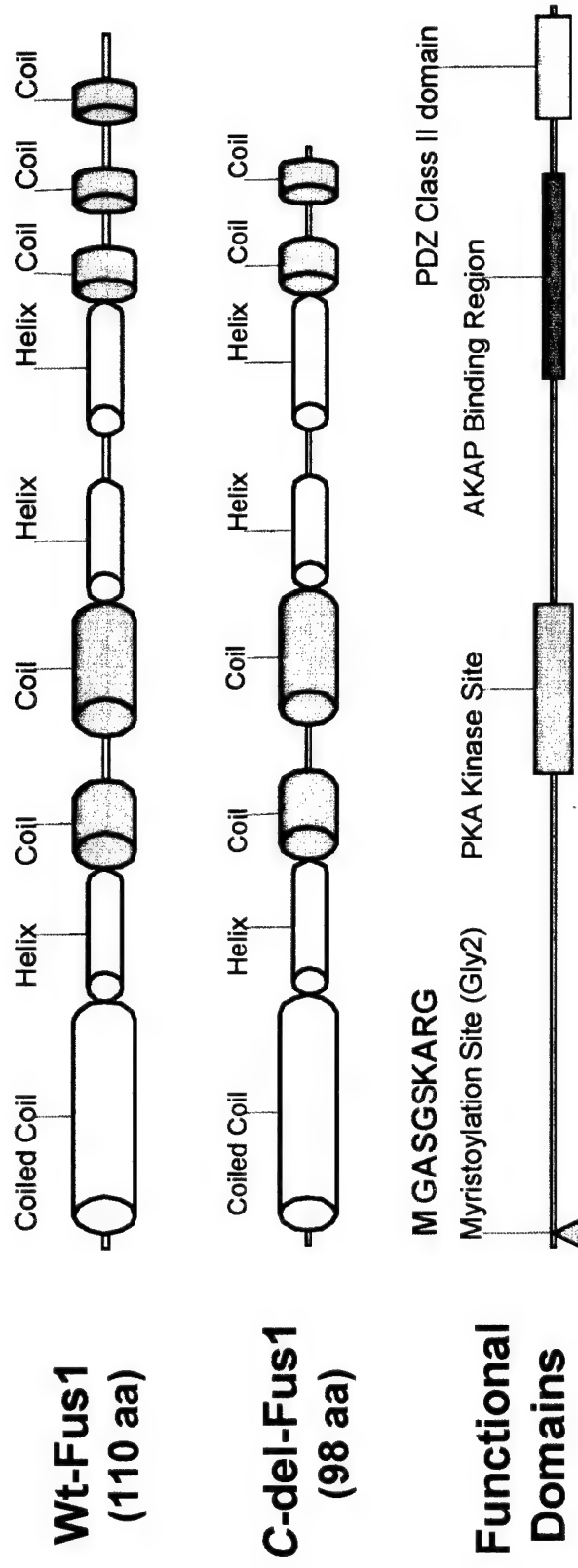
beginning of the treatment in each group. The mean tumor volumes  $\pm$  SE from these experiments are shown. ANOVA was performed to determine statistical significance between each treatment group using Statistica software (StatSoft Inc. Tulsa, OK), and  $P \leq 0.05$  was considered significant. **B.** Effect of systemic administration of *FUS1*-Lipoplex on development of A549 experimental lung metastases in nude mice. All animals were injected intravenously with various lipoplexes every 2 days for 3 times at a dose of 25  $\mu$ g plasmid DNA:10 nmol liposome each in 100  $\mu$ l of D5W per animal; PBS alone was used as a mock control and *LacZ* as a negative control. Each treatment group consisted of 10 animals. Lungs were harvested 2 weeks after the last injection, and metastatic colonies on the surfaces of lung were counted without knowledge of the treatment groups. Error bars represent standard error (SE). A nonparametric t-test (Wald-Wolfowitz Runs Test) was performed to determine the statistical significance between each treatment group using Statistica software (StatSoft Inc.), and  $P \leq 0.05$  was considered significant. A significant inhibition of metastasis development was observed in mice treated with wt-*FUS1* ( $P < 0.001$ ) and dmt-*FUS1* ( $P < 0.001$ ), compared to mice treated with PBS or *LacZ*, but there was no significant inhibition in mice treated with, myr-mt-FUS1 ( $P = 0.892$ ). The representative India ink-stained lungs and hematoxylin and eosin-stained formalin-fixed/ paraffin-embedded tissue sections in each treatment group are shown in **C**. The white spots on the lung surfaces indicate the metastatic tumor colonies. **D.** Induction of apoptosis by wt-Fus1 expression *in vivo*. The A549 experimental metastases tumor-bearing mice were treated with Fus1-lipoplexes for three times within a week at a same dose mentioned in **B**. Forty-eight h after last treatment, animals were killed and lungs were harvested and freshly frozen. Induction of apoptosis was analyzed using an In Situ Apoptosis Detection Kit with FITC-dUTP-labeled TUNEL reaction (Roche Biochemicals) and florescence images were examined under a



fluorescence microscope and recorded with an equipped digital camera (panels **a-c**). The tumor morphology was shown in photographs **d-f**, taken at the same positions as above **a-c** under regular optical light source.



A.



${}^2\text{MGASGSKARG} \rightarrow {}^2\text{MAASGSKARG} \text{ (GCC)}$

**Myr-mt-Fus1**  
(Gly<sub>2</sub> → Ala<sub>2</sub>)

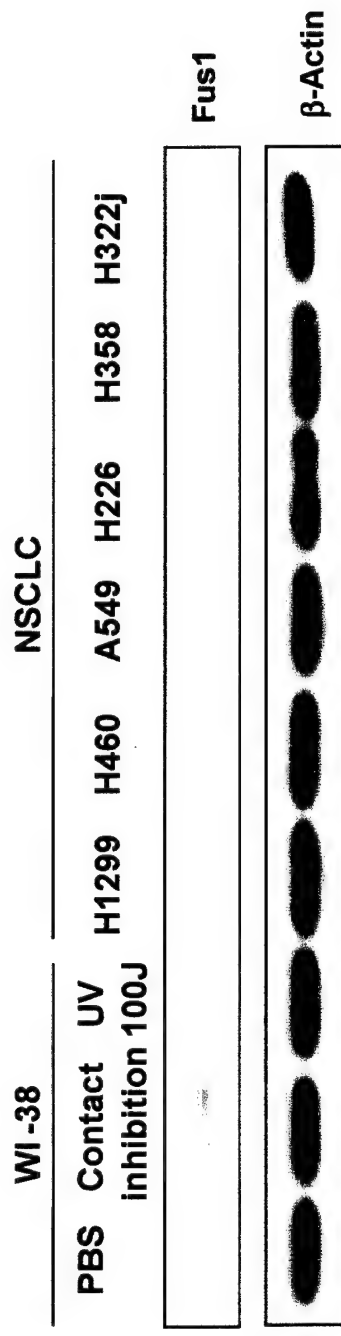
**87<sup>91</sup> NL PQG VKG → NL<sup>87</sup> PQG<sup>91</sup> VKG (ATT) (CCT) (ATC) (CCC)**

**Dmt-Fus1**  
(Ile<sub>87</sub>, 91 → Pro<sub>87</sub>, 91)

**Figure 1A**



**B.**



**C.**

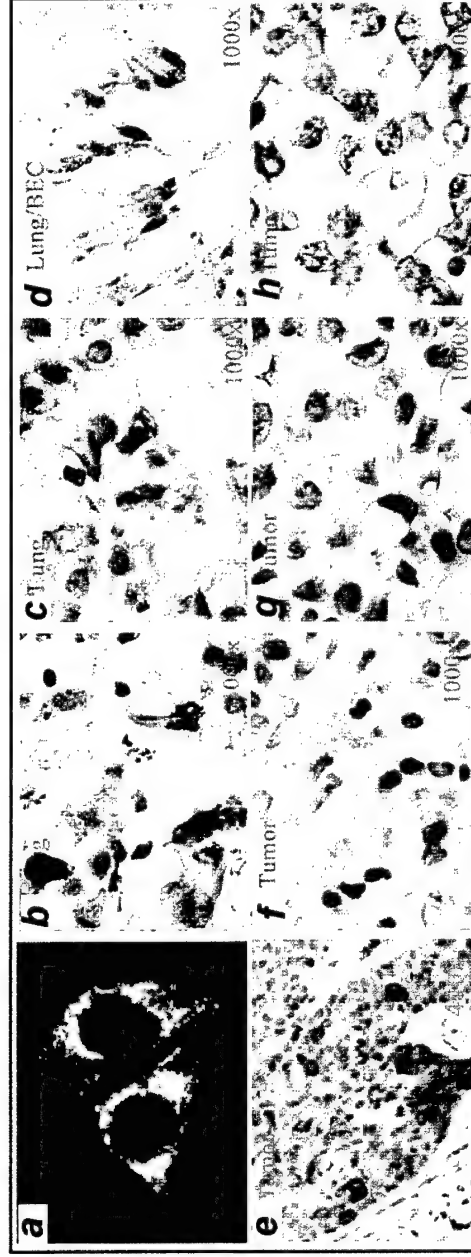
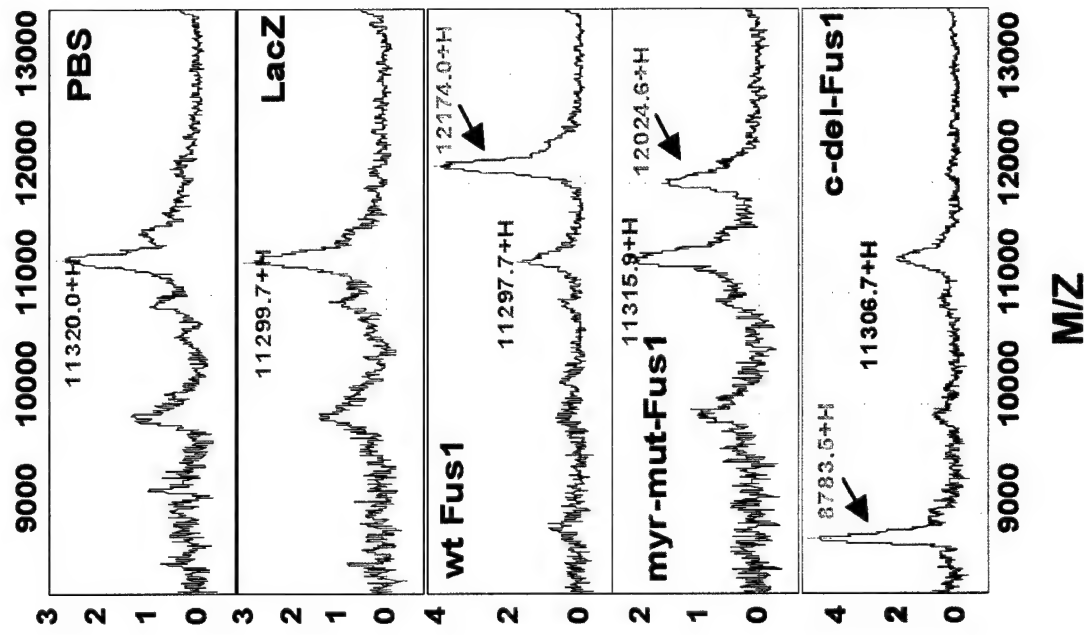


Figure 1B and C



**A.**



**B.**

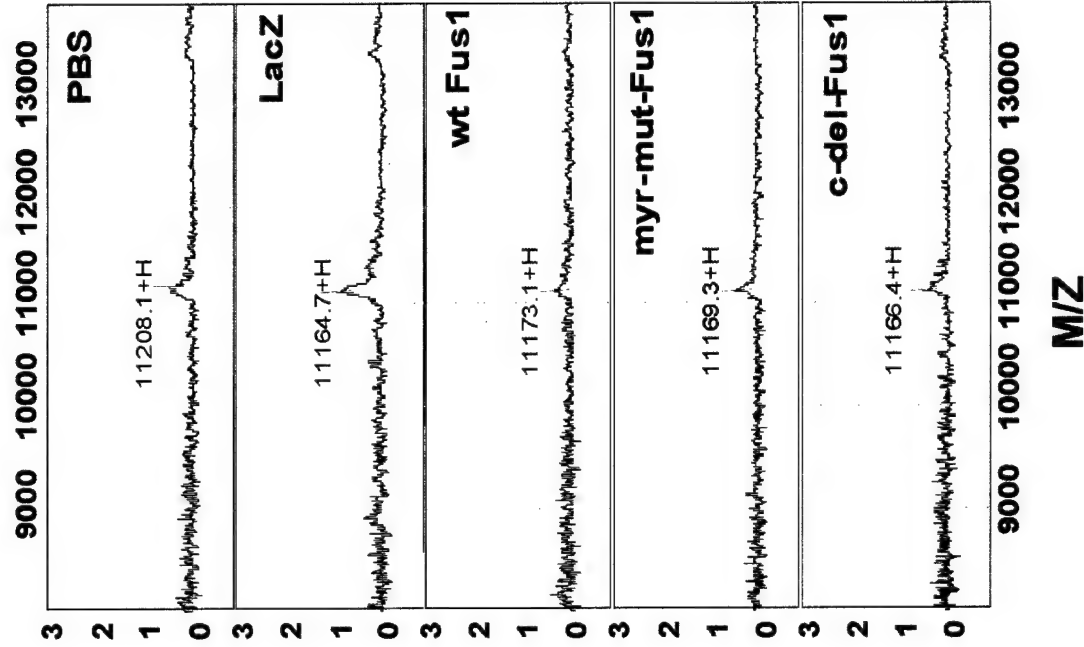


Figure 2A,B



C.

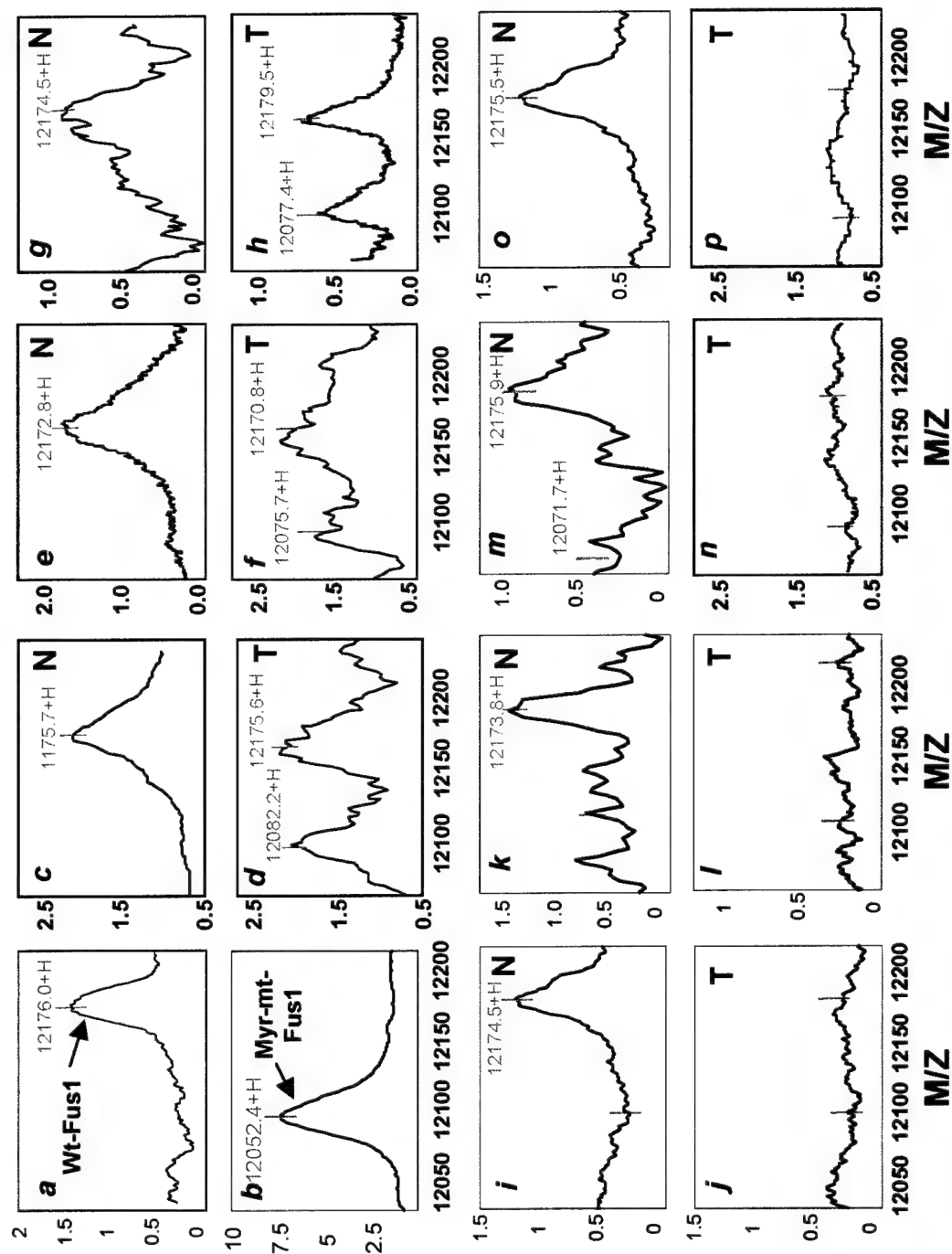


Figure 2C



D.

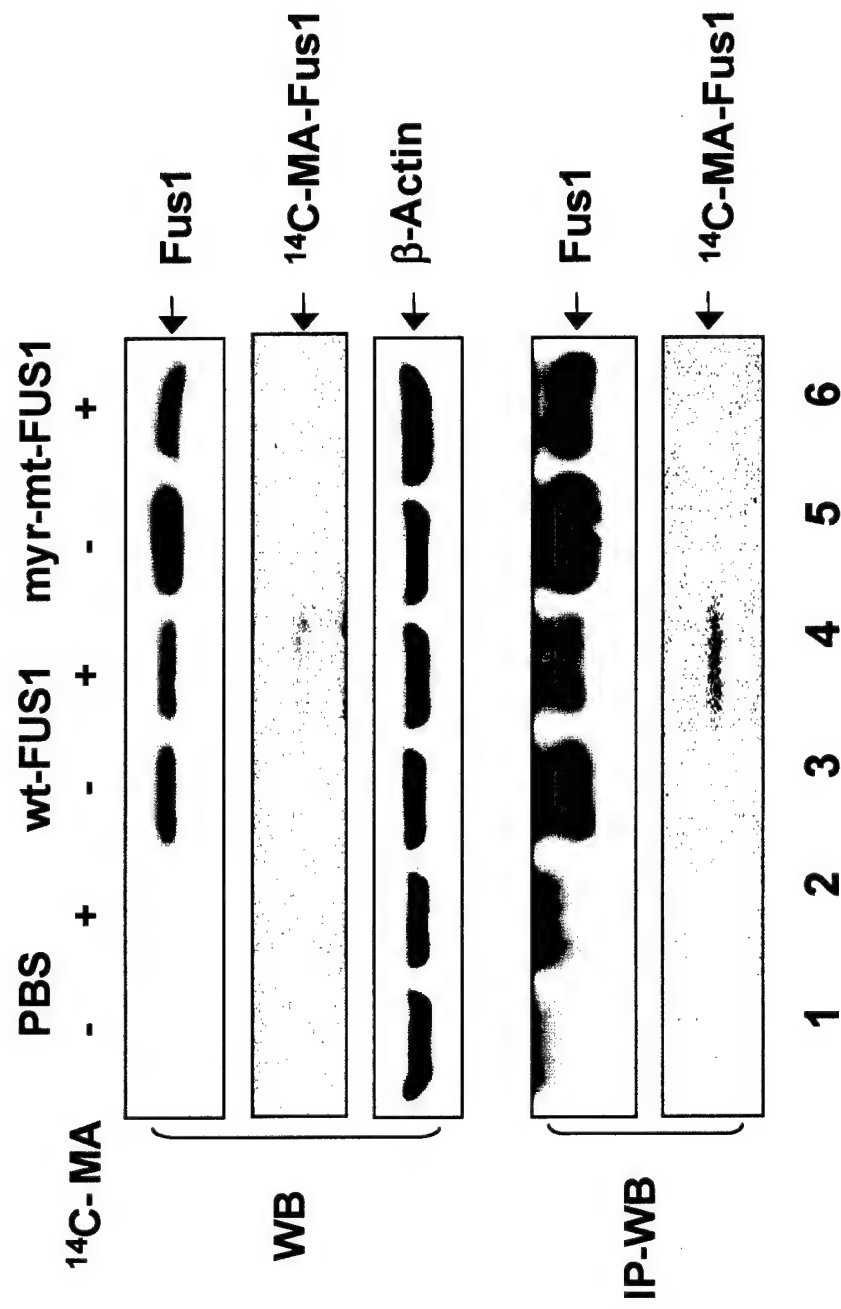


Figure 2D



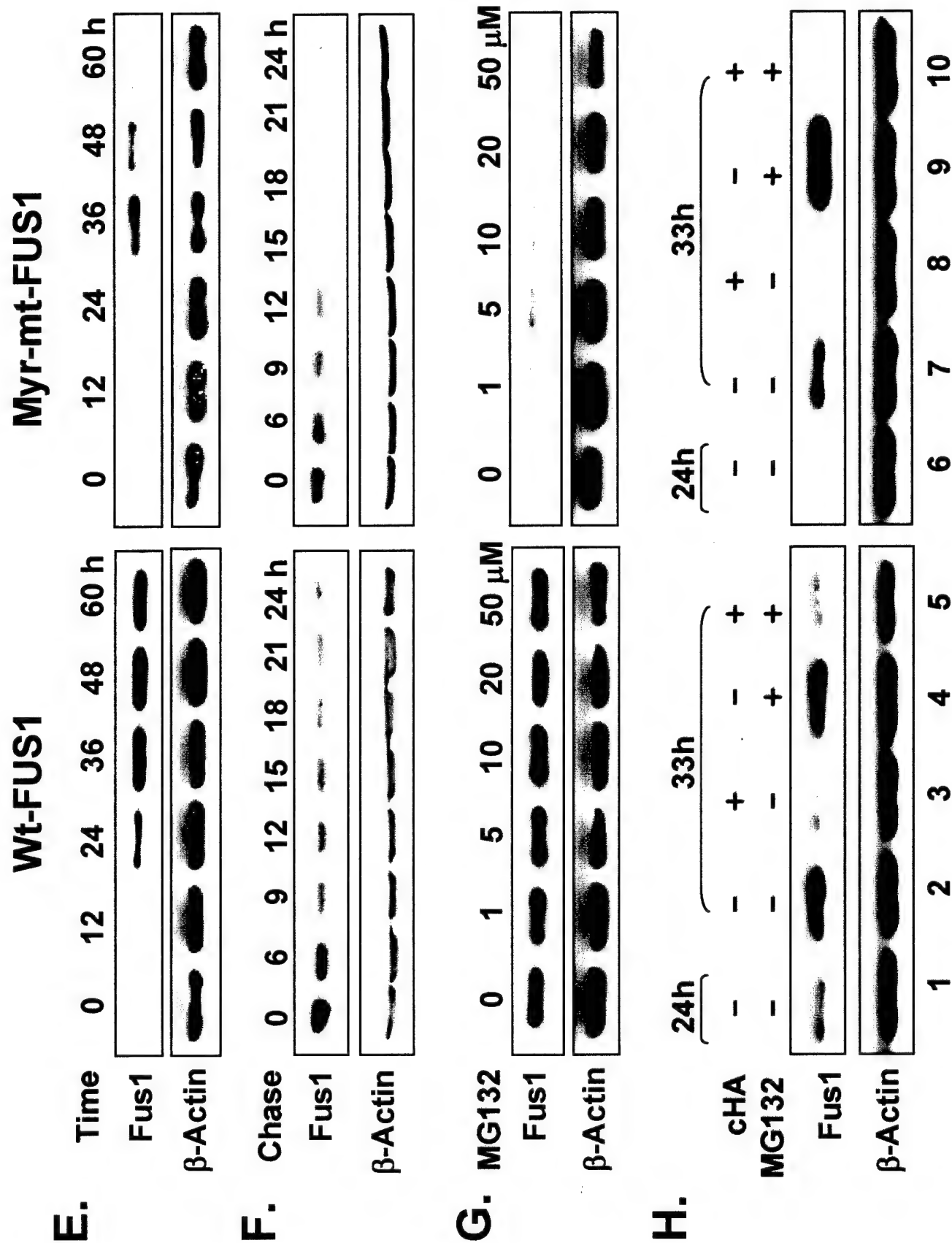
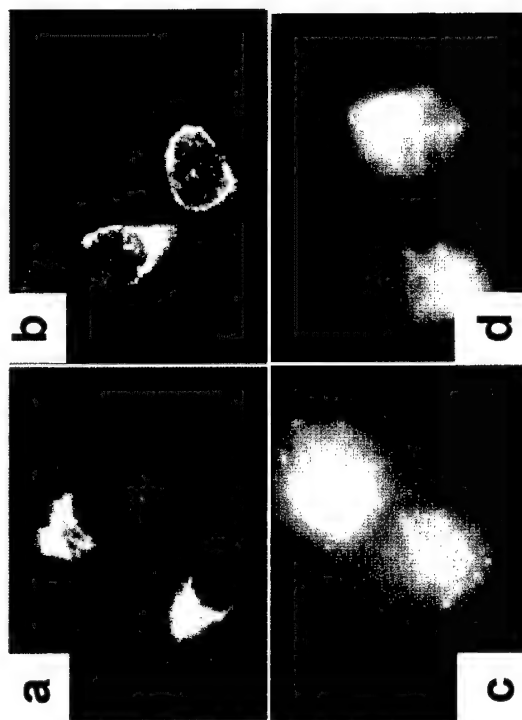


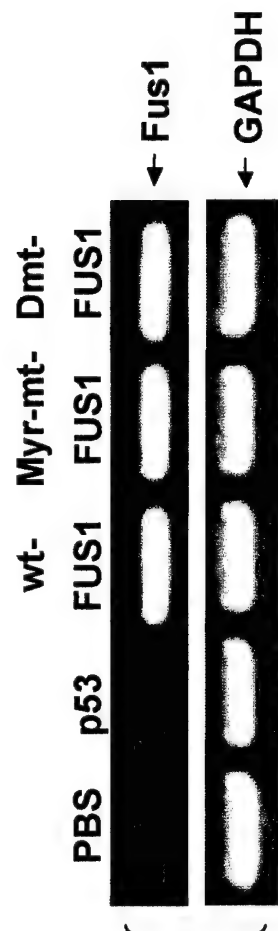
Figure 2E-H



A.



B.



C.

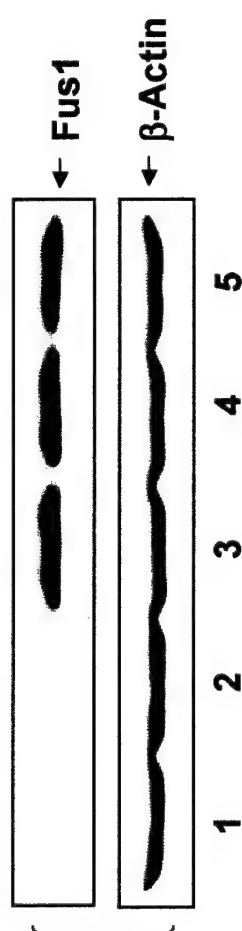

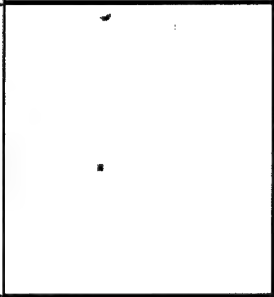
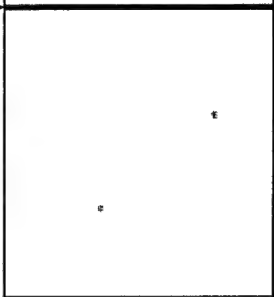
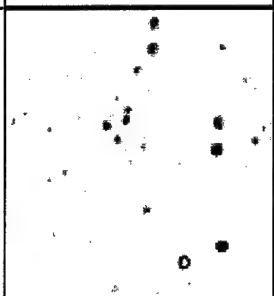
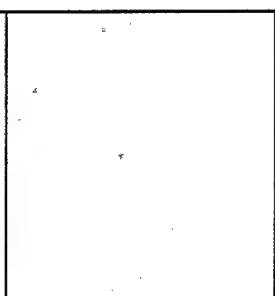


Figure 3A,B,C



D.

pcDNA3.1	pcDNA3.1 + wt-p53	pcDNA3.1 + wt-FUS1	pcDNA3.1 + myr-mt-FUS1	pcDNA3.1 + dmt-FUS1
				

E.

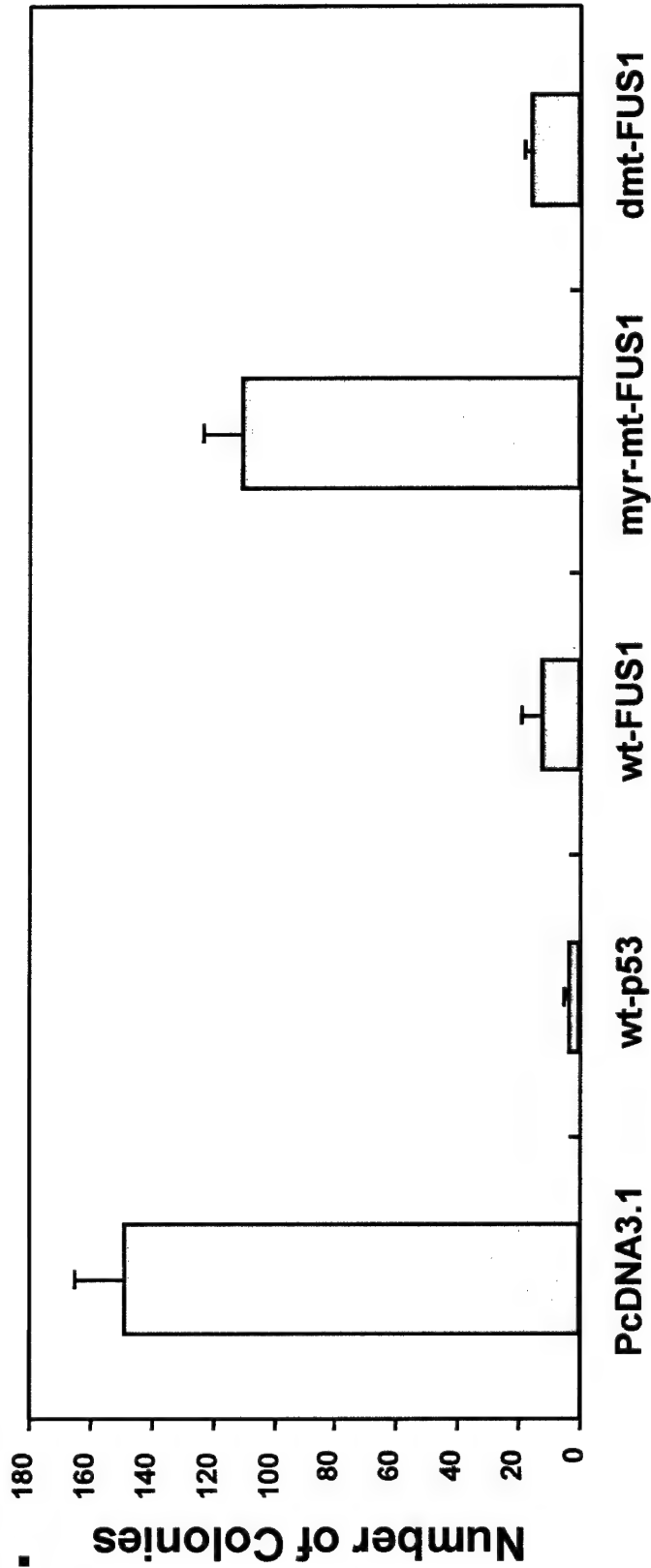


Figure 3D,E



A.

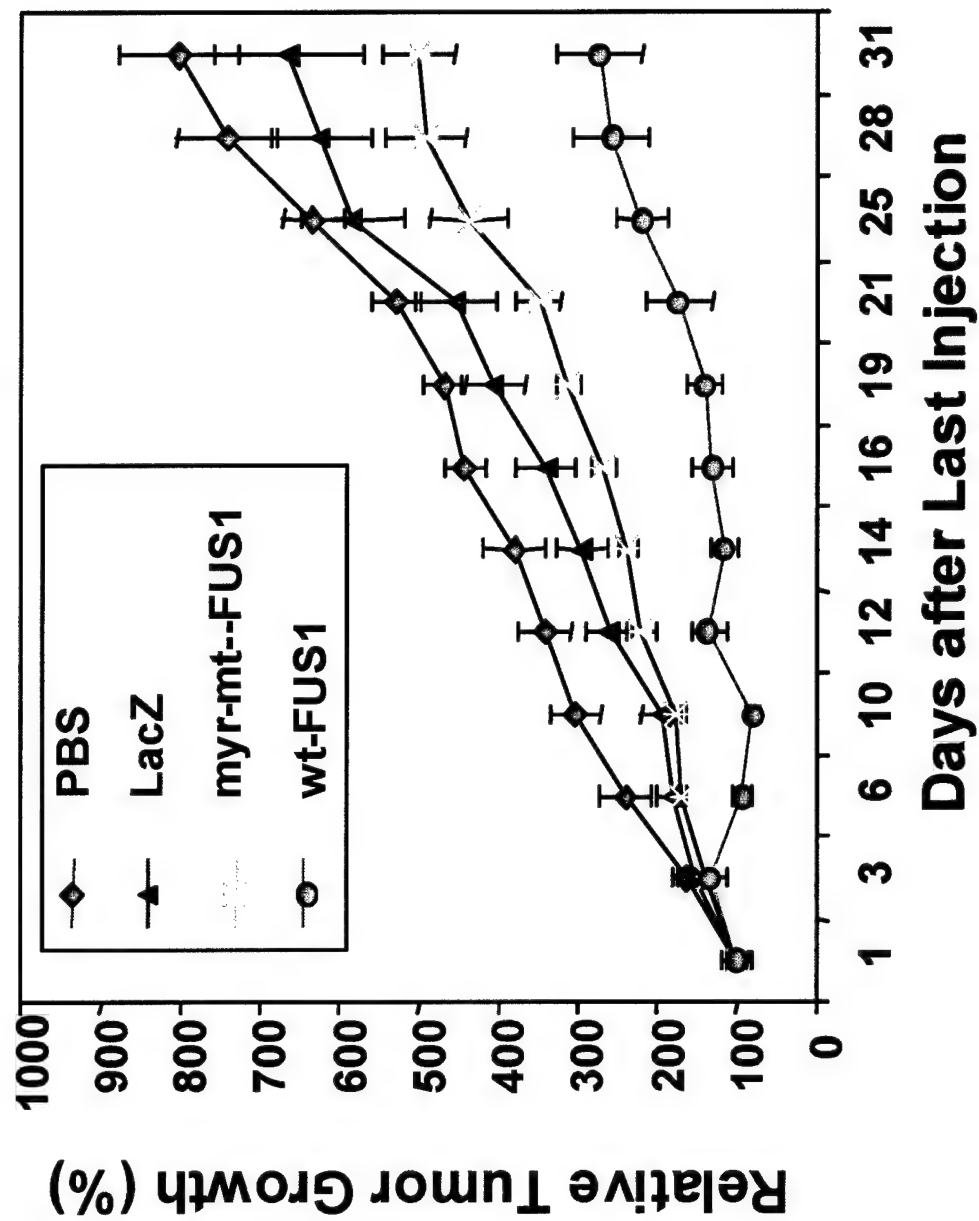
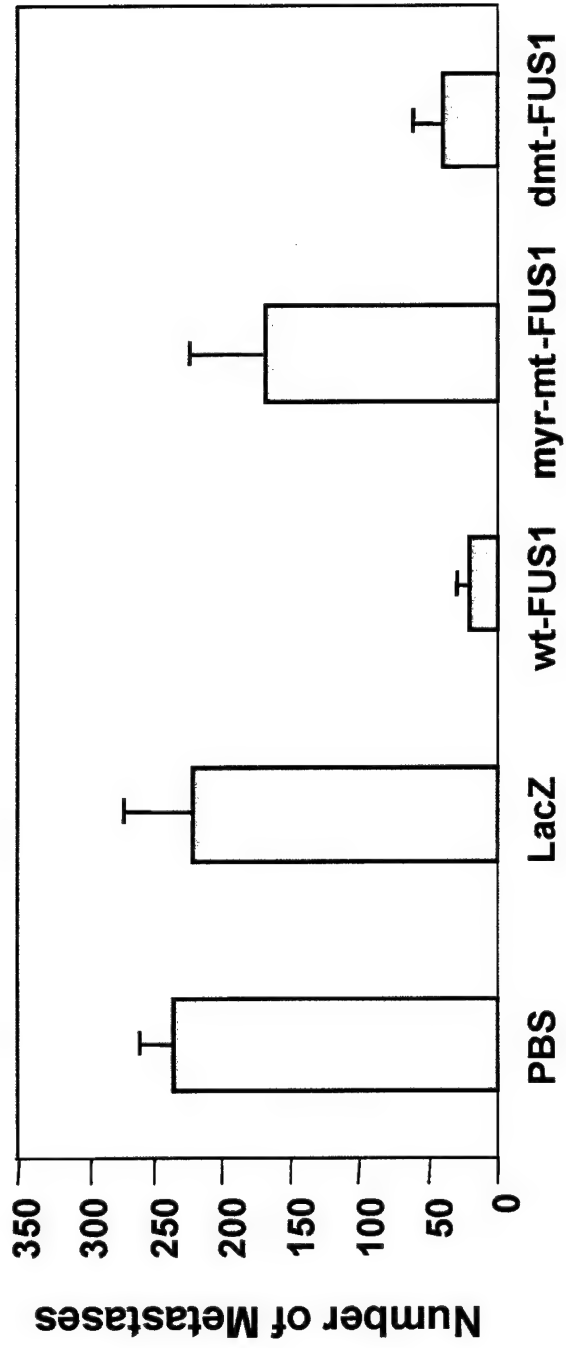


Figure 4A



**B.**



**C.**

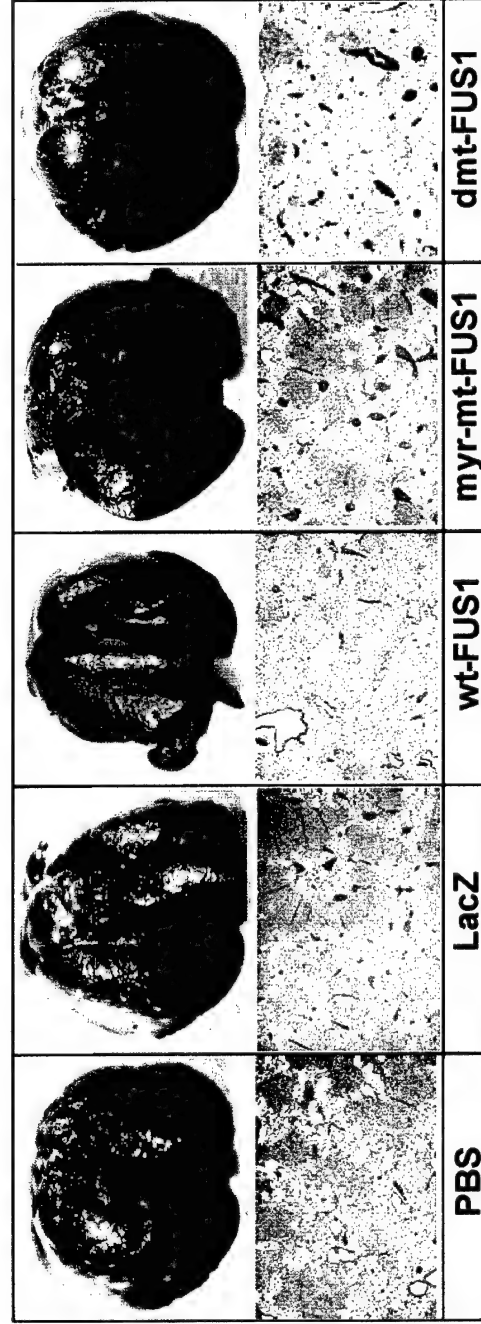


Figure 4B, C



**D.**

	<b>PBS</b>	<b>wt-FUS1</b>	<b>myr-mt- FUS1</b>
--	------------	----------------	---------------------

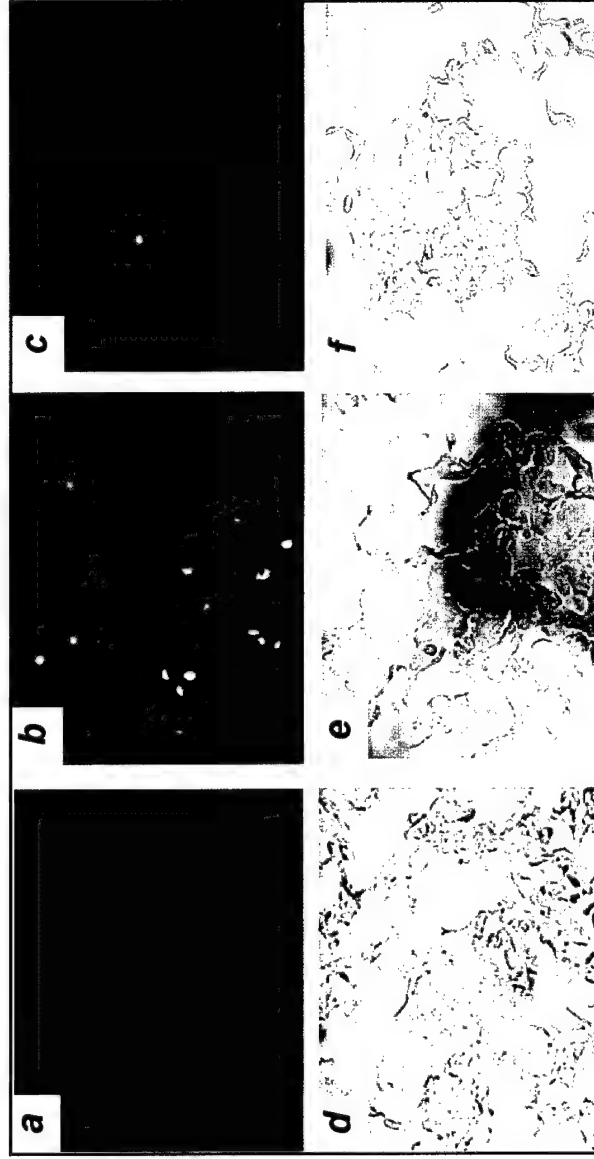


Figure 4D





# Department of Biostatistics

## **DECISION ANALYSIS OF PROPHYLACTIC CRANIAL IRRADIATION FOR PATIENTS WITH SMALL CELL LUNG CANCER**

**B. Nebiyou Bekele, J. Jack Lee, Scott B. Cantor  
Xian Zhou, and Jin Soo Lee**

Technical Report #002-03

April 2003

1515 Holcombe Boulevard, Unit 447

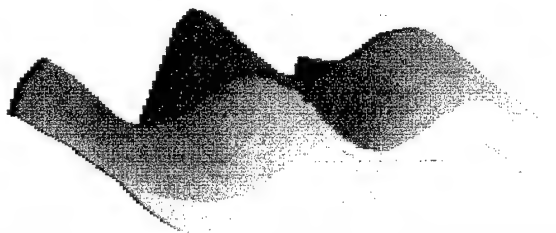
Houston, Texas USA 77030-4009

Telephone: (713) 745-5984 Facsimile: (713) 745-4940

<http://www.mdanderson.org/depts/biostatistics>

E-mail: [statreport@odin.mdacc.tmc.edu](mailto:statreport@odin.mdacc.tmc.edu)

THE UNIVERSITY OF TEXAS  
MD ANDERSON  
CANCER CENTER



TECHNICAL REPORT #002-03  
APRIL 2003  
DECISION ANALYSIS OF PROPHYLACTIC  
CRANIAL IRRADIATION FOR PATIENTS WITH  
SMALL CELL LUNG CANCER  
B. NEBIYOU BEKELE, J. JACK LEE, SCOTT B. CANTOR,  
XIAN ZHOU, AND JIN SOO LEE  
1515 HOLCOMBE BOULEVARD, UNIT 447  
HOUSTON, TEXAS USA 77030-4009  
TELEPHONE: (713) 745-5984 FACSIMILE: (713) 745-4940  
WWW.MDANDERSON.ORG/DEPTS/BIOSTATISTICS  
E-MAIL: STATREPORT@ODIN.MDACC.TMC.EDU



# Decision Analysis of Prophylactic Cranial Irradiation for Patients with Small Cell Lung Cancer<sup>1</sup>

B. Nebiyu Bekele,<sup>2,3</sup> Ph.D., J. Jack Lee,<sup>2,3,4</sup> Ph.D.,  
Scott B. Cantor,<sup>2</sup> Ph.D., Xian Zhou,<sup>2</sup> M.S., Jin Soo Lee,<sup>5</sup> M.D.

<sup>1</sup>Supported in part by grants from the National Cancer Institute CA16672, CA91844 and grants from the Department of Defense DAMD17-01-1-0689, DAMD17-02-1-0706.

<sup>2</sup>The University of Texas M. D. Anderson Cancer Center

<sup>3</sup>BNB and JJJ contributed equally to the work.

<sup>4</sup>To whom requests for reprints should be addressed:

Department of Biostatistics, The University of Texas M. D. Anderson Cancer Center,

1515 Holcombe Blvd., Unit 447, Houston, Texas 77030-4009

Telephone: (713) 794-4158

Fax: (713) 745-4940

Email: jjlee@mdanderson.org

<sup>5</sup>National Cancer Center Hospital of Korea, 809 Madul-dong, ilsan-gu, Gyeonggi-do, 411-764, Republic of Korea.

Running Title: Decision Analysis of PCI in SCLC

Keywords: Quality-adjusted life expectancy, long-term toxicity, two-way sensitivity analysis, decision analysis



## **ABSTRACT**

**Background:** Although prophylactic cranial irradiation (PCI) is shown to have some survival benefit in patients with small cell lung cancer (SCLC) who have achieved a complete response, this treatment may also produce neurotoxicity (NT) and impaired cognitive function. We developed a decision-analytic model to compare quality-adjusted life expectancy (QALE) in a cohort of SCLC patients who do and do not receive PCI.

**Methods:** We explored the effect of various NT and 5-year survival rates on quality of life (QOL). The impact of QOL of PCI was assessed using quality-adjusted survival, quality-adjusted life expectancy, and evaluated by sensitivity analyses.

**Results:** At current achievable survival rates (i.e., 26% 5-year survival rate with PCI and 22% without PCI) PCI maintains a small benefit over No PCI (PCI QALE=4.23, No PCI QALE=3.81) when we assumed a 30% NT rate at year 5. If the PCI survival rate increases to 40% (36% for No PCI), No PCI is preferred over PCI for NT rates greater than 40%. Two-way sensitivity analyses show that No PCI is preferred for high NT rates and increased survival rates. As the survival rate for SCLC continues to improve, NT rate must be controlled to maintain a favorable risk benefit ratio for recommending PCI.

**Conclusions:** The current data suggest PCI offers better quality-adjusted life expectancy yet the risk-benefit ratio of PCI depends on the underlying NT rate and its impact on QOL, and the cure fraction. The role of PCI in SCLC patients needs to be critically reviewed as survival rates increase, especially for those patients who have achieved complete response.

## **INTRODUCTION**

The brain is recognized as a frequent site of metastasis in small cell lung cancer (SCLC) patients and about 10% of SCLC patients have demonstrable central nervous system metastases at initial presentation, usually in



combination with other extrathoracic sites. The brain is also recognized as a frequent site of first metastasis in SCLC patients even after initial response to chemotherapy. The incidence of clinically detectable brain metastases rises with increased length of survival and reaches 50% at 2 years [1,2]. The probability is even higher if the autopsy cases are included. Nugent et al. reported 80% probability of CNS metastases at 2 years [3]. Moreover, treatment of brain metastases is unsatisfactory; only about half of patients achieve a useful palliation after whole brain irradiation and median survival is less than 3 months after the brain metastasizes [4].

Taking into account the poor outcome of patients who developed brain metastases, Hansen proposed prophylactic brain irradiation for all patients with SCLC in 1973 [5]. The idea behind the use of prophylactic brain irradiation, later renamed prophylactic cranial irradiation (PCI) in SCLC was based on the success in reducing CNS relapse in childhood leukemia [6]. Although neurotoxicity was observed in childhood leukemia after PCI therapy, an early study reported no long-term side effects of PCI in SCLC [7]. However, subsequent investigators reported chronic long-term neurotoxicities following treatment of SCLC with PCI [8].

To date, various randomized trials have been reported in the literature [9-24] comparing survival rates in SCLC for PCI and No PCI treated groups. The results of those studies confirmed a significant reduction in the incidence of brain metastases following PCI. Moreover, a meta-analysis of the research has shown that PCI has a survival benefit [25]. PCI has been recommended for SCLC patients who have achieved complete remission (CR). Since the early 1980s, major textbooks follow these recommendations [26].

Based on the retrospective analysis of NCI data, Rosen et al, recommended PCI be given to only those who achieved CR [27].



PCI is routinely recommended for those patients who achieved a complete response to chemotherapy [26]. However, given that these patients have a greater potential for long-term survival, they may be at increased risk of chronic neurotoxicity. Moreover, as more effective chemotherapy and combined chemo-radiation improves the overall outcome and long-term survival of SCLC patients, the potential risk of chronic neurotoxicity will be greater and the quality of life becomes a more important consideration among the long-term survivors.

The purpose of this research is to explore the potential benefits of PCI therapy in SCLC patients who have achieved a complete response after accounting for the negative effects of neurotoxicity due to PCI therapy. We examine the risk-benefit ratio of PCI by varying the cure fraction and neurotoxicity rate. We postulate that if the “cure fraction” (we use 5-year survival as a surrogate for cure fraction) increases as a result of improved therapy, there will be increased risk and severity of neurotoxicity. Our results support the concept that as cure rate increases the benefit of PCI is mitigated and therefore we propose that the role of PCI in SCLC therapy should be re-evaluated, especially for those who have a greater potential for a cure.

## **METHODS**

We examine quality-adjusted life expectancy (QALE) for patients receiving PCI and compare their QALE with patients not receiving PCI after considering the impact of NT on quality of life (QOL). A decision-analytic model was used to compare QALE in the PCI and No PCI treated groups using a cohort of simulated SCLC patients. To incorporate the impact of chronic neurotoxicity on the quality of life of PCI treated patients, we calculated the quality-adjusted life expectancy based on the following assumptions. We modeled survival times in a large cohort (N=100,000) of 60 year-old, SCLC patients in complete remission with and without PCI based



on the published meta-analysis results [25]. The age of 60 was chosen because that was the median age of patients included in the meta-analysis.

#### Assumptions for the onset and frequency of Neurotoxicity

In this analysis, we explored various neurotoxicity rates. For the base case we assumed that 30% of patients who had received PCI would, *if they continue to survive*, eventually experience neurotoxicity. It should be noted that this 30% is a latent neurotoxicity rate because most patients do not survive long enough to experience neurotoxicity. If we assume a 26% 5-year survival rate, this 30% latent neurotoxicity rate results in only 10% of patients who survive long enough to actually experience onset of neurotoxicity because *most patients die before the effects of neurotoxicity are observed*. These results are consistent with the results that show a 5-year incidence of neurotoxicity of 10% as reported by Shaw et al. [28].

We assumed that the cumulative probability of neurotoxicity at time  $t$  follows a generalized logistic function

$$\text{cumulative probability of NT at time } t = \frac{\Delta}{1 + 60 \times \exp(-1.05 \times t)}$$

The functional form presented above has the following properties:

- 1)  $\Delta$  is the maximum cumulative NT rate.  $\Delta = 0.30, 0.40$  and  $0.50$ .
- 2) The cumulative NT rate of neurotoxicity is relatively low within the first 2 years after PCI treatment while the frequency increases markedly after 2 years
- 3) The cumulative NT rate begins to plateau after 6 years.

Figure 1 depicts the functional form of the overall cumulative neurotoxicity rate for 30% and 50% cumulative neurotoxicity rates.



{Figure 1 about Here}

#### Assumption for the effect of NT on Quality of Life

Neurotoxicity is degenerative in nature. Decreasing QOL after onset of NT can be captured by constructing a utility function with utility of 1 corresponding to a fully functional, healthy life and 0 corresponding to death. A non-linear utility function with a mixture of exponential distributions was applied. We explored a case in which the minimum utility reaches 0.40 (mild declining utility case) and a case in which the minimum utility reaches 0.20 (moderate declining utility case). The plots of the utility functions can be found in Figure 2. In the mild declining utility case, we assumed that the quality of life, as measured by utility, will decrease to 76% by one year after onset of neurotoxicity, and continued to decrease to 65% by two years. After this 2-year time-point, utility will decrease to 45% by 10 years after onset of neurotoxicity and to 40% by 15 years then stay at 40% thereafter. The utility rapidly declines in the first five years after onset of NT and reaches its minimum at 15 years. Another scenario we explored was to assume that the utility eventually decreases to 0.20 after onset of neurotoxicity.

The utility functions were constructed as follow. Define  $c_i$  to be the number of survival days prior to the onset of neurotoxicity and let  $d_i$  be the number of survival days after onset of neurotoxicity for the  $i$ th patient where  $i$  goes from 1 to 100,000. The total unadjusted survival time for patient  $i$  is  $S_i = c_i + d_i$ . Furthermore, define  $U_{ij}$  to be the utility of the  $i$ th patient on the  $j$ th day.



For the mildly decreasing utility case,  $U_{ij}$  is

$$U_{ij} = \begin{cases} 1.0 & \text{for } j < c_i \\ 0.378e^{-.0023(j-c_i)} + 0.28e^{-.00022(j-c_i)} + 0.342e^{-.000014 \times 10^{-5}(j-c_i)} & \text{for } c_i \leq j \leq 5478.75 + c_i \\ 0.40 & \text{for } 5478.75 + c_i < j < S_i \end{cases}$$

For the moderately decreasing utility case,  $U_{ij}$  is

$$U_{ij} = \begin{cases} 1.0 & \text{for } j < c_i \\ 0.668e^{-.0026(j-c_i)} + 0.06e^{-.00056(j-c_i)} + 0.272e^{-.000057 \times 10^{-5}(j-c_i)} & \text{for } c_i \leq j \leq 5478.75 + c_i \\ 0.20 & \text{for } 5478.75 + c_i < j < S_i \end{cases}$$

{Insert Figure 2 about Here}

### Survival Functions

Survival functions after treatment with and without PCI were based on a 1999 meta-analysis [25]. The meta-analysis was used to determine the general form of the survival curves and the benefit of PCI therapy relative to No PCI. The meta-analysis also provided us with a measure of the relative failure rate (RFR) of PCI to No PCI at 5 years. Specifically, failure rates for the PCI group and No PCI group are 81% and 86%, respectively. The resulting 5-year RFR of PCI to No PCI is 94.2%. Because improved therapy has resulted in marked improvement in survival rates since the completion of the meta-analysis, more current 5-year survival rates for PCI treated patients were obtained from a recently reported intergroup SCLC study reported by Turrisi et al [29]. The intergroup study was then incorporated to better model more up-to-date 5-year survival rates. Specifically, the 5-year survival rate for the PCI group was 26% per the inter-group results [29]. Taking this updated 5-year survival rate for the PCI group in conjunction with the 5-year RFR of PCI to No PCI obtained from the meta-analysis [25] (i.e., 94.2%), we calculated the updated No PCI 5-year survival rate to be 22%.



Survival times were modeled using a truncated log normal distribution. Although the standard log-normal distribution mimicked the survival curves associated with this patient population quite well, it has an extremely heavy tail (i.e. many observations with large values) which results in implausible death-times (e.g., death at 200 years). To mitigate this problem we used the log normal distribution to model the survival curves of patients receiving PCI for the first 15 years after treatment with or without PCI. After 15 years, we assumed that surviving patients were essentially cured and that survival rates for this cohort would then follow the life tables for the general population at that age [30].

It should be noted that as we varied the 5-year survival rates in the PCI and No PCI groups for the purpose of sensitivity analysis, the 5-year relative benefit of PCI to No PCI was held constant for all scenarios when cure rate increases as a result of more effective chemotherapy. This is based on the assumptions that (1) in the No PCI group, the portion of failure with and without brain metastasis remains the same, and (2) the percent brain metastasis reduction of PCI with respect to No PCI remains the same, and (3) the portion of failure with and without brain metastasis remains the same in the PCI group as well. Assumption (3) is conservative in favor of a survival benefit for the PCI group. Since PCI is a non-systematic therapy, it should not protect patients from metastases occurring at other sites.

#### Quality-Adjusted Life Expectancy

We modeled the effect of NT on QOL using a mixture of exponential functions as described before. The relationship between QOL and survival is summarized by the quality-adjusted life years (QALE). QALE for the  $i$ th patient receiving PCI therapy ( $QALY_i$ ) is defined as.



$$QALY_i = \frac{\sum_{j=1}^{S_i} U_{ij}}{365.25}$$

We obtain the QALE by taking the average of the QALY's for all patients receiving PCI therapy

$$QALE = \frac{\sum_{i=1}^{N_{PCI}} QALY_i}{N_{PCI}}$$

## RESULTS

### Quality-Adjusted Survival and Quality-Adjusted Life Expectancy

Quality-adjusted survival curves for various neurotoxicity rates and 5-year survival rates are given in Figure 3.

Estimated survival curves for PCI without neurotoxicity were included for reference purposes. The adjusted survival plots were calculated assuming that utility decreases to 0.40 over 15 years after onset of neurotoxicity.

Figure 3a shows that PCI is always better than No PCI but as NT increases and/or the cure rate increases, the No PCI curve remains the same while the quality-adjusted PCI curve drops. As a result when neurotoxicity is 30% and the No PCI 5-year survival rate is 22% the QALE for the PCI group is 4.23 years while the group without PCI had a QALE of 3.81 years which supports the use of PCI at current survival rates if we look only at the point estimates of QALE in the two groups. If the neurotoxicity rate is actually 50% then, although PCI is still preferred, the benefit of this treatment is decreased relative to the benefit observed when the NT rate is 30% (Figure 3c). If the No PCI cure rate is 36% and the NT rate is 30%, the No PCI has only a slightly lower QALE relative to the PCI group (Figure 3d) and has better QALE than PCI at 40% and 50% NT rates.

{Insert Figure 3 about Here}



Assuming that utility decreases to 0.20 over ten years after onset of neurotoxicity, quality-adjusted survival curves for various neurotoxicity rates and 5-year survival rates are given in Figure 4. Figure 4a shows that when neurotoxicity is 30% and the No PCI 5-year survival rate is 22% the QALE for the PCI group is 4.09 years while the group without PCI had a QALE of 3.81 years which again supports the use of PCI at current survival rates. The potential negative effects of PCI become apparent in Figures (4c-4f). In each of those scenarios, No PCI has better QALE compared to PCI. For example, in the scenario depicted by Figure 4f in which the NT rate is 50% and the cure rate in the No PCI group is 36%, the QALE in the PCI group is 5.26%, which is 12% lower than in the No PCI group.

{Insert Figure 4 about Here}

#### Two-Way Sensitivity Analysis

Figure 5 is a contour plot showing the regions in which No PCI is preferred over PCI or vice versa when utility is assumed to decrease to 0.40 over 15 years. In this two-way sensitivity analysis, PCI is preferred below the solid line and No PCI is preferred above this line (gray-shaded area). At current 5-year survival rates of 22% and 26% for the No PCI and the PCI groups, respectively, it is clear that PCI is preferred except when the neurotoxicity rate is above 52%. At a 30% neurotoxicity rate the 5-year No PCI survival rate must be 42% (PCI survival rate of 46%) before No PCI is preferred over PCI. At a neurotoxicity rate of 50%, No PCI is preferred when the 5-year No PCI survival rate is 23% (PCI survival rate of 27%) or higher (a very plausible scenario given current clinical trends).

{Insert Figure 5 about Here}

Figure 6 is a contour plot showing the regions in which No PCI is preferred over PCI when utility is assumed to decrease to 0.20 over 15 years. For this case, at a 30% cumulative neurotoxicity rate No PCI is preferred over



PCI when the 5-year No PCI survival rate is 32% (36% survival rate for PCI group). At neurotoxicity rates of 50%, No PCI is preferred when the 5-year survival rates are as low as 17 % (21% PCI survival rate). Two-way sensitivity analysis shows that as the 5-year survival rate of no PCI group continues to increase, NT rate must be controlled to maintain a favorable risk benefit ratio for recommending PCI.

{Insert Figure 6 about Here}

## DISCUSSION

Chemotherapy, with or without chest radiotherapy, improves the survival of SCLC patients and even cures a small fraction of patients who present with limited stage disease. However, as a pharmacological sanctuary site, the brain is a frequent site of relapse even after complete response and the brain has been considered. Because SCLC is a radiosensitive tumor, PCI has been advocated for small cell lung cancer since 1973 [5]. Historically, there had been growing concerns about late neurotoxicities. Johnson et al. reported that among 20 long-term survivors ranging between 2.4 years and 10.6 years, fifteen (75%) had neurological complaints which included memory loss, walking or writing difficulties, weakness [31]. Fifteen (75%) of them also had abnormal brain CT findings and 12 (60%) had abnormal mental status examination. Lee et al. reported 3 cases of severe dementia, confusion, and ataxia among 24 long-term survivors [8] Similarly, Fonseca et al. reported leuko-encephalopathy in 5 of 35 patients (14%) who received PCI, where the mean time to onset of symptoms after termination of irradiation was approximately one year [32]. Although prospective randomized studies rarely reported serious neurotoxicities, the follow-up period in these trials is relatively short thus making it difficult to draw any meaningful conclusions. Accordingly, the role of PCI in the management of small cell lung cancer needs to be critically reviewed in the light of existing evidence of chronic neurotoxicity and prospect of better survival outcome in the future.



This research has revealed key points related to issues that physicians should consider for patients with SCLC who have achieved a complete response before deciding whether to recommend PCI therapy for the management of patients with good long-term disease control and cure potential. It is clear that at current survival rates, PCI therapy is beneficial in extending the survival of patients with small cell lung cancer who have achieved a complete response. Under various scenarios we showed that the benefit of PCI relative to No PCI highly depends on the rate and severity of neurotoxicity rate and the cure fraction.

As the 5-year survival rates increase due to improved therapies, PCI may have inferior QALE relative to No PCI. More importantly, the role of PCI in SCLC patients who have achieved complete response needs to be carefully evaluated as these patients are expected to have better 5-year survival rates. Furthermore, there may be subsets of patients, who because of their baseline characteristics (such as younger patients and females), have higher cure potential than the "average" patient. In those patient populations, we should better understand the severity of neurotoxicity so as to better delineate the most appropriate treatment options.

It has been noted that increased total dose and higher dose fractionation reduces the CNS relapse rate. However, because of the fear that higher dose fraction might be associated with more neurotoxicity, 2.5 Gy X 10 fractions are more widely recommended at this point. How this modification of dose/dose fraction schedule will affect the outcome is unclear. Our analysis suggests that with 40% minimum utility and a 30% plausible NT rates (i.e. 30%), PCI is associated with decreased QALE if the 5-year survival rate is greater than 42% in the No PCI group. This lead us to conclude that as the cure fraction of SCLC continues to increase as a result of improved systematic therapy PCI may result in inferior QALE. The role of PCI in SCLC patients needs to be critically reviewed as survival rates increase, especially for those patients who have achieved complete



response. Efforts need to be made to increase the effectiveness of tumor control rate while reducing long-term toxicity to make PCI as safe and effective as possible.



## REFERENCES

1. Bunn BA, Nugent JL, Matthews MJ. Central nervous system metastases in small cell lung carcinoma. *Semin Oncol* 1978;5:314-22.
2. Komaki R, Cox JD, Whitson W. Risk of brain metastases from small carcinoma of the lung related to length of survival and prophylactic irradiation. *Cancer Treat Rep* 1981;65:811-14.
3. Nugent JL, Bunn PA, Matthews MJ, Inde DC, Cohen MH, Gazder A, Minna JD. CNS metastases in small cell bronchogenic carcinoma: Increasing the frequency and changing pattern with lengthening of survival. *Cancer* 1979;44:1885-93.
4. Carmichael J, Crane JM, Bunn PA, Glatstein E, Ihde DC. Results of Therapeutic cranial Irradiation in small cell lung cancer. *Int J Radiat Oncol Biol Phys* 1988;14:455-59.
5. Hansen HH: Should initial treatment of small cell carcinoma include systemic chemotherapy and brain irradiation? *Cancer Chemother Rep* 1973; Part 3 4:239-241.
6. Bleyer WA, Poplack DG: Prophylaxis and treatment of leukemia in the central nervous system and other sanctuaries. *Semin Oncol* 1985;12:131-48.
7. Catane R, Schwade JG, Yarr I, et al: Follow-up neurological evaluation in patients with small cell lung carcinoma treated with prophylactic cranial irradiation and chemotherapy. 1981; *Int J Radiat Oncol Biol Phys* 7:105.
8. Lee JS, Umsawasdi T, Lee YY, Barkley WT, Murphy WK, Welch S, Valdivieso M. Neurotoxicity in Long-Term Survivors of Small Cell Lung Cancer. *International Journal of Radiation Oncology Biol Phys* 1986;12:313-321.
9. Arriagada R, Le Chevalier T, Borie F, et al. Prophylactic cranial irradiation for patients with small-cell lung cancer in complete remission. *Journal Natl Cancer Inst* 1995;87:183-90.
10. Gregor A, Cull A, Stephens RJ, et al. Prophylactic cranial irradiation is indicated following complete response to induction therapy in small cell lung cancer: results of a multicenter randomized trial. *Eur J Cancer* 1997;33:1752-8.
11. Jackson DV Jr, Richards F II, Copper MR, et al. Prophylactic cranial irradiation in small cell carcinoma of the lung: a randomized study. *JAMA* 1977;237:2730-3.
12. Cox JD, Petrovich Z, Paig C, Stanley K. Prophylactic cranial irradiation in patients with inoperable carcinoma of the lung: preliminary report of a cooperative trial. *Cancer* 1978;42:1135-40.
13. Beiler DD, Kane RC, Bernath AM, Cashdollar MR. Low dose elective brain irradiation in small cell carcinoma of the lung. *Int J Radiat Oncol Biol Phys* 1979;5:941-5.



14. Hansen HH, Dombernowsky P, Hirsch FR, Hansen M, Rygard J. Prophylactic irradiation in bronchogenic small cell carcinoma: A comparative trial of localized versus extensive radiotherapy including prophylactic cranial irradiation in patients receiving combination chemotherapy. *Cancer* 1980;46:279-84.
15. Maurer LH, Tulloh M, Weiss RB, et al. A randomized combination modality trial in small cell carcinoma of the lung: comparison of combination chemotherapy-radiation therapy versus cyclophosphamide-radiation therapy effects of maintenance chemotherapy and prophylactic whole brain irradiation. *Cancer* 1980;45:30-9.
16. Eagan RT, Frytak S, Lee RE, Creagan ET, Ingle JN, Nichols WC. A case for preplanned thoracic and prophylactic whole brain radiation therapy in limited small cell lung cancer. *Cancer Clin Trials* 1981;4:261-6.
17. Katsenis AT, Karpasitis N, Giannakakis D, Maragoudakis N, Kiparissiadis P. Elective brain irradiation in patients with small-cell carcinoma of the lung: preliminary report. In: Protifex G, ed. *Lung cancer: etiology, epidemiology, prevention, early diagnosis, treatment*. Amsterdam: Excerpta Medica, 1982:277-84.
18. Moutain CF, Vincent R, Wilson HE, Stanley K. Intensive chemotherapy and radiotherapy of small cell carcinoma of the lung-regional disease. In: *Abstracts of the Third World Conference on Lung Cancer*, Tokyo, Japan, May 17-20, 1982;153.
19. Seydel HG, Creech R, Pagano M, et al. Prophylactic versus no brain irradiation in regional small cell lung carcinoma. *Am J Clin Oncol* 1985;8:218-23.
20. Niiranen A, Holsti P, Salmo M. Treatment of small cell lung cancer: Two-drug versus four drug chemotherapy and loco-regional irradiation with or without prophylactic cranial irradiation. *Acta Oncol* 1989;28:501-5.
21. Aroney RS, Aisner J, Wesley MN, et al. Value of prophylactic cranial irradiation given at complete remission in small cell lung carcinoma. *Cancer Treat Rep* 1983;67:675-82.
22. Ohonoshi T, Ueoka H, Kawahara S, et al. Comparative study of prophylactic cranial irradiation in patients with small cell lung cancer achieving a complete response: a long-term follow-up result. *Lung Cancer* 1993;10:47-54.
23. Laplanche A, Monnet I, Santos-Miranda S, et al. Controlled clinical trial of prophylactic cranial irradiation for patients with small cell lung cancer in complete remission. *Lung Cancer* 1998;21:193-201.
24. Wagner H, Kim K, Turrisi A. A randomized phase III study of prophylactic cranial irradiation versus observation in patients with small cell lung cancer achieving a complete response: final report of an incomplete trial by the Eastern Cooperative Oncology Group and Radiation Therapy Oncology Group (E3589/R92-01). *Proc Am Soc Clin Oncol* 1996;15:376.
25. Auperin A, Arriagada R, Pignon JP, Le Pechoux C, Gregor A, Stephens RJ, Kristjansen PEG, Johnson BE, Ueoka H, Wagner H, Aisner J. Prophylactic Cranial Irradiation for Patients with Small-Cell Lung Cancer in Complete Remission. *New Engl J Med* 1999;341:476-84.



26. Minna JD, Higgins GA, Glatstein EJ: Cancer of the lung, in Devita VT, Hellman SJ, Rosenberg SA (eds): Cancer: Principles & Practice of Oncology. Second Edition. Philadelphia J.B. Lippincott Company 1985;507-97.
27. Rosen ST, Makuch RW, Lichter AS, Ihde DC, Matthews MJ, Minna JD, Glatstein E, Bunn PA. Role of the Prophylactic Cranial Irradiation in Prevention of Central Nervous System Metastases in Small Cell Lung Cancer. *Am J Med* 1983;74:615-24.
28. Shaw EG, Su JQ, Eagan RT, Jett JR, Maksymiuk AW, Deigert FA. Prophylactic Cranial Irradiation in Complete Responders with Small-Cell Lung Cancer: Analysis of the Mayo Clinic and North Central Cancer Treatment Group Data Bases. *J Clin Oncol* 1994: Volume 12: 3227-32.
29. Turrisi AT, Kim K, Blum R, Sause WT, Livingston RB, Komaki R, Wagner H, Aisner S, Johnson DH. Twice-Daily Compared with Once-Daily Thoracic Radiotherapy in Limited Small-Cell Lung Cancer Treated Concurrently with Cisplatin and Etoposide. *New Engl J Med* 1999: Volume 340: 265-271.
30. National Center for Health Statistics. Vital statistics of the United States, 1995, preprint of vol II, mortality, part A sec 6 life tables. Hyattsville Maryland. 1998.
31. Johnson BE, Becker B, Goff WB 2nd, Petronas N, Krehbiel MA, Makuch RW, McKenna G, Glatstein E, Ihde DC: Neurologic, neuropsychologic, and computed cranial tomography scan abnormalities in 2- to 10-year survivors of small-cell lung cancer. *J Clin Oncol* 1985;3(12):1659-67.
32. Fonseca R, O'Neill BP, Foote RL, Grill JP, Sloan JA, Frytak S: Cerebral toxicity in patients treated for small cell carcinoma of the lung *Mayo Clin Proc* 1999 May;74(5):461-5.



## **FIGURE LEGEND**

Figure 1. Comparative cumulative risk of neurotoxicity over time with 30% or 50% of the patients developed neurotoxicity eventually.

Figure 2. Utility functions reflecting loss in quality of life over time upon the onset of neurotoxicity for scenarios with a minimum utility of 20% and 40%, respectively.

Figure 3. Quality-adjusted survival curves for PCI and No PCI groups with 40% minimum utility.

Figure 4. Quality-adjusted survival curves for PCI and No PCI groups with 20% minimum utility.

Figure 5. Two-way sensitivity analysis by varying 5-year survival rate in No PCI group and neurotoxicity rate with 40% minimum utility.

Figure 6. Two-way sensitivity analysis by varying 5-year survival rate in No PCI group and neurotoxicity rate with 20% minimum utility.



Figure 1.

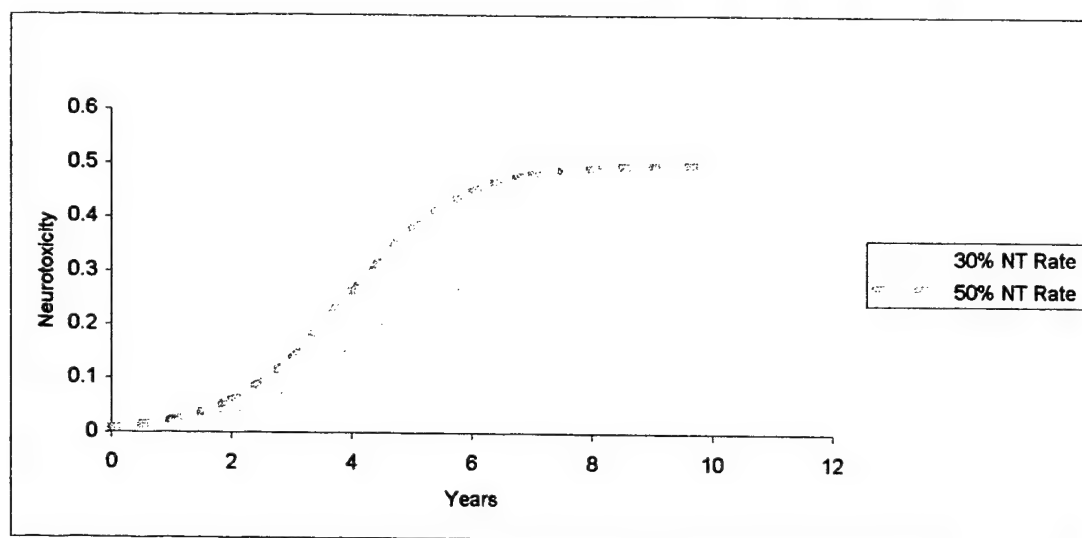




Figure 2.

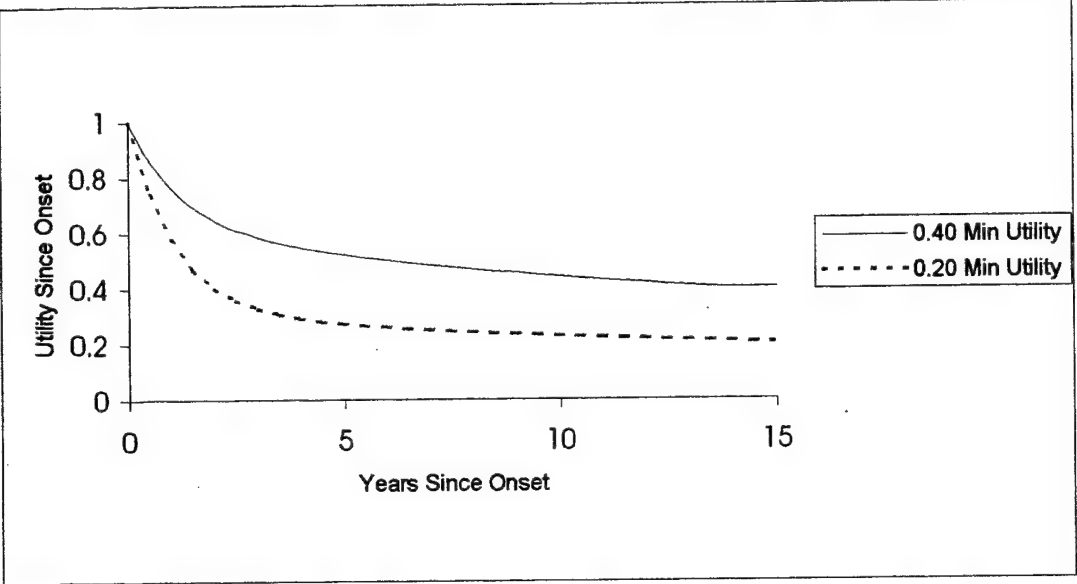




Figure 3

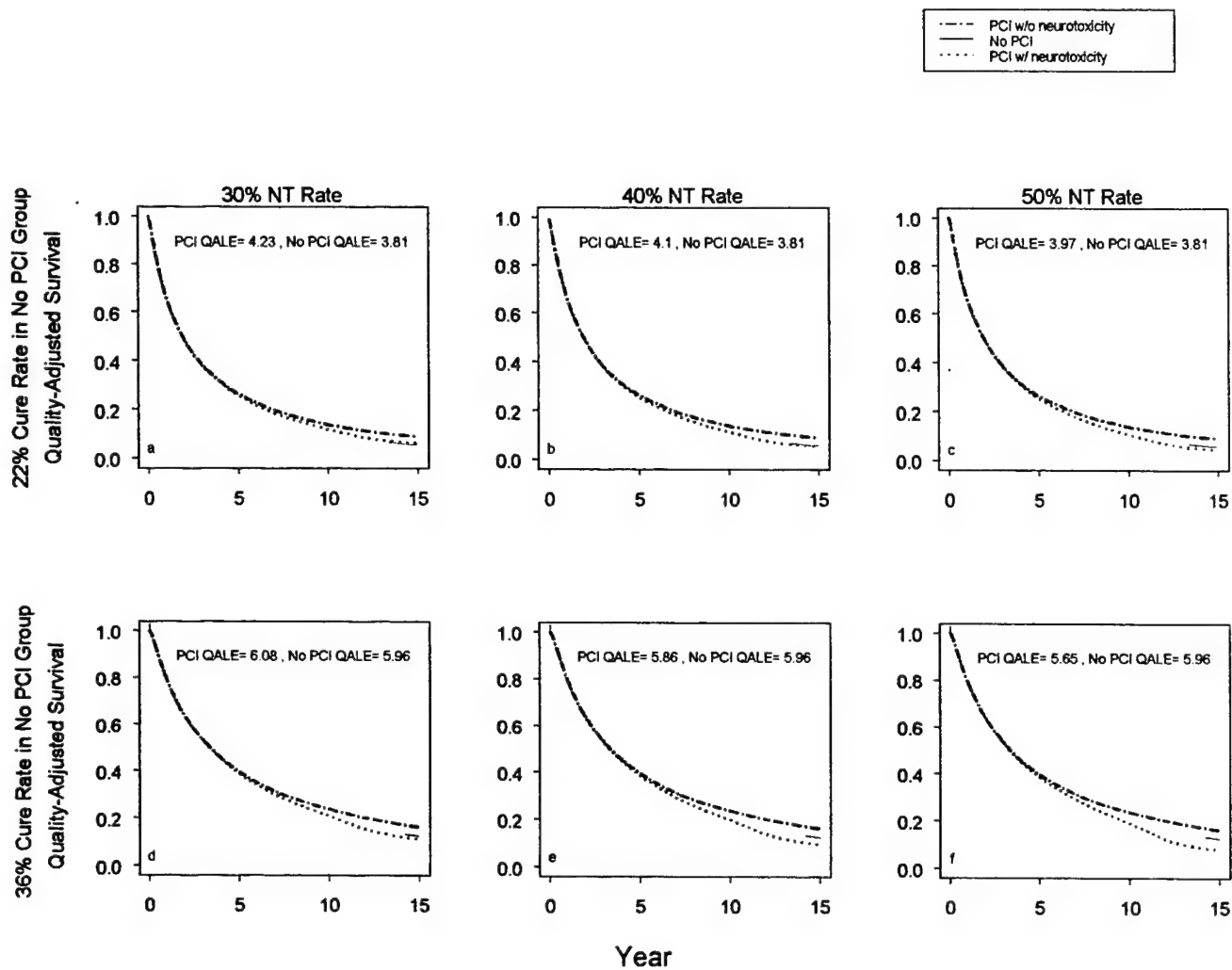




Figure 4.

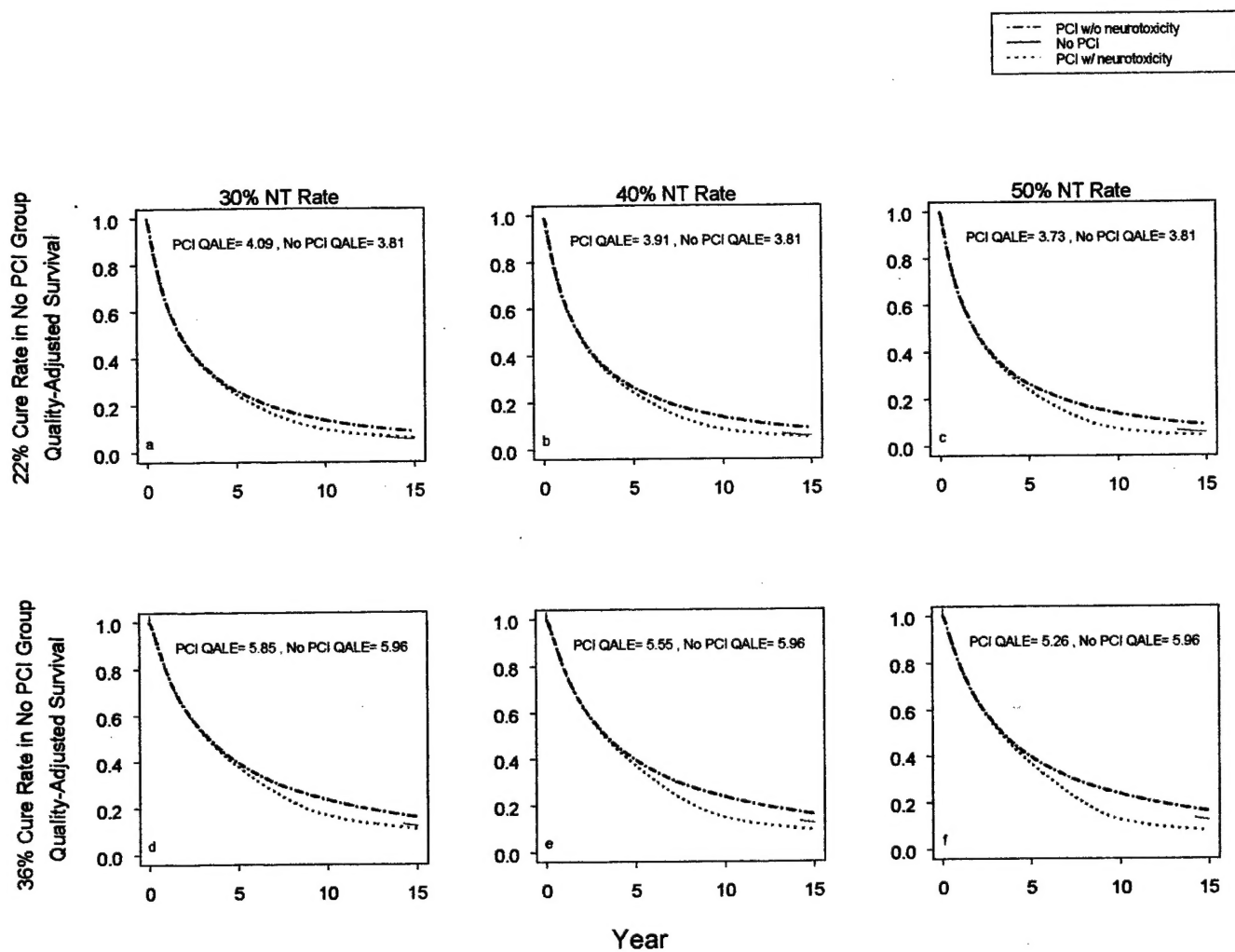




Figure 5.

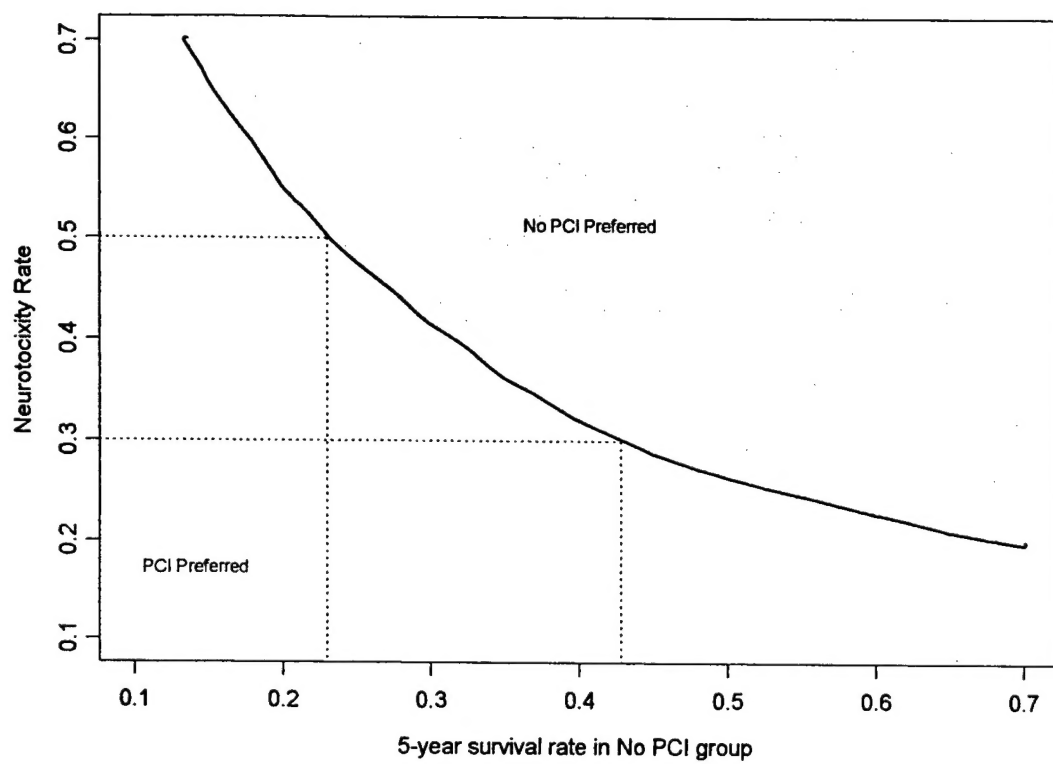
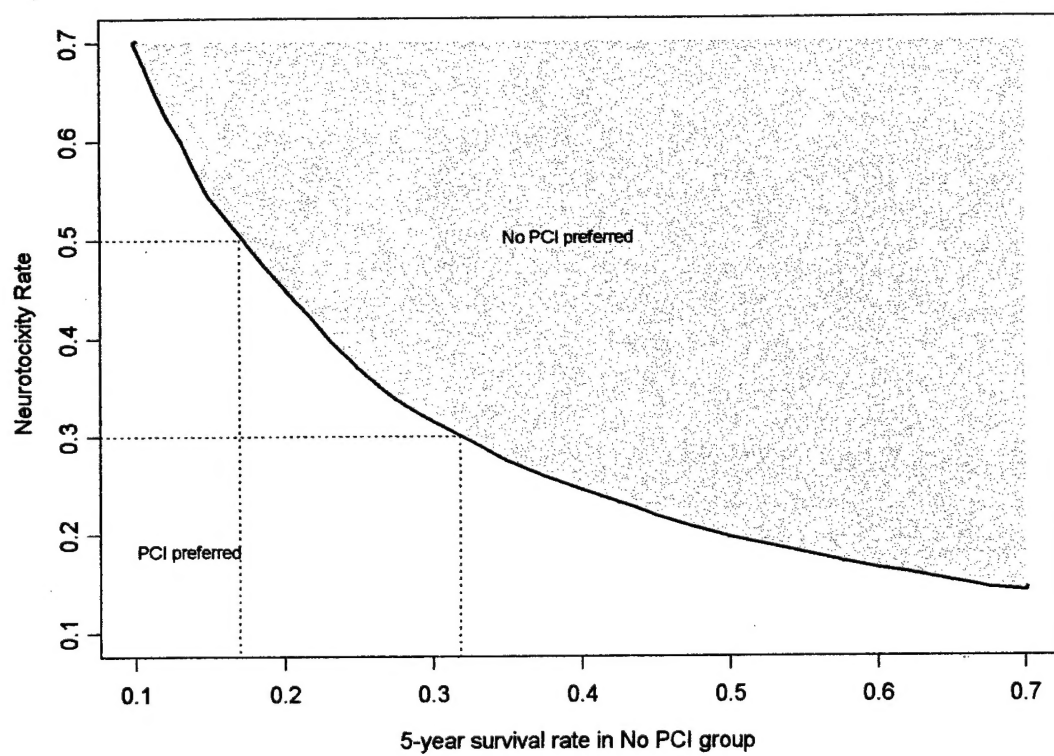




Figure 6.





**Technical Reports of the Department of Biostatistics, The University of Texas M. D. Anderson Cancer Center**  
(List of archived reports available at <http://www.mdanderson.org/depts/biostatistics>)

UTMDABTR-006-01 Thall PF, Inoue L, Berry DA: Seamlessly expanding a randomized phase II trial to phase III

UTMDABTR-007-01 Thall PF, Sung H-G, Choudhury A: Dose-finding based on feasibility and toxicity in T-cell infusion trials

UTMDABTR-008-01 Stallard N, Thall PF: Decision-theoretic designs for pre-phase II screening trials in oncology

UTMDABTR-009-01 Thall PF: Bayesian clinical trial design in a cancer center

UTMDABTR-010-01 Thall PF, Sung H-G, Estey EH: Multi-course treatment strategies for clinical trials of rapidly fatal diseases

UTMDABTR-011-01 Thall PF, Estey EH: Graphical methods for evaluating covariate effects in the Cox model

UTMDABTR-012-01 Cheung YK, Thall PF: Monitoring the rates of composite events with censored data in phase II clinical trials

UTMDABTR-013-01 Rosner GL, Stadler W, Ratain MJ: The randomized discontinuation design: application to cytostatic antineoplastic agents

UTMDABTR-014-01 Thall PF, Inoue LYT, Martin TG: Adaptive decision-making in a lymphocyte infusion trial

UTMDABTR-015-01 Wu D, Rosner GL, Broemeling L: Bayesian inference of age-dependent sensitivity, sojourn time and transition rate in screening

UTMDABTR-016-01 Broemeling L, Wu D: Power functions for Bayesian tests with application to the design of clinical trials: the fixed-sample case

UTMDABTR-017-01 Coombes KR, Highsmith WE, Krogmann TA, Baggerly KA, Stivers DN, Abruzzo LV  
Identifying and quantifying sources of variation in microarray data using high-density cDNA membrane arrays

UTMDABTR-018-01 Thall PF: Ethical Issues in Oncology Biostatistics

UTMDABTR-019-01 Morris JS, Wang N, Lupton JR, Chapkin RS, Turner ND, Hong MY, Carroll RJ: A Bayesian analysis of colonic crypt structure and coordinated response to carcinogen exposure incorporating missing crypts

UTMDABTR-020-01 Morris JS, Vannucci M, Brown PJ, Carroll RJ: Wavelet-based nonparametric modeling of hierarchical functions in colon carcinogenesis

UTMDABTR-001-02 Cheng Y, Su F, Berry DA: Asymptotic optimal group sequential strategies in two-armed bandit problems

UTMDABTR-002-02 Thall PF, Wathen JK, Bekele BN, Champlin RE, Baker LO, Benjamin RS  
Hierarchical Bayesian approaches to phase II trials in diseases with multiple subtypes

UTMDABTR-003-02 Broemeling LD: Studies in the history of probability and statistics: the Bayesian contributions of Edmond Lhoste

UTMDABTR-004-02 Cheng Y, Rosner GL: Asymptotic optimal sample sizes for discovering a promising treatment in phase II group sequential clinical trials

UTMDABTR-005-02 Moon H, Lee JJ, Ahn H, Nikolova RG: Web-based simulator for sample size and power estimation in animal carcinogenicity studies

UTMDABTR-006-02 Moon H, Ahn H, Lee JJ, Kodell RL: A weight-adjusted Peto's test when cause of death is not assigned

UTMDABTR-007-02 De Iorio M, Müller P, Rosner GL, MacEachern SN: An ANOVA model for dependent random measures

UTMDABTR-008-02 Thall PF, Millikan RE, Müller P, Lee S-J: Dose-finding with two agents in phase I oncology trials

UTMDABTR-009-02 Estey EH, Thall PF: New designs for phase II clinical trials

UTMDABTR-010-02 Morris JS, Baggerly KA, Coombes KR: Bayesian shrinkage estimation of the relative abundance of mRNA transcripts using SAGE

UTMDABTR-011-02 Do KA, Broom B, Wen S: GeneClust

UTMDABTR-012-02 Do K, McLachlan GJ, Bean R, Wen S: Some recent methods in clustering microarray gene expression data and applications

UTMDABTR-013-02 Huang X, Wolfe RA, Hu C: A test for independent censoring using correlated survival data

UTMDABTR-014-02 Bekele BN, Thall PF: Dose-finding based on multiple ordinal toxicities in phase I oncology trials

UTMDABTR-015-02 Baggerly KA, Deng L, Morris JS, Aldaz CM: Differential expression in SAGE: accounting for normal between-library variation

UTMDABTR-016-02 Thall PF, Lee SJ: Practical model-based dose-finding in phase I clinical trials: methods based on toxicity

UTMDABTR-001-03 Baggerly KA, Morris JS, Coombes KR: Cautions about reproducibility in mass spectrometry: Joint analysis of several proteomic data sets

UTMDABTR-002-03 Bekele BN, Lee JJ, Cantor SB, Zhou X, Lee JS: Decision analysis of prophylactic cranial irradiation for patients with small cell lung cancer

**Best Available Copy**